PRECLINICAL PHARMACOKINETICS AND SKELETAL PHARMACOLOGY OF A SELECTIVE ANDROGEN RECEPTOR MODULATOR

DISSERTATION

Presented in Partial Fulfillment of the Requirements for

the Degree Doctor of Philosophy in the Graduate

School of The Ohio State University

By

Jeffrey Dale Kearbey, B.S.

*****

The Ohio State University

2004

Dissertation Committee:

Dr. James T. Dalton, Advisor

Dr. Thomas D. Schmittgen

Dr. Robert J. Lee

Approved by

_____

Advisor
Pharmacy Graduate Program

ABSTRACT

Osteoporosis poses a significant health threat to the elderly population. Upon aging, females lose between 35-50% of their trabecular bone and 25-30% of their cortical bone. Men lose between 15-45% of their trabecular bone and 5-15% of their cortical bone. The lifetime risk for hip, spine, and distal forearm fractures are 40% and 13% in women and men, respectively. Mortality rates in the six months following hip fracture are 10-20% higher in patients than in age-matched controls, and, of those surviving, the majority experienced pain and limped or required a cane. As the longevity of the population increases, it becomes increasingly important to develop appropriate treatments to either preserve or rebuild bone in order to prevent fractures and/or promote healing.

Many lines of evidence point to the fact that androgens play a pivotal role in bone biology. However, side effect profiles and poor oral bioavailability limit the application of currently available androgen formulations. The discovery of nonsteroidal AR agonists with tissue selective pharmacologic effects provides a unique opportunity to more clearly define the role of androgens in skeletal growth and maintenance, as well as explore these new therapeutic entities for the treatment of osteoporosis. We employed a rational experimental design to test the hypothesis that treatment of ovariectomy-induced osteoporosis in animal models with an orally bioavailable nonsteroidal agonist for the AR (S-4) would exert a protective and proliferative effect on the skeleton.

The specific aims of this project were to: evaluate the therapeutic potential of S-4 based on its pharmacokinetic parameters in rats (Chapter 2) and delineate the protective (Chapter 3) and/or proliferative (Chapter 4) effects of SARMs on bone *in vivo.*

We hypothesized that S-4 would be rapidly and completely absorbed after oral administration and avoid some of the historical drawbacks of testosterone administration due to its nonsteroidal structure. As expected, we observed decreased metabolic clearance and enhanced oral bioavailability compared to testosterone. S-4 demonstrates complete bioavailability, short time to peak plasma concentration, and relatively slow metabolic clearance at doses capable of eliciting maximal pharmacologic effect. These properties favor the continued development of S-4 as an orally bioavailable nonsteroidal SARM.

In order to examine the protective effects of S-4 on bone loss, we evaluated the pharmacologic activity of S-4 in a rat model of accelerated bone loss. Our studies clearly show that OVX-induced changes in whole body BMD, body weight, percent fat mass, L5-L6 BMD, femoral BMD, femoral CT, femoral CC, femoral PC, trabecular density, biomechanical strength, and biological markers of bone resorption and formation are modulated by a nonsteroidal SARM. S-4 fully restored whole body BMD, L5-L6 BMD, femoral BMD, cortical content, and biomechanical strength in ovariectomized animals. Taken together, these data suggest that S-4 could provide a novel pharmacological intervention in the prevention of bone loss in postmenopausal women.

Finally, we assessed the anabolic activity of S-4 in an osteopenic rat model. Whole body BMD was fully restored in animals receiving > 0.1 mg/day S-4. Regional analysis of the L5-L6 vertebra and the femur by DEXA showed that S-4 completely

restored BMD. pQCT results confirmed anabolic effects on the cortical bone in the femur, but trabecular density in the distal femur was unchanged with drug treatment. The lack of effect in trabecular bone was likely due to the lack of preexisting architecture upon which to rebuild lost bone. Complete restoration of the biomechanical strength in the femur further supports our conclusion that S-4 is anabolic in bone. These data suggest that S-4 is likely to significantly reduce the fracture risk in patients with osteoporosis through direct anabolic action on both muscle and bone. S-4 performed as well or better than DHT in these assays. As S-4 is anabolic in bone, orally bioavailable, tissue-selective, and does not cross-react with other steroid hormone receptors, it offers significant advantages over currently available therapies for osteoporosis.

Dedicated to my wife

Tara L. Kearbey

and to my parents

Roger and Shirley Kearbey

ACKNOWLEDGMENTS

I would like to express my sincere appreciation and gratitude to my advisor, Dr. James T. Dalton, for his friendship, support, and guidance. His pursuit of scientific excellence and depth of knowledge have never ceased to inspire. I would like to thank the members of my dissertation committee, Dr. Thomas D. Schmittgen and Dr. Robert J. Lee, for their comments and discussions. I appreciate Dr. Duane D. Miller for his guidance and constructive criticism. I am grateful to Dr. Duane D. Miller's research group, Dr. Kiwon Chung, Dr. Yali He, and Dr. Seoung Soo Hong for synthetic method development and synthesis of the compounds used in my studies. I would like to thank Dr. Charles R. Yates and Dr. Donghua Yin for their friendship, guidance, and discussions. I am grateful to Dr. Di Wu, Ms. Wenqing Gao, Mrs. Eunju Hurh, and Mrs. Huiping Xu for their assistance with experimental design, implementation, and data interpretation of the studies performed herein. I wish to thank the other members of Dr. Dalton's laboratory for their friendship and help. I would like to thank my parents, Roger and Shirley Kearbey, and my brother, Robert Kearbey, for their encouragement and support. Finally, I cannot begin to express my appreciation and gratitude to my wife, Tara Kearbey, for her enduring support and encouragement, without which I could not have achieved this goal.

This research was supported in part by grants from NIH (R01 DK59800) and GTx Inc. Memphis, TN to Dr. James T. Dalton.

VITA

April 15, 1975……. Born – Poplar Bluff, Missouri

1993…….Poplar Bluff Senior High School

1998…….B.S. Animal Sciences, University of Missouri

1999-2000……... Graduate Teaching Assistant, University of Tennessee

2000-Present……Graduate Teaching and Research Assistant, The Ohio State University

PUBLICATIONS

Research Publications

1. Rogers TD, Gades NM, Kearbey JD, Virgous CK, and Dalton JT. Chronic Restraint Via Tail Immobilization in Mice: Effects on Corticosterone Levels and Other Physiologic Indices of Stress. Contemporary Topics in Laboratory Animal Science, 41(1):46-50, 2002.

2. Yin D, Gao W, Kearbey JD, Xu H, Chung K, Miller DD, and Dalton JT. Pharmacodynamics of Selective Androgen Receptor Modulators. Journal of Pharmacology and Experimental Therapeutics, 304(3):1334-1340, 2003.

3. Yates CR, Chang C, Kearbey JD, Yasuda K, Schuetz EG, Miller DD, Dalton JT, and Swaan PW. Structural Determinants of P-glycoprotein-Mediated Transport of Glucocorticoids. Pharmaceutical Research, 20(11):1794-1803, 2003.

4. Kearbey JD, Gao W, Miller DD, and Dalton JT. Pharmacokinetics of S-3-(4-acetylamino-phenoxy)-2-hydroxy-2-methyl-N-(4-nitro-3-trifluoromethyl-phenyl)-propionamide, a Nonsteroidal Selective Androgen Receptor Modulator. Xenobiotica, 34(3):273-280, 2004.

FIELD OF STUDY

Major Field: Pharmacy

TABLE OF CONTENTS

LIST OF TABLES

LIST OF FIGURES

CHAPTER 1

INTRODUCTION

1.1 Androgens

Androgens are important mediators of many physiological processes in both males and females. Development and maintenance of the male phenotype as well as regulation of spermatogenesis and male sexual behavior are perhaps the most well known effects of androgens. However, androgen receptors (AR) are widely distributed throughout the body in tissues such as muscle, bone, hair, skin, kidney, lipoproteins, central nervous system, liver, and reproductive tissues in males and females indicating the diverse functions of androgens [1, 2].

The AR is a member of the nuclear hormone receptor superfamily. Other prominent members of this superfamily include estrogen receptor (ER), progesterone receptor (PR), glucocorticoid receptor (GR), mineralocorticoid receptor (MR), retinoid X receptor (RXR), vitamin D receptor (VDR), thyroid hormone receptor (TR), and peroxisome proliferator-activated receptor (PPAR) as well as others. In the classical (ligand-dependent) model of nuclear hormone receptor action, these receptors mediate

cellular response in the nucleus through direct regulation of specific gene expression [3]. Specifically, the receptors are bound to heat shock proteins (HSP) and other chaperone proteins in the absence of ligand. Upon ligand binding, a conformational change in the receptor causes HSP to dissociate, dimerization, phosphorylation, binding to hormone response elements (HRE), and stimulation of transcription. The HRE for each receptor is different and allows selective activation of specific genes in response to each hormone [4]. A schematic representation of this pathway is illustrated in Figure 1.1. Although our research is focused on the ligand-dependent activation of the AR, ligand-independent activation of AR has also been reported [5, 6]. There is evidence showing that cyclin-dependent kinases and mitogen activated protein kinases can phosphorylate nuclear hormone receptors in the absence of ligand and stimulate transcription of genes under the control of the HRE [7].

There are two endogenous androgens testosterone and dihydrotestosterone (DHT). Testosterone is the primary circulating androgen in males and females [1]. In males, testosterone is secreted by testicular Leydig cells in response to luteinizing hormone (LH). In females, 50% of the circulating testosterone is secreted by the adrenal gland and the ovaries and 50% is produced by peripheral conversion of the androgen precursors dehydroepiandrosterone (DHEA) and androstenedione (A) [8]. The major biochemical pathways for the synthesis of sex steroids are shown in Figure 1.2.

The androgenic effect of testosterone is multiplied in some tissues by the local conversion of testosterone to DHT by 5a-reductase. DHT is the most potent endogenous androgen, binds the AR with a higher binding affinity than testosterone, and is able to

activate the receptor at a lower concentration [1]. DHT is considered the primary androgen in reproductive tissues and skin [1].

Pathological androgen deficiencies as well as declining androgen levels in aging patients are well characterized and have been linked to decreased well being, unexplained fatigue, sexual dysfunction, decreased bone density, decreased muscle strength, and changes in body composition [2, 9, 10]. A comprehensive review of several placebo controlled studies focused on androgen deficiencies in men found that testosterone replacement resulted in beneficial effects on body composition, muscle strength, sexual function, well being, bone mineral density, and some cognitive improvements [11]. However, risks from the side effects of testosterone supplementation limit its application to patients with markedly decreased androgen levels as opposed to patients with low to normal androgen levels that would also experience benefits from the androgen replacement [11]. Androgen therapy is absolutely contraindicated in patient populations with a history of breast cancer, prostate cancer, or a hematocrit above 55% [12]. Androgen supplementation in females remains controversial due to inadequate preparations and doses for females, dose limiting side effects such as virilization, and lack of randomized clinical trials [13, 14]. However, novel therapeutic agents that exploit the AR but exhibit better side effect profiles and a more narrow pharmacologic action than endogenous ligands offer many potential therapeutic advantages in both males and females [14].

1.2 Discovery of Selective Androgen Receptor Modulators

Our laboratory was the first to report the discovery of a series of nonsteroidal agonists for the AR [15]. These compounds were discovered during attempts to find electrophilic AR affinity ligands through structural modification of known nonsteroidal antiandrogens (structures shown in Figure 1.3). Following this initial discovery, our laboratory synthesized several novel series of nonsteroidal AR agonists and explored their anabolic and androgenic structure-activity relationships both *in vitro* and *in vivo* [16, 17, 18, 19]. Several compounds were identified that exhibited higher AR binding affinities than the antiandrogens from which they were derived. Many of these compounds were in the series of bicalutamide analogs. The functional activity of these AR ligands ranged from antagonist to full agonist. Although, the affinity for the AR did not correlate with the functional activity, structural features necessary for agonist versus antagonist activity were identified [17]. These newly discovered compounds bound the AR with affinity similar to that of testosterone and mimicked the effects of known steroidal agonists on receptor-mediated transcriptional activation [15]. However, the lead compound from AR binding studies and transcriptional activation studies, acetothiolutamide, exhibited relatively low *in vivo* activity [18]. In an effort to resolve the apparent disparity between *in vitro* and *in vivo* results, the pharmacokinetics and metabolism of acetothiolutamide were characterized. It was subsequently determined that extensive hepatic metabolism led to a rapid clearance of the drug, which minimized drug exposure and accounted for the lack of androgenic activity of this compound [18]. It was clear from the metabolism studies that oxidation, mainly at the sulfur linkage, was

the main route of metabolism. Therefore, a new series of compounds with an ether linkage, in place of the thioether linkage in acetothiolutamide, was synthesized in an effort to reduce metabolic clearance of these compounds.

During *in vitro* AR binding affinity and *in vivo* pharmacologic activity characterization of the new ether-linked bicalutamide derivatives, S-3-(4-acetylamino-phenoxy)-2-hydroxy-2-methyl-N-(4-nitro-3-trifluoromethyl-phenyl)-propionamide (S-4) (structure shown in Figure 1.4) emerged as our lead compound [19]. S-4 is a ligand with potent AR binding affinity (Ki = 4.0 ± 0.7 nM) that exhibits tissue-selective androgenic and anabolic effects in rats [19]. Other studies in our laboratory showed that S-4 is specific for the AR and does not activate the other steroid hormone receptors in a transcriptional activation assay (data not published). In castrated male rats, S-4 showed dose-dependent effects in the levator ani muscle. These effects were similar in potency and efficacy to those of testosterone propionate (TP). However, S-4 was only a partial agonist in the prostate and seminal vesicles, restoring them to 34% and 28% of intact animals, respectively [19]. These results clearly show that S-4 exhibits tissue specific activity and is a strong candidate for clinical development as the first nonsteroidal selective androgen receptor modulator (SARM).

The tissue selectivity of SARMs may offer many therapeutic advantages for androgen replacement therapy. For example, S-4 was only a partial agonist in prostate tissue. Therefore, it is possible that patients with prostate cancer could still benefit from the anabolic effects of SARMs in muscle or bone without the detrimental effects that might be observed with testosterone therapy.

1.3 Bone Physiology

Bone is a dynamic structure that is continuously remodeling as we age. The skeleton is comprised of two different types of bone, cortical bone and trabecular (cancellous) bone as shown in Figure 1.5. Cortical bone comprises about 80% of the skeleton and is referred to as compact bone. Trabecular bone, also known as spongy or cancellous bone, comprises approximately 20% of the skeleton and is mainly found in the vertebrae and the ends of long bones. The Basic Multicellulat Unit (BMU) is responsible for bone remodeling. There are several sequential steps in bone remodeling. The first step is origination of a BMU as a result of mechanical stress, microdamage, or random osteoclast action. Osteoclasts are large multi-nucleated, bone resorbing cells found in the bone marrow. It is widely believed that cytokines and growth factors are the chemical signals for origination. These signals summon osteoclasts to the bone surface. Resorption by osteoclasts typically lasts about two weeks in any one particular area. Following bone resorption, osteoclasts most likely undergo apoptosis, and osteoblasts, bone forming cells, are recruited to lay down osteoid in the resorption pit. Osteoid is the collagen-rich matrix into which minerals are deposited. Once the osteoid has reached a thickness of about six microns, mineralization begins. Over the following months, the minerals pack tighter together and the density of the bone is increased. Finally, the osteoblasts become either lining cells or osteocytes. Lining cells regulate calcium efflux from the bone, while osteocytes are capable of sensing mechanical stresses in the bone [20].

Bone resorption and bone formation are tightly coupled processes. However, depending on the stage in life, there can be a slight deficit in one or the other. In the earlier stages of life, bone formation outpaces bone resorption, resulting in bone growth. During the middle stages of life, the rate of bone resorption and bone formation are approximately equal, while in the later stages of life the rate of bone resorption is faster than the rate of bone formation. It is in this latter stage of life when we are losing bone density that problems may arise.

1.4 Osteoporosis: The Clinical Problem

The National Institutes of Health reported that health care expenditures related to osteoporosis were $17 billion in 2001. Osteoporosis is defined as bone mineral density or bone mineral content more than 2.5 standard deviations below the young adult reference mean [21]. This disease already affects 10 million Americans, and another 34 million Americans are believed to suffer from low bone mass. One third of Caucasian women over the age of fifty have osteoporosis, yet nearly 80% remain undiagnosed. The most common cause for diagnosis is a fracture. By the age of 60, about 7% of women and 3% of men have suffered a fracture resulting from osteoporosis [22]. The lifetime risk for hip, spine, and distal forearm fractures are 40% and 13% in women and men, respectively [23]. Gender differences in osteoporosis are well documented. The incidence of osteoporosis is significantly higher in women than in men. Upon aging, females lose between 35-50% of their trabecular bone and 25-30% of their cortical bone. Men lose between 15-45% of their trabecular bone and 5-15% of their cortical bone [22,

24]. Schneider and Guralnik [25] predict the number of individuals in the United States over the age of 65 will increase from 32 million in 1990 to 69 million by 2050, and the number of individuals over the age of 85 will increase from 3 to 15 million during the same period. Based on the current incidence of hip fractures, inflation, and population growth, healthcare costs related to treating hip fractures could triple by the year 2040 [25], similar figures were reported by Cummings *et al*. [26]. More important than the economic cost are the clinical consequences of hip fractures. Mortality rates in the six months following fracture are 10-20% higher in patients than in age-matched controls [27, 28], and, of those surviving, the majority experienced pain and limped or required a cane [27, 29]. As the longevity of the population increases, it becomes increasingly important to develop appropriate treatments to either preserve or rebuild bone in order to prevent fractures and/or promote healing.

1.5 *In Vitro* Osteoporosis Models

Both *in vitro* and *in vivo* models have been developed to study the effects of various hormones and drugs on bone. It is widely believed that cells from the osteoblast (bone forming) lineage produce factors that activate osteoclasts (bone resorbing) and promote osteoclastogenesis [30]. Therefore, most of the *in vitro* research in the area of bone cells focuses on osteoblasts. Osteoblasts have been derived from the use of primary cell cultures of both human [31, 32] and rodent bones [33] or osteosarcoma cell lines, developed from either rodent [34] or human bone tumors [35, 36, 37]. Primary cell cultures are currently the only source of osteoclast cells. As with other primary cell

culture systems, the heterogeneity of the osteoclast cell populations is a significant concern in interpreting the results from these studies.

Cultured osteoblast cells provided a simplified model system in which to screen new drug candidates, elucidate the mechanism of action of current and novel therapeutic agents, study the physiology of bone formation, and delineate the role of osteoblast cells in bone resorption [38]. Since bone tissue is comprised of a complex mixture of different cell types embedded in an extracellular matrix, it is necessary to isolate individual cell types in order to investigate the molecular mechanisms by which these cells are regulated [39]. However, it is important to keep in mind that these *in vitro* systems are far less complex than the *in vivo* bone environment. Therefore, the results from an *in vitro* system should be confirmed, if possible, in an *in vivo* model, as interactions between different cell types *in vivo* may be important to the cellular regulation of the pathway being studied. The role of drug disposition in drug efficacy is also not adequately addressed by *in vitro* models.

Many different endpoints can be used for *in vitro* systems. Assays designed to measure cell proliferation, protein secretion, and mRNA production are a few examples of techniques that can be employed to describe the effects of different therapeutic agents on these systems. The variety of parameters that can be measured and the relative speed in which these experiments can be performed are significant advantages of *in vitro* systems. Protein secretion and mRNA expression are direct measures of the physiological effects of therapeutic agents. Ultimately, the production and modulation of proteins are responsible for the effects of drugs in cells. However, assays for protein

concentration and activity often lack the sensitivity to detect small changes. Therefore mRNA expression provides a more sensitive measure of drug effects in *in vitro* systems.

1.6 *In Vivo* Osteoporosis Models

While a great deal of mechanistic and cell signaling data has been generated from the use of cell culture models, *in vitro* model systems are not always an accurate predictor of *in vivo* response [39]. Therefore, it is more clinically relevant to use an animal model for the evaluation of therapeutic treatments. The majority of *in vivo* studies utilize the ovariectomized female rat as a model of postmenopausal osteoporosis. The United States Food and Drug Administration (FDA) has specified the ovariectomized female rat as the appropriate small animal model of osteoporosis [40]. One reason this model is so widely used is that it has responded positively to every therapeutic regimen clinically used to treat postmenopausal osteoporosis [41]. However, there are some physiological differences in bone modeling and remodeling between the ovariectomized rat and humans. Unlike humans, the growth plates in rats never fuse, so the bones never completely stop growing. However, at twenty-three weeks of age, the growth rate has significantly slowed making it easier to separate the drug effects from normal bone growth [42]. Rats also lack Haversian remodeling [43]. Therefore, bone remodeling in rats occurs at the surface of the bone and not within the bone. Even with these differences, rats provide an accepted and economical model to investigate new drug therapies.

Now that we have a relevant model in which to measure changes in bone, we must carefully choose which biological parameters to measure. Until recently, most animal studies used changes in urine or serum markers, along with histomorphometry of excised bones as endpoints. Clinically, the focus has been on biological markers, since histomorphometry of the iliac crest is both invasive and expensive. There are many markers of both bone resorption and bone formation. Markers of bone formation include serum alkaline phosphatase, serum osteocalcin (bone Gla protein, BGP), serum type I collagen propeptides, C-terminal propeptide (PICP), and N-terminal propeptide (PINP) [44]. Markers of bone resorption include urine hydroxyproline, serum tartrate-resistant acid phosphatase (TRAP), urine hydroxylysine glycosides, pyridinoline cross-links (PYR, DPD), urine N-terminal-to-helix-cross-links (NTX), urine C-terminal-to-helix-cross-links (CTX), and serum C-terminal-to-helix-cross-links (ICTP) [44]. In the following studies, we chose serum osteocalcin as a marker of bone formation and deoxypryidinoline (DPD) as a marker of bone resorption. Osteocalcin has been validated as a specific marker for bone formation in a variety of pathological conditions, including osteoporosis [44]. Osteocalcin is synthesized by osteoblasts and most of the protein is immediately bound to the bone mineral. However, a proportion of the osteocalcin is released into the blood and can be measured as an indicator of osteoblastic activity. DPD links collagen molecules together in the final stage of fibril formation. It is released following tissue degradation. Although small amounts of DPD have been identified in some other tissues such as muscle and the cardiovascular system, the vast majority of DPD in the urine comes from the degradation of bone tissue, and is therefore considered bone specific [45].

While changes in serum and urine markers mirror the changes in bones, they do not directly measure the changes in bone mineral density. With the recent advances in dual energy x-ray absorptiometry (DEXA), one can measure sequential changes in bone mineral density within a single animal. DEXA is considered the "gold standard" for measuring bone mineral density *in vivo* [46]. Briefly, two energies of x-rays are passed through the subject. The lower energy x-rays are able to pass through the soft tissue but not the bone. The higher energy x-rays are able to pass through both the soft tissue and the bone. The detector collects the signal from the x-ray source. Based on the attenuation of the x-rays through the subject, the computer determines the amount of bone, fat tissue, and lean tissue. To determine bone mineral density, the DEXA instrument measures bone mineral content and divides this number by the calculated bone area. Therefore, DEXA provides us with an areal density (g/cm^2) rather than a volumetric density (g/cm^3).

1.7 Skeletal Effects of Androgens *In Vitro*

There is an abundance of evidence suggesting that androgens play an important role in skeletal development. AR have been identified in a number of bone cells, including osteoblasts [47, 48, 49, 50, 51, 52], osteoclasts [53], marrow derived stromal cells [54], osteocytes [55], and hypertrophic chondrocytes [55]. Normal human osteoblasts express up to 3,000 AR per cell [47] and up to 3,900 estrogen receptors per cell [56]. Androgens exert effects on the activity of osteoblasts [54, 57, 58, 59]. A number of studies examined the effects of androgens on bone cells in culture. In

osteoblastic cell culture, both transcriptional activation [60] and AR expression [50] are up-regulated in response to treatment with DHT. Another study by Kasperk *et al.* [61] reported increased osteoblast proliferation after treatment with DHT. DHT treatment of a human osteoblastic cell line decreased Interleukin-6 (IL-6) production [62]. IL-6 is a multifunctional cytokine that is implicated in stimulating bone resorption following estrogen depletion [63]. Specifically, IL-6 secreted from osteoblasts acts as a paracrine mediator of osteoclastogenesis [64]. There is also some evidence to suggest that IL-6 is required for estrogen deficiency-induced bone loss. Both IL-6 knock-out mice [63] and normal mice [64] that were administered an IL-6 neutralizing antibody failed to lose bone following ovariectomy. DHT has also been shown to increase Insulin-like Growth Factor-I (IGF-I) six-fold in a human osteoblast cell line [65]. IGF-1 is a growth promoting polypeptide that has been correlated to bone growth [66]. IGF-1 has also been shown to enhance osteoblast differentiation [67].

1.8 Skeletal Effects of Androgens *In Vivo*

Animal models have provided some insight into the effects of androgen on bone. Testicular feminized male rats (i.e., rats that have mutated AR that do not bind androgens) have bone properties similar to that of female rats (i.e., smaller bones and lower bone turnover rates) [68]. Androgen treatment in orchidectomized male animals prevents reduction of the periosteal bone formation rate [69]. More recent studies by Hanada *et al.* [70] showed that a tetrahydroquinoline-derived SARM (S-40503) exhibits anabolic effects in an orchidectomized rat model of bone loss. They showed that S-

40503 was able to maintain cancellous bone in a gonadectomized male rat, but not in an ovariectomized female model. However, S-40503 increased cortical bone mineral density (BMD) in both models. Although S-40503 shows less tissue selectivity and is less potent than S-4 in the levator ani muscle [19, 70], these studies provide evidence that a SARM can modulate bone mass. Tobias *et al*. showed that DHT partially restored cancellous bone in ovariectomized female rats [71]. They found that DHT increased both trabecular number and thickness. However, they concluded that increases in trabecular thickness appeared to be the primary mechanism for the increases seen in cancellous bone volume. DHT effects were also noted in cortical bone, but these results did not reach statistical significance. The authors concluded that the study duration might have been too short for significant alterations in cortical bone to occur. They also performed histological analysis of osteoclast surface, a measure of bone resorption effects. DHT reduced these parameters at a dose rate of 1 mg/kg/day, indicating an anti-resorptive role for androgens in bone loss [71]. As a whole, their data suggest that androgens demonstrate both anti-resorptive and anabolic effects on bone, but they were unable to determine the predominate mechanism in cancellous bone. Another study found that androgens stimulate bone formation in cancellous bone [72]. These studies were of a relatively short duration (14 days), and therefore parameters such as the ratio of bone volume to tissue volume (BV/TV) remained unchanged even though DHT treatment increased trabecular thickness.

While animal model data provides valuable insights into the pharmacological activity of androgens, it is important to look at data generated in human populations. In humans, androgen insensitive males have decreased bone density [73] and skeletal mass

[74]. Testosterone treatment before epiphyseal closure in patients with isolated gonadotrophin deficiency causes rapid increases in bone mass [75, 76, 77]. Other studies by Stanhope [78] and Keenan [79] showed that nonaromatizable androgens increase linear bone growth. Male bones have thicker cortical walls and more mass than female bones [80, 81, 82]. Male hypogonadism is also associated with osteoporosis, and there is a correlation between testosterone levels and bone mass in aging men [83, 84, 85, 86, 87]. In fact, up to 20% of men with vertebral crush fractures are hypogonadal [88]. All of these data support the hypothesis that androgens play a significant role in bone homeostasis.

Clinical trials have shown that testosterone therapy can increase bone mineral density or decrease markers of bone resorption in osteoporotic hypogonadal men [89, 90, 91, 92, 93], glucorticoid-induced osteoporosis [94], osteoporotic eugonadal men [95], and gonadotrophin releasing hormone (GnRH) deficient men [96]. In summary, these studies found that testosterone therapy resulted in a positive increase in bone mineral density of about 5% [20]. Estimates from osteoporosis studies in women suggest that a 5% increase in bone mineral density would result in a decrease in fracture risk by about 50% [20].

1.9 Current Androgen Formulations

Synthesized steroidal androgens are used to treat a wide variety of conditions resulting from endogenous androgen deficiencies in both male and female patients. Unfortunately, nearly all of the current formulations suffer from severe limitations [97, 98]. Testosterone, in its pure form, suffers from low systemic bioavailability when

administered orally [99]. Testosterone esters (e.g., testosterone propionate, testosterone enanthate, testosterone cypionate, and testosterone buciclate) were developed in order to achieve a more desirable pharmacokinetic profile. Testosterone esters are usually administered intramuscularly in oil. Since the esters are less polar than free testosterone, they are more slowly absorbed and therefore offer a prolonged duration of action [100]. Peak plasma concentrations are not reached until 2-5 days after the injection, and plasma concentrations return to normal levels in 10-14 days [101]. Therefore, supraphysiological plasma levels can be reached shortly after the injections and levels fall to subphysiological levels before the next injection, which can result in a "roller coaster" effect of symptoms (i.e., symptom response fluctuates with plasma concentrations) [101] and increases the likelihood of testosterone related side effects [12]. 17-Alkylated testosterones (e.g., methyltestosterone and oxandrolone) are orally bioavailable, but they cause unacceptable hepatic toxicity and are less efficacious. Therefore, they are not recommended for long-term administration [101, 102, 103, 104]. Testosterone can be administered transdermally via a skin patch, but patches must be replaced daily and skin irritation is a frequent occurrence [105]. Transdermal gels have also been formulated for daily drug delivery. Gels have shown lower incidence of skin irritation than patches, but inadequate absorption of transdermal preparations may limit their effectiveness [101]. The high cost of transdermal formulations (~$100/month) compared to injectable formulations (~$10/month) also makes them a less favorable option for androgen therapy [12]. Buccal testosterone preparations are also available, but require frequent administration throughout the day to maintain therapeutic plasma levels [12]. Another drawback of testosterone administration is the cross reactivity of both testosterone and its

metabolites with the other steroid hormone receptors [98, 106]. As shown in Figure 1.2, testosterone can be converted directly to estradiol by aromatase.

1.10 Scope and Objectives of Dissertation

Many lines of evidence point to the fact that androgens play a pivotal role in bone biology. However, side effect profiles and poor oral bioavailability limit the application of currently available androgen formulations. The discovery of nonsteroidal AR agonists with tissue selective pharmacologic effects provides a unique opportunity to more clearly define the role of androgens in skeletal growth and maintenance, as well as explore these new therapeutic entities for the treatment of osteoporosis. We employed a rational experimental design to test the hypothesis that treatment of ovariectomy-induced osteoporosis in animal models with an orally bioavailable nonsteroidal agonist for the AR (S-4) would exert a protective and proliferative effect on the skeleton.

The specific aims of this project were to: evaluate the therapeutic potential of S-4 based on its pharmacokinetic parameters in rats (Chapter 2) and delineate the protective (Chapter 3) and/or proliferative (Chapter 4) effects of SARMs on bone *in vivo.* A summary of our findings and analysis of future perspectives for SARM research in osteoporosis is presented in Chapter 5.

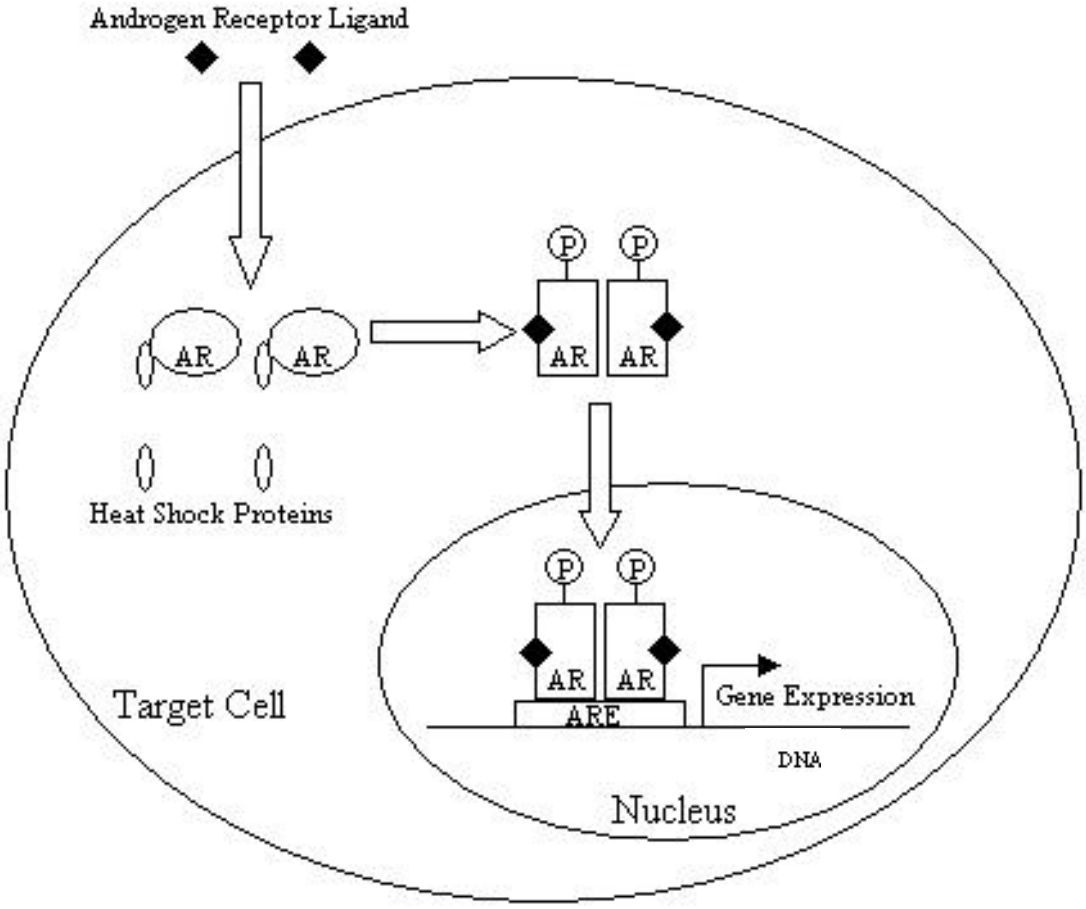

Figure 1.1: Ligand-dependent model of androgen receptor action.

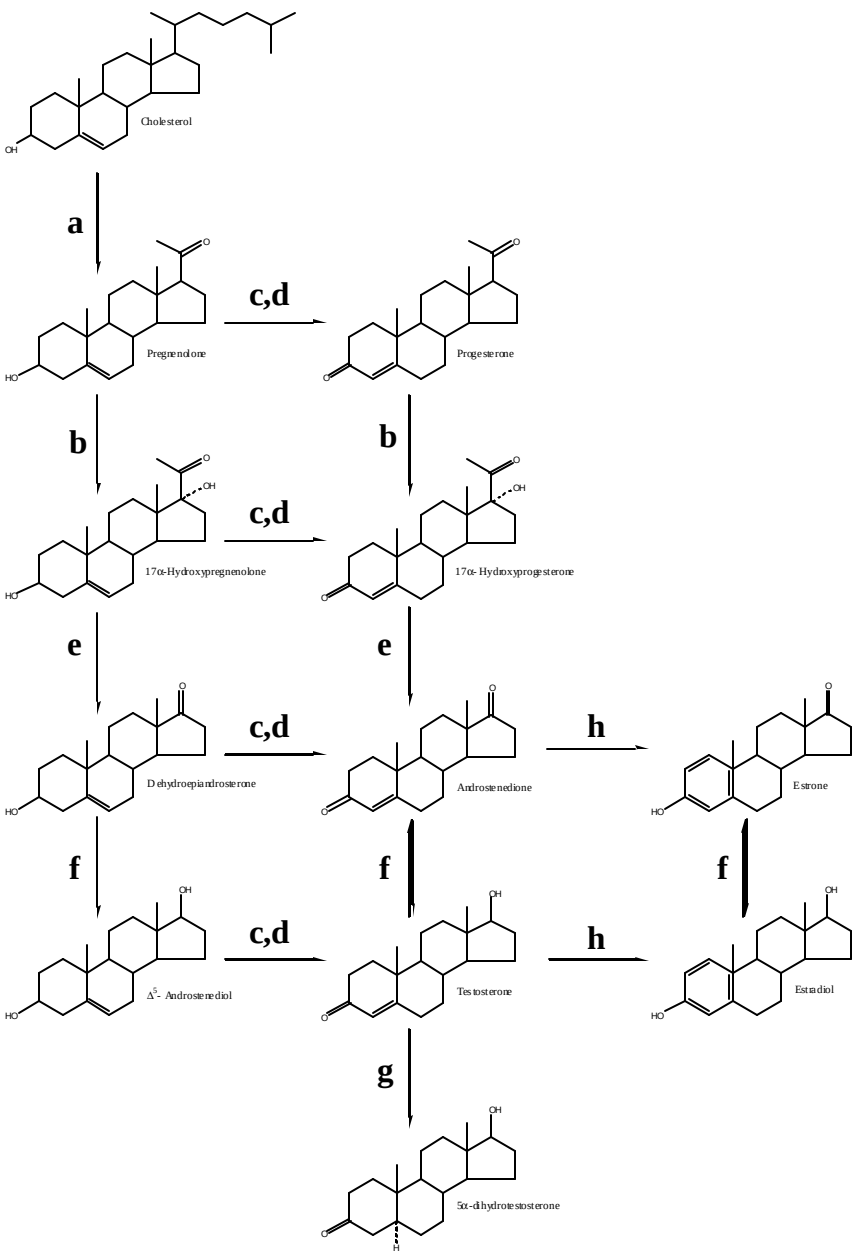

Figure 1.2: Sex steroid biosynthesis pathways. (a) side chain cleavage, (b) 17α-hydroxylase, (c) 3β-hydroxysteroid dehydrogenase, (d) 3-oxosteroid-4,5-isomerase, (e) 17,20-lyase, (f) 17β-hydroxysteroid dehydrogenase, (g) 5α-reductase, and (h) aromatase.

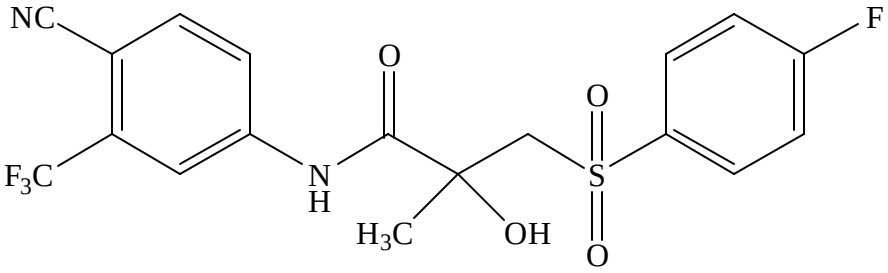

Bicalutamide (Casodex)

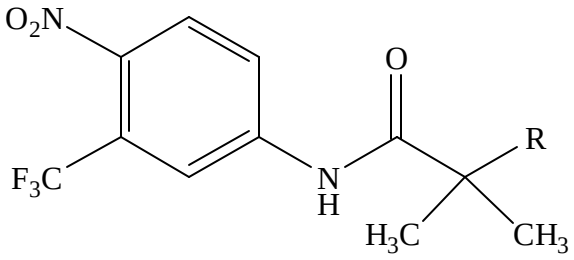

Flutamide (Eulexin) R=H
Hydroxyflutamide R=OH

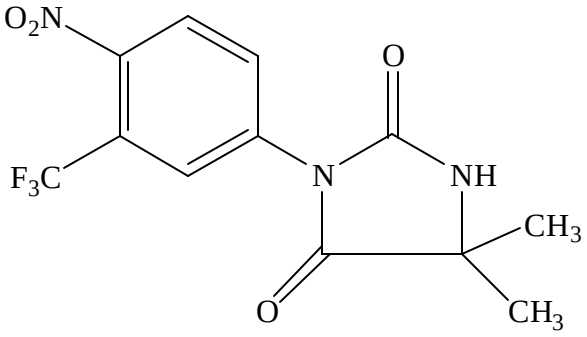

Nilutamide (Anadron)

Figure 1.3: Structures of nonsteroidal antiandrogens.

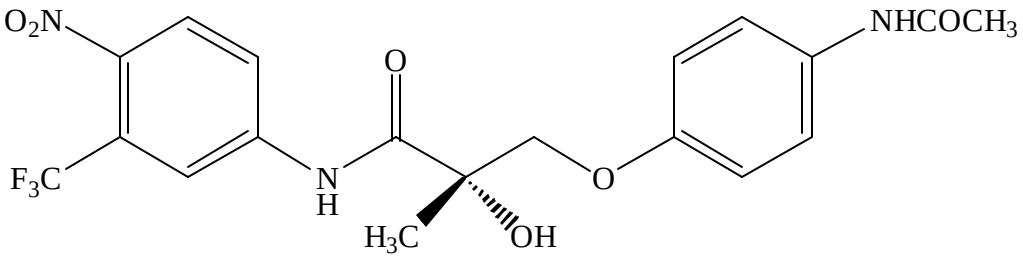

Figure 1.4: Structure of S-3-(4-acetylamino-phenoxy)-2-hydroxy-2-methyl-N-(4-nitro-3-trifluoromethyl-phenyl)-propionamide (S-4).

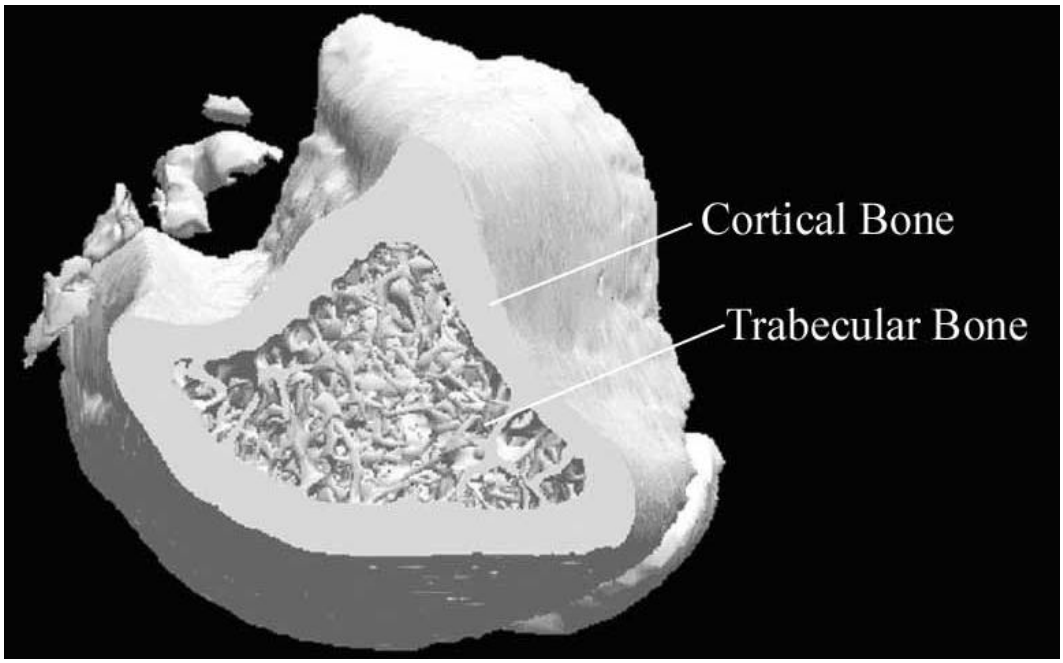

Figure 1.5: Cortical versus trabecular bone. (pQCT image of a proximal rat tibia)

CHAPTER 2

Pharmacokinetics of S-3-(4-acetylamino-phenoxy)-2-hydroxy-2-methyl-N-(4-nitro-3-trifluoromethyl-phenyl)-propionamide in Rats

2.1 Introduction

The effects of androgens are well documented in many different tissues. However, poor pharmacokinetic properties and side effect profiles limit the therapeutic application of testosterone to a small subset of the population. With the discovery of SARMs, it may be possible to overcome some of the pharmacokinetic and side effect problems associated with current androgen formulations [15]. Negro-Vilar [14] defined the ideal anabolic SARM as 'orally active, ideally with a pharmacokinetic profile consistent with once a day administration, with anabolic effects on muscle and bone, but lesser activity in the prostate and seminal vesicles'. An orally active anabolic SARM would be a valuable therapeutic agent for a variety of indications including muscle wasting diseases, male hypogonadism, male fertility, and osteoporosis. Given its

nonsteroidal structure, we hypothesized that S-3-(4-acetylamino-phenoxy)-2-hydroxy-2-methyl-N-(4-nitro-3-trifluoromethyl-phenyl)-propionamide (hereafter referred to as, S-4, to coincide with previously published research) would be rapidly and completely absorbed after oral administration and avoid some of the historical drawbacks of testosterone administration. In our previous pharmacodynamic studies, S-4 was administered via subcutaneous osmotic pumps [19]. Therefore, the purpose of the current studies was to test our hypothesis that the nonsteroidal structure of S-4 would result in decreased hepatic metabolism and increased oral bioavailability as compared to testosterone and identify it as the first of a series of orally active and tissue-selective anabolic agents. To this end, we examined the pharmacokinetics and oral bioavailability of S-4 in rats as a means to further demonstrate the promising preclinical properties of a representative SARM.

2.2 Materials and Methods

2.2.1 Animals

The Institutional Laboratory Animal Care and Use Committee (ILACUC) of The Ohio State University approved this study. Thirty-five male Sprague Dawley® rats weighing approximately 250 g were purchased from Harlan (Indianapolis, IN). Eighteen hours prior to dosing, a catheter was implanted in the right jugular vein of each animal, and food (Harlan Teklad 22/5 rodent diet, Harlan, Indianapolis, IN) was removed. The

animals were provided water *ad libitum* and weighed immediately prior to dose administration. Food was returned twelve hours after dosing.

2.2.2 Chemicals and Formulations

S-4 was synthesized using previously described methods [107]. Chemical purity was confirmed using elemental analysis, mass spectrometry, and proton NMR. Dosing solutions were prepared immediately prior to administration and consisted of a cosolvent mixture of polyethylene glycol-300 (Sigma Chemical Company, St. Louis, MO, Lot 30K0174) and ethanol (Pharmco Products Inc., Brookfield, CT, Lot T022001).

2.2.3 Study Design

Animals were randomized into seven groups, with five animals per group. Intravenous (i.v.) doses (0.5, 1, 10, and 30 mg kg^{-1}) were administered via the jugular vein catheter. Dosing solutions were prepared at an appropriate concentration to deliver the dose in a final volume of 0.2 to 0.3 ml. A 1 ml syringe graduated to 0.1 ml was used to volumetrically deliver the dose. After dose administration, the catheters were flushed with an aliquot (three times the volume of the administered dose) of sterile heparinized saline. Oral (p.o.) doses (1, 10, and 30 mg kg^{-1}) were introduced directly into the stomach via oral gavage in a volume of 0.2 to 0.3 ml. These doses were chosen to

represent the range of S-4 doses used during preclinical pharmacology, safety, and toxicology studies.

2.2.4 Sample Collection and Preparation

Blood samples (~250 µl each) were withdrawn from the jugular vein catheter prior to each dose and at 5, 10, 20, 30, 60, 120, 240, 480, 720, and 1440 min after i.v. doses of 0.5, 1, and 10 mg kg^{-1}, and prior to and at 30, 60, 90, 180, 240, 360, 480, 720, 1440, and 2160 min after dose administration for the 1 and 10 mg kg^{-1} p.o. doses. For the 30 mg/kg i.v. and p.o. dose groups, blood samples were drawn immediately prior to and at 20, 40, 60, 90, 120, 240, 360, 480, 720, and 1440 min after dose administration. A volume of heparinized saline (100 units/ml) equal to the volume of blood removed was infused following each blood draw. Blood samples were collected into 1.5 ml heparinized microcentrifuge tubes and placed on ice until plasma was separated by centrifugation at 800 g for 10 min at 4ºC. Plasma samples were stored at –20 ºC until analysis. Metabolic cages were used to collect urine samples from the high dose group over the 0-24 hr and 24-48 hr time periods following administration of each dose.

2.2.5 Plasma Extraction for HPLC

S-4 was extracted from plasma using a liquid/liquid extraction method. Aliquots of plasma (100 µl) were spiked with internal standard (2-ethyl-2-hydroxy-N-(4-nitro-3-

trifluoromethyl-phenyl)-butyramide, MW 320, a structural analog of S-4) and vortexed briefly. Plasma proteins were precipitated by the addition of acetonitrile (500 µl) and separated from the solution by centrifuging at 9300g for 2 min. The supernatant was aspirated into 12 ml glass extraction tubes and 1.0 ml of phosphate buffered saline (pH 7.4) and 7.0 ml of ethyl acetate were added. Extraction tubes were shaken horizontally at 180 oscillations per min for 40 min on an Eberbach (Ann Arbor, MI) reciprocating shaker. The mixture was then centrifuged at 1540 g for 10 min to facilitate phase separation. The organic phase was removed, placed in a glass centrifuge tube, and evaporated to dryness under nitrogen. The residue was reconstituted in 150 µl of mobile phase, centrifuged at 9300 g for 2 min to separate any residual particulate matter, and 100 µl was injected into the HPLC.

2.2.6 HPLC Plasma Analysis

Plasma concentrations for the 10 mg kg^{-1} i.v. dose group and the 30 mg kg^{-1} i.v and p.o. dose groups were determined using a validated HPLC method. HPLC analysis was performed on a Waters Chromatographic System consisting of a model 510 pump, Nova-Pak® C18 3.9mm x 150mm x 4µm column, model 717 autosampler, and a model 486 UV detector (Waters Corporation, Milford, MA). The mobile phase consisted of acetonitrile:water (40:60) with 30 mM ammonium acetate at a flow rate of 1 ml min^{-1}. The eluent was monitored for UV absorbance at 270 nm. Standard curves were linear (R^2 = 0.989) over the concentration range 1 to 150 µg ml^{-1}, and all quality control standards predicted values were within 85-115% of the actual concentration. Intra- and

inter-day variability was less than 14.9% and 8.2%, respectively, at the lower limit of quantitation.

2.2.7 HPLC/MS Plasma and Urine Analysis

Plasma concentrations for the 0.5 and 1 mg kg^{-1} i.v. dose and 1 and 10 mg kg^{-1} p.o. dose were determined using a validated HPLC/MS method. S-4 was extracted from plasma aliquots using a liquid/liquid extraction method. Aliquots of plasma (100 µl) were spiked with internal standard (deuterated compound S-4, MW 444) and vortexed briefly. Plasma proteins were precipitated by the addition of acetonitrile (500 µl) and separated from the solution by centrifuging at 16,100 g for 30 min. The supernatant was aspirated into 1.5 ml Eppendorf® tubes and evaporated to dryness under nitrogen. The residue was reconstituted in 150 µl of mobile phase, centrifuged at 16,100 g for 5 min to separate any residual particulate matter, and 20 ml was injected into the HPLC/MS system column. HPLC analysis was performed on an Agilent 1100 Series System (binary pump, G1312A; degasser, G1379A; autosampler, G1367A; autosampler thermostat, G1330B; thermostatted column compartment, G1316A; Palo Alto, CA) with a 2.1 x 50 mm, 5 µm particle size, Zorbax® SB-phenyl column (Agilent, Palo Alto, CA). The mass spectrometer was a single quadrupole mass selective detector (Agilent SL G1946D). LC/MS analyses were performed using an electrospray ionization source and the following conditions: negative single ion mode; dry gas flow 10 l min^{-1}; capillary voltage 2500 V; nebulizer pressure 25 psig; drying gas temperature 350 °C; fragmentor voltage 174 V; peak width 0.15 min; time filter on; run time 12.3 min; post run time 6

min; column temperature 28 °C; and a flow rate of 0.15 ml min^{-1}. A gradient mobile phase consisting of two solutions was used. Solution A was an aqueous solution containing 5% acetonitrile, 10 mM ammonium formate, and 0.1% formic acid. Solution B contained 95% acetonitrile, 5% water, 10 mM ammonium formate, and 0.1% formic acid. The percentage of solution B in the mobile phase increased linearly from 40 to 100% during the first six minutes of each chromatographic run, was maintained at 100% from 6 to 12.0 minutes, and then decreased linearly to 40% at 12.2 minutes for the remainder of the run. S-4 was identified as the ion with 440.3 m/z while the deuterated compound S-4 was identified as the ion with 443.3 m/z. Data acquisition was performed with Agilent® ChemStation Software (Version A.08.04). Standard curves for plasma were linear (R^2 = 0.984) over the concentration range 0.005 to 0.050 µg ml^{-1}, and all quality control standards predicted values were within 85-115% of the actual concentration. Rat urine samples were centrifuged at 800 g for ten minutes to separate particulates, and then filtered through a 0.22 µm syringe filter. Filtered rat urine samples were diluted 200 times with HPLC grade water and a 15 µl aliquot was injected into the LC/MS. The HPLC separation and MS operating conditions for the urine samples were identical to those used for plasma analysis. Standard curves for urine specimens were linear over the range of 0.005 to 0.5 µg/ml. Intra- and inter-day variability was less than 12% and 11%, respectively, at the lower limit of quantitation for these assays.

2.2.8 Pharmacokinetic Data Analysis

The plasma concentration-time data were analyzed by noncompartmental methods using WinNonlin® (version 3.1, Pharsight Corporation, Mountain View, CA). The area under the plasma concentration-time curve from time zero to infinity (AUC) was calculated by the trapezoidal rule with extrapolation to time infinity. The terminal half-life ($T_{1/2}$) was calculated as 0.693 $?_z^{-1}$, where $?_z$ was the terminal phase rate constant. The plasma clearance (CL) was calculated as $CL = Dose_{iv}\ AUC_{iv}^{-1}$, where $Dose_{iv}$ and AUC_{iv} were the intravenous dose and the corresponding area under the curve from time 0 to infinity, respectively. The maximal plasma concentration (C_{max}) and the time at which it occurred (T_{max}) for the p.o. doses were determined by visual inspection of the concentration time-profiles. The apparent volume of distribution at equilibrium (V_{ss}) was calculated as:

$$V_{ss} = Dose\ AUMC_{0-\infty}\ (AUC_{0-\infty})^{-2}$$

where $AUMC_{0-\infty}$ was the area under the first moment of the plasma concentration-time curve extrapolated to infinity. The mean residence time (MRT) was calculated as:

$$MRT = AUMC_{0-\infty}\ (AUC_{0-\infty})^{-1}$$

Oral bioavailability (F) for each dose was calculated as:

$$F = AUC_{po}\ \ Dose_{iv}\ \ (AUC_{iv}\ Dose_{po})^{-1}$$

where $Dose_{po}$, $Dose_{iv}$, AUC_{iv}, and AUC_{po} were the mean p.o., mean i.v. dose, and the corresponding mean areas under the curve from time 0 to infinity, respectively.

2.2.9 Statistical Analysis

Statistical analyses were performed by single factor analysis of variance (ANOVA). P-values of less than 0.05 were considered as statistically significant differences. Pharmacokinetic parameters are presented as mean ± S.E.M.

2.3 Results

2.3.1 Pharmacokinetics of S-4 After I.V. Doses

S-4 achieved average maximal plasma concentrations of 1.6, 2.3, 28, and 168 µg ml^{-1} following i.v. doses of 0.5, 1, 10, and 30 mg kg^{-1}, respectively (Figure 2.1). The average steady state volume of distribution for S-4 (0.45 L kg^{-1}) was slightly less than total body water (0.67 L kg^{-1}) [108]. CL remained relatively constant for the 0.5, 1 mg kg^{-1}, and 10 mg kg^{-1} doses at 1.92, 2.12, and 1.52 ml min^{-1} kg^{-1}, respectively. However, the CL of S-4 was lower (1.00 ml min^{-1} kg^{-1}, $p<0.05$) at the 30 mg kg^{-1} dose. Accordingly, the area under the plasma concentration time curve increased proportionally

with dose up to the 10 mg kg^{-1} dose, (Table 2.1). However, at an i.v. dose of 30 mg kg^{-1}, the AUC increased disproportionately to 29 mg min ml^{-1}. Urinary excretion data showed that less than 0.15% of the drug was excreted unchanged, indicating that renal elimination of S-4 as unchanged drug was negligible. The $T_{1/2}$ of S-4 was 154, 182, 223, and 316 min after doses of 0.5, 1, 10, and 30 mg kg^{-1}, respectively. MRT increased from 222 and 240 min at the 0.5 and 1 mg kg^{-1} doses to 305 and 423 min following the 10 and 30 mg kg^{-1} doses, respectively, due to the decrease in clearance. Pharmacokinetic parameters for the intravenous doses are summarized in Table 2.1.

2.3.2 Pharmacokinetics of S-4 After P.O. Doses

S-4 achieved average maximal plasma concentrations of 1.4, 11, and 20 µg ml^{-1} following p.o. doses of 1, 10, and 30 mg kg^{-1}, respectively (Figure 2.2). The time to reach the maximal plasma concentration (T_{max}) was 48, 84, and 336 min for the 1, 10, and 30 mg kg^{-1} doses, respectively. S-4 was completely bioavailable for the 1 and 10 mg kg^{-1} doses. However, following the 30 mg kg^{-1} dose, the bioavailability of S-4 decreased to 57%. The $T_{1/2}$ of S-4 was 203, 173, and 266 min after doses of 1, 10, and 30 mg kg^{-1}, respectively. Pharmacokinetic parameters for the p.o. doses are summarized in Table 2.2.

2.4 Discussion

Analysis of variance showed no significant difference in the CL of S-4 at doses of 0.5, 1, and 10 mg kg^{-1}, ($P>0.05$). Previous *in vivo* studies in our laboratory showed that the dose required to restore the levator ani muscle weight in castrated animals, an indicator of anabolic activity, to that of intact animals was less than 4 mg kg^{-1} day^{-1}[19]. Thus, S-4 demonstrates linear pharmacokinetics within the dose range needed to exert maximal pharmacologic effects.

The lack of parent drug in the urine suggests that S-4 was extensively metabolized. Assuming a hepatic blood flow of 13.8 ml min^{-1} in the rat [108] and that S-4 is exclusively eliminated by hepatic metabolism, the hepatic extraction ratio of S-4 would be less than 0.05. Based on this hepatic extraction ratio we predicted greater than 95% bioavailability (i.e., less than 5% of the drug would be removed by first pass metabolism). Our results confirmed this prediction, as S-4 was completely bioavailable following pharmacologically relevant doses (i.e., doses = 10 mg kg^{-1}).

Although S-4 is structurally similar to bicalutamide, a clinically used antiandrogen, its total body CL was quite different. In rats, bicalutamide is eliminated with a half-life of 17 to 21 h [109]. S-4 is cleared much more rapidly with an average half-life of about 4 h. The oral bioavailability of bicalutamide (61%) following a 25 mg kg^{-1} oral dose [109] is nearly identical to the oral bioavailability of S-4 (57%) following the 30 mg kg^{-1} dose. Like bicalutamide, a very small percentage (0.15%) of S-4 is excreted unchanged in the urine. As a whole, these data suggest that the primary difference in pharmacokinetic parameters for S-4 and bicalutamide is a result of

differences in metabolism and not other factors such as drug absorption, distribution, or renal excretion.

The observed decrease in oral bioavailability and the prolonged time to peak plasma concentration observed after 30 mg kg^{-1} oral doses of S-4 were most likely due to the poor aqueous solubility of the compound (about 80 µg ml^{-1}). Similar behavior was noted for bicalutamide during preclinical pharmacokinetic studies [109]. Decreased oral bioavailability at higher doses may serve as a protective mechanism given the potential for abuse of an anabolic drug such as S-4. However, it is important to note that S-4 demonstrated high oral bioavailability and a short time to peak plasma concentration at doses capable of eliciting maximal pharmacologic effect [19].

A similar trend was observed in half-life following i.v. administration. As the dose was increased, the $?_z$ value decreased ($P<0.001$) and the half-life of S-4 increased ($P<0.01$). This observation also supports the conclusion that the CL of the drug was diminished at the highest doses. The CL of S-4 at a dose of 0.5 mg kg^{-1} (1.92 ml min^{-1} kg^{-1}) was significantly ($P<0.001$) greater than that observed for the 30 mg kg^{-1} dose (1.00 ml min^{-1} kg^{-1}). These data suggest that saturation of the drug metabolizing enzymes may be occurring at this higher dose. Therefore, we would expect to see further suppression of CL following doses greater than 30 mg kg^{-1}. However, due to the potency of S-4, we do not anticipate the need for such high doses during clinical usage. Forthcoming data from our laboratory will provide needed information regarding the hepatic metabolism and pharmacokinetics of S-4 in this and other species.

The pharmacologic activity and pharmacokinetics of S-4 in rats suggest that this compound has the properties of an ideal SARM as defined by Negro-Vilar [14]. It is

rapidly absorbed following oral doses (T_{max}, 48 - 84 minutes), and it exerts tissue-specific anabolic effects *in vivo*, with anabolic effects in muscle and bone but lesser effects in the prostate and seminal vesicles [19, 110]. S-4 and testosterone have similar binding affinities 4.0±0.7 and 1.1±0.2 nM respectively [19, 111], log P values of 4.4±0.6 and 3.5±0.3 respectively (data not published), and similar anabolic potency and efficacy [19], however, the metabolic clearance of S-4 and testosterone are markedly different, ~2.1 ml min^{-1} kg^{-1} and ~181 ml min^{-1} kg^{-1} [112] respectively. These data support our hypothesis since the nonsteroidal structure of S-4 resulted in decreased metabolic clearance and enhanced oral bioavailability compared to testosterone. These properties, coupled with forthcoming reports from our laboratory regarding the pharmacologic effects of S-4 in other pertinent animal models and its pharmacokinetics and metabolism in dogs and humans, favor the continued development of S-4 as an orally bioavailable nonsteroidal SARM.

2.5 Acknowledgments

I would like to thank Dr. Di Wu for the development and validation of the analytical methods as well as the sample analysis, Ms. Wenqing Gao for her assistance with the animals and valuable discussions, Dr. Duane Miller's group for synthesis of S-4, and Ms. Huiping Xu and Dr. James Dalton for their valuable discussions and manuscript review. This chapter was originally published in *Xenobiotica*, 2004. 34(3): p. 273-280.

Parameter	I.V. Dose			
	0.5 mg kg^{-1}	**1 mg kg^{-1}**	**10 mg kg^{-1}**	**30 mg kg^{-1}**
CL (mL min^{-1} kg^{-1})	1.92 ± 0.20	2.12 ± 0.07	1.52 ± 0.12	1.00 ± 0.08
Vss (L kg^{-1})	0.42 ± 0.06	0.48 ± 0.08	0.44 ± 0.04	0.42 ± 0.14
l_z **(min^{-1})**	0.0045 ± 0.00046	0.0038 ± 0.00077	0.0031 ± 0.00044	0.0022 ± 0.0008
MRT (min)	222 ± 43	240 ± 45	305 ± 32	423 ± 158
AUC (mg min mL^{-1})	0.24 ± 0.03	0.46 ± 0.16	6.0 ± 0.5	28 ± 3

Table 2.1: Pharmacokinetics of S-4 in rats after IV administration. Data presented as Mean ± S.E.M. Individual pharmacokinetic data for each animal are presented in Tables A.8, A.9, A.10, and A.11 of Appendix A.

Parameter	P.O. Dose		
	1 mg kg^{-1}	**10 mg kg^{-1}**	**30 mg kg^{-1}**
l_z **(min^{-1})**	0.0034 ± 0.00032	0.004 ± 0.0004	0.0026 ± 0.00021
C_{max} (µg ml^{-1})	1.39 ± 0.49	11.32 ± 3.7	20 ± 11
T_{max} (min)	48 ± 16	84 ± 61.5	336 ± 156
AUC (mg min mL^{-1})	0.55 ± 0.08	6.0 ± 1.6	16 ± 6
F (%)	120	100	57

Table 2.2: Pharmacokinetics of S-4 in rats after oral administration. Data presented as Mean ± S.E.M. Individual pharmacokinetic data for each animal are presented in Tables A.12, A.13, and A.14 of Appendix A.

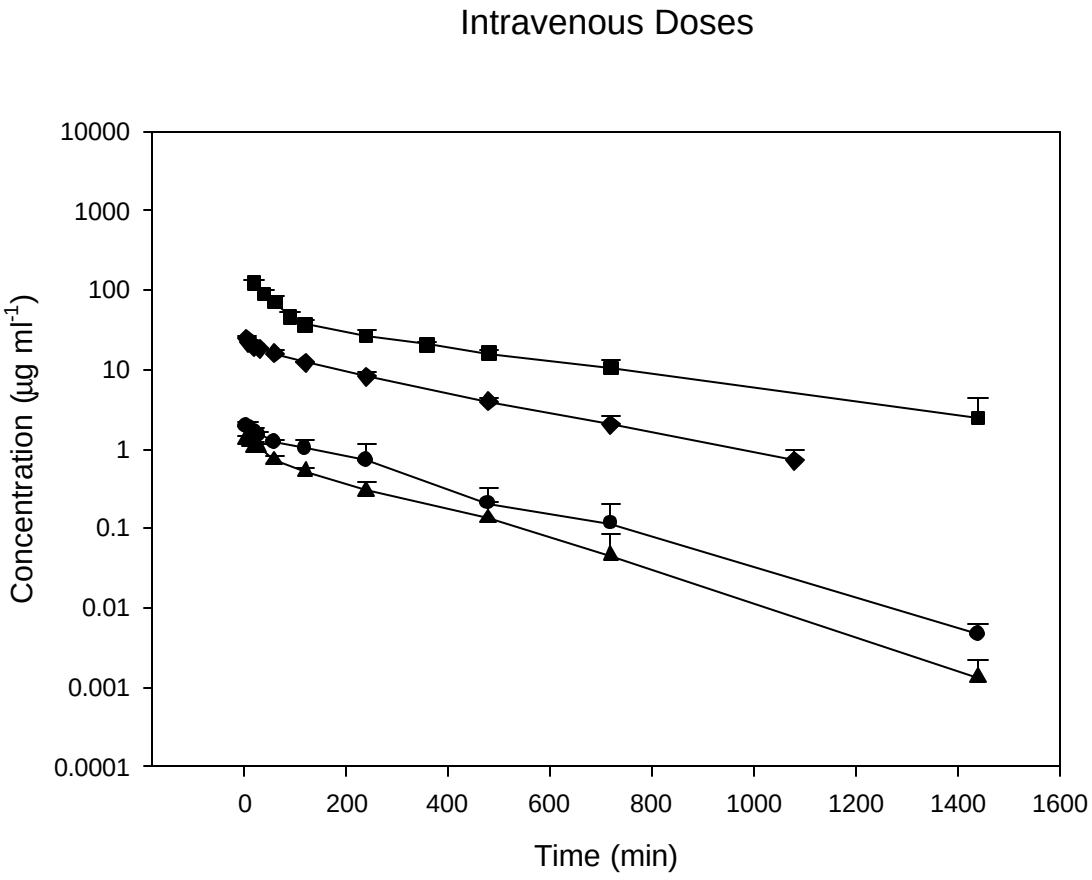

Figure 2.1: Mean plasma concentration-time profiles following intravenous doses of S-4 in male rats. Square: 30 mg kg^{-1}; Diamonds: 10 mg kg^{-1}; Circle 1 mg kg^{-1}; and Triangle: 0.5 mg kg^{-1}. Data are presented as mean ± S.D., for n=5 in each group. Individual plasma concentration-time data for each animal are presented in Tables A.1, A.2, A.3, and A.4 of Appendix A.

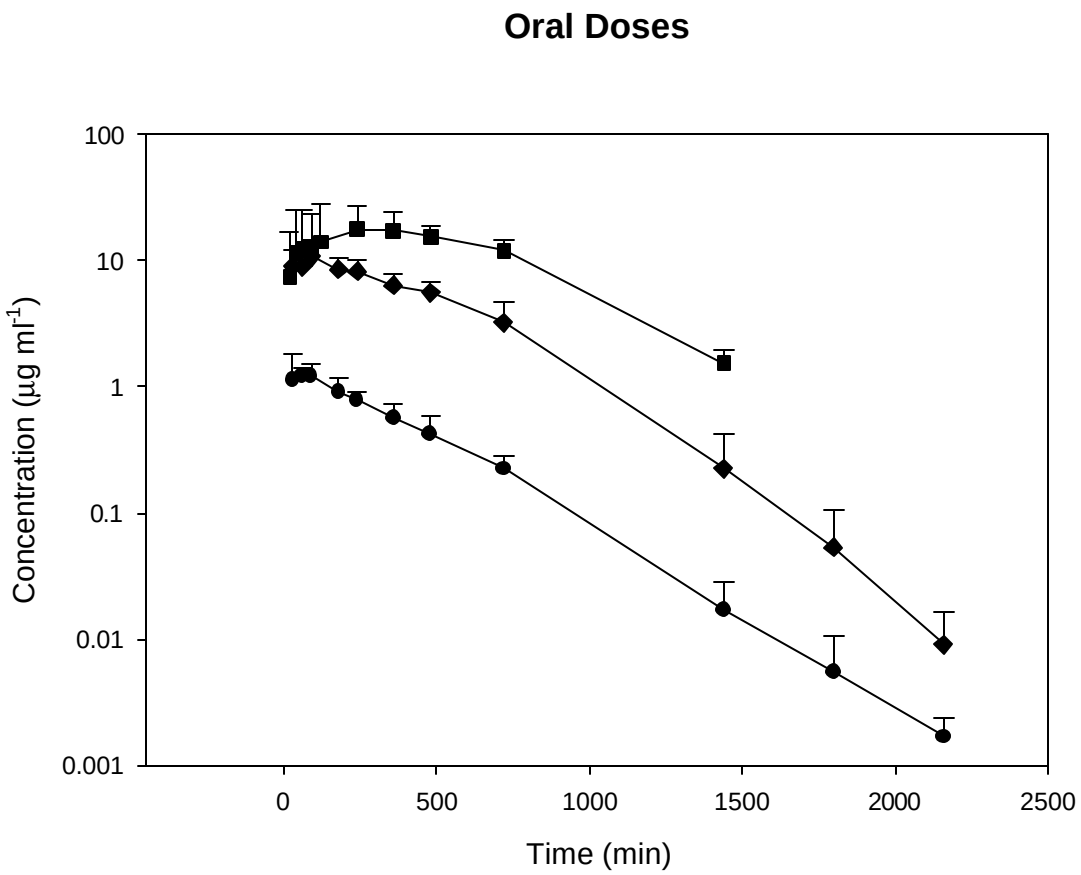

Figure 2.2: Mean plasma concentration-time profiles following oral doses of S-4 in male rats. Square: 30 mg kg^{-1}; Diamonds: 10 mg kg^{-1}; and Circle 1 mg kg^{-1}. Data are presented as mean ± S.D., for n=5 in each group. Individual plasma concentration-time data for each animal are presented in Tables A.5, A.6, and A.7 of Appendix A.

CHAPTER 3

Protective Effects of S-3-(4-acetylamino-phenoxy)-2-hydroxy-2-methyl-N-(4-nitro-3-trifluoromethyl-phenyl)-propionamide on the Skeleton of Ovariectomized Rats

3.1 Introduction

Clearly, both androgens and estrogens mediate bone turnover. However, the relative contributions of androgenic versus estrogenic effects are not well defined. Cross reactivity with the estrogen receptor (ER) and peripheral conversion of endogenous androgens to estradiol have complicated the delineation of pure androgenic effects in bone. For this reason, the mechanism by which androgens exert their effect in bone is poorly understood even though the protective skeletal effects of androgens are well documented [71, 113, 114, 115, 116]. The use of androgens as a therapeutic intervention for osteoporosis has been limited due to the side effects, lack of convenient dosage formulations, and the conversion of androgens to estrogens in peripheral tissues. Selective androgen receptor modulators (SARMs) offer a unique mechanism to study androgen effects in bone. S-4, a model SARM, shows no cross-reactivity with the other

steroid hormone receptors [17] and is not a substrate for aromatase. Additionally, S-4 has a high affinity for the AR, exhibits tissue selective anabolic action [19], and is orally bioavailable [117]. We hypothesized that a nonsteroidal selective androgen receptor modulator would reduce bone loss. Therefore, we chose to evaluate the protective skeletal effects of S-4 in an animal model of accelerated bone loss to more precisely define the role of androgens in bone homeostasis.

3.2 Materials and Methods

3.2.1 Animals

One hundred twenty female Sprague-Dawley rats were purchased from Harlan (Indianapolis, IN). The animals were housed with three animals per cage and were allowed free access to tap water and commercial rat chow (Harlan Teklad 22/5 rodent diet - 8640). During the course of the study, the animals were maintained on a 12 hr light:dark cycle. This study was reviewed and approved by the Institutional Laboratory Care and Use Committee of The Ohio State University. At 23 weeks of age, the animals were ovariectomized (OVX) or sham-operated and then assigned to one of 12 treatment groups (Table 3.1) of 10 animals as follows: (1) OVX+S-4 (0.1 mg/day); (2) OVX+S-4 (0.3 mg/day); (3) OVX+S-4 (0.5 mg/day); (4) OVX+S-4 (0.75 mg/day); (5) OVX+S-4 (1.0 mg/day); (6) OVX+S-4 (3.0 mg/day); (7) OVX+DHT (1 mg/day); (8) OVX+S-4+Antiandrogen (0.5 + 1.0 mg/day); (9) OVX+Vehicle; (10) intact+S-4 (1 mg/day); (11) intact+DHT (1mg/day); (12) intact+Vehicle. The doses of S-4 were chosen based on a

pilot study and prior pharmacodynamic studies performed in our laboratory [19]. Since DHT cannot be aromatized to estradiol, DHT treatment was included in both intact and ovariectomized animals to serve as a positive control group to evaluate the skeletal effects of a pure androgen. Intact and ovariectomized animals receiving vehicle alone served as negative controls. Another control group received an antiandrogen along with S-4 in an effort to delineate the AR-mediated versus AR-independent effects of S-4. During the course of the study, five animals died from non-drug related causes. Therefore, groups 1, 6, and 10 were composed of nine animals each and group 4 was composed of eight animals. Dosing solutions were prepared daily by dissolving drug in dimethyl sulfoxide (DMSO) and diluting in polyethylene glycol 300 (PEG 300). All doses were administered for 120 days via daily subcutaneous injections in a volume of 0.20 ml.

3.2.2 Whole Body DEXA Analysis

Total body bone mineral density (BMD), percent fat mass (FM), body weight (BW), bone mineral content (BMC), bone mineral area (BMA), and lean mass (LM) were determined by dual energy x-ray absorptiometry (DEXA) (GE, Lunar Prodigy™) using the small animal software (Lunar enCORE, version 6.60.041) on days 0 and 120. Animal BW was also determined by standard gravimetric methods using a 700 series Ohaus triple beam animal balance (Florham Park, NJ). For scanning, the animals were anesthetized with ketamine:xylazine (87:13 mg/kg) and positioned in a prone position as demonstrated in Figure 3.1. Total body data was obtained by selecting an area encompassing the

entire animal as the region of interest during data processing. The parameters determined to be the most sensitive to estrogen withdrawal (i.e., largest differences between intact and OVX control groups) were used and reported herein in order to focus our analyses on the most hormone-sensitive measures with a larger dynamic range.

3.2.3 *Ex Vivo* DEXA Analysis

Immediately following the whole body DEXA scan on day 120, groups 1 through 11 were sacrificed, and the lumbar vertebra, femurs, and tibia were excised and cleared of soft tissue. Group 12 was sacrificed at day 210. The excised bones were scanned through a 3-inch deep room temperature water bath to simulate soft tissue. The proximal femur, distal femur, proximal tibia, L2-L4 vertebra, and L5-L6 vertebra were selected as regions of interest from the DEXA scan and analyzed for BMD. Femoral images were also subdivided into ten equal regions of interest, as shown in Figure 3.2, from proximal (region 1) to distal (region 10), and the BMD of each region was determined by the Lunar enCORE small animal software. We observed the greatest difference in BMD between the intact and OVX groups in femoral region 4. Therefore, femoral analysis between all groups was performed in region 4.

3.2.4 Femoral pQCT Analysis and Biomechanical Testing

The right femurs from the OVX + 1.0 mg/day S-4 (Group 5), OVX + 3.0 mg/day S-4 (Group 6), OVX + 1.0 mg/day DHT (Group 7), OVX control (Group 9), intact + 1

mg/day S-4 (Group 10), and intact control (Group 12) were sent to Skeletech, Inc. (Bothell, WA) for peripheral quantitative computed tomography (pQCT) analysis and biomechanical testing. The femur was subjected to pQCT scanning using a Stratec XCT RM and associated software (Stratec Medizintechnik GmbH, Pforzheim, Germany. Software version 5.40 C). The femur was analyzed at both the mid-shaft and distal regions. The length of the femur was determined using scout scan views, and the mid-shaft region was chosen at 50% of the length of the femur. The distal region was chosen at 20% of the length of the femur starting at the distal end. One 0.5 mm slice perpendicular to the long axis of the femur was used for analysis. Total bone mineral content, total bone area, total bone mineral density, cortical bone mineral content, cortical bone area, cortical bone mineral density, cortical thickness, periosteal perimeter (circumference) and endosteal perimeter were determined at the mid-shaft of the femur. At the distal femur total bone mineral content, total bone area, total bone mineral density, trabecular bone mineral content, trabecular bone area and trabecular bone mineral density were determined. After pQCT analysis, the de-fleshed whole femur was used in the three-point bending test. The anterior to posterior diameter (APD) (unit:mm) at the midpoint of the femoral shaft was measured with an electronic caliper. The femur was placed on the lower supports of a three-point bending fixture with the anterior side of the femur facing downward in an Instron Mechanical Testing Machine (Instron 4465 retrofitted to 5500)(Canton, MA). The length (L) between the lower supports was set to 14 mm. The upper loading device was aligned to the center of the femoral shaft. The load was applied at a constant displacement rate of 6 mm/min until the femur broke. The mechanical testing machine directly measured the maximum load (F_u) (unit:N), stiffness

(S) (units:N/mm), and energy absorbed (W) (unit:mJ). The axial area moment of inertia (I) (unit:mm^4) was calculated by the software during the pQCT analysis of the femoral mid-shaft. Stress (σ) (units:N/mm^2), elastic modulus (E) (unit:Mpa), and toughness (T) (units:mJ/m^3) were calculated by the following formulas: stress: $\sigma = (F_u * L *(a/2)) / (4* I)$; elastic modulus: $E = S*L^3/(48*I)$; and toughness: $T = 3*W*(APD/2)^2/(L*I)$. The parameters determined to be the most sensitive to estrogen withdrawal are reported herein.

3.2.5 Vertebral Biomechanical Testing

The L5 vertebra from the OVX + 1.0 mg/day S-4 (Group 5), OVX + 3.0 mg/day S-4 (Group 6), OVX + 1.0 mg/day DHT (Group 7), OVX control (Group 9), intact + 1 mg/day S-4 (Group 10), and intact control (Group 12) were sent to Skeletech, Inc. (Bothell, WA) for biomechanical testing of vertebral crush strength. The posterior pedicle arch, spinous process, cranial end, and caudal end were removed from each vertebra using a low-speed diamond saw in order to obtain a vertebral body specimen with two parallel surfaces. Widths in the medial-lateral (MLD) (unit:mm) and anterior-posterior directions (APD) (unit:mm) were measured with digital calipers at both the cranial and caudal ends. The average MLD and APD values from the cranial and caudal measurements were used to calculate cross-sectional area. The height (H) (unit:mm)of the vertebral body specimen was determined with digital calipers. The core vertebra sample was placed between two platens and loaded at a constant displacement rate of 6 mm/min until failure in an Instron Mechanical Testing Machine (Instron 4465 retrofitted

to 5500). The mechanical testing machine directly measured the maximum load (F_u) (unit:N), stiffness (S) (units:N/mm), and energy absorbed (W) (unit:mJ). Stress (σ) (units:N/mm^2), elastic modulus (E) (unit:Mpa), toughness (T) (units:mJ/m^3), and cross-sectional area (CSA) were calculated by the following formulas: stress: $\sigma = F_u/(CSA)$; elastic modulus: $E = S/(CSA/ H)$; cross-sectional area: $CSA = \pi * (APD)*(MLD)/4$; and toughness: $T = W/(CSA * H)$. The parameters determined to be the most sensitive to estrogen withdrawal are reported herein.

3.2.6 Urine and Serum Markers

Five days prior to sacrifice, five animals per group were placed in metabolism cages overnight (15 h) for urine collection. Food was removed 8 h prior to and during urine collection. Samples were stored at -20°C until analysis. Urine levels of deoxypyridinoline (DPD) were analyzed by METRA™ DPD enzyme-linked immunosorbent assay (ELISA) kit (catalog number: 8007, Quidel® Corporation, San Diego,CA) according to the manufacturer's instructions. DPD levels were normalized for urine creatinine levels measured by METRA ™ Creatinine Assay kit (catalog number: 8009, Quidel® Corportation) according to the manufacturer's instructions. Blood samples taken at the time of sacrifice were allowed to clot at room temperature and serum was separated by centrifugation at 800 g for 10 min at 4ºC. Serum samples were stored at -20°C until analysis. Serum concentrations of osteocalcin and IGF-1 were determined using a commercially available rat osteocalcin enzyme immuno assay (EIA) kit (catalog number: BT-490, Biomedical Technologies Inc., Stoughton, MA) and ACTIVE® rat

IGF-1 EIA kit (catalog number: DSL-10-2900, Diagnostic Systems Laboratories, Inc., Webster, TX), respectively, according to the manufacturer's instructions. Urine and serum markers were analyzed in the OVX control (Group 9), OVX + 1.0 mg/day S-4 (Group 5), OVX + 3.0 mg/day S-4 (Group 6), and OVX + 1.0 mg/day DHT (Group 7) only.

3.2.7 Statistical Analysis

Statistical analyses were performed by single factor analysis of variance (ANOVA). P-values of less than 0.05 were considered as statistically significant differences. Raw data is presented in tabular form in Appendix B.

3.3 Results

3.3.1 Whole Body DEXA Analysis

Figure 3.3 shows the BMD for all groups at day 120. As expected, the BMD in OVX animals (0.196 g/cm^2) was significantly less than that observed in intact controls (0.214 g/cm^2) at day 120. S-4 treatment either partially (i.e., BMD significantly greater than OVX controls) or fully (i.e., BMD not significantly different than intact controls) prevented the loss of skeletal BMD in OVX animals at doses greater than 0.1 mg/day.

DHT partially maintained BMD in the OVX animals. However, in intact animals, DHT caused a significant decrease in BMD. S-4 treatment in intact animals maintained BMD at the level of intact controls. Co-administration of bicalutamide, a pure antiandrogen, partially prevented the effects of S-4 suggesting that the AR was important for regulating the bone response to the drug.

The average body weight for all groups at the beginning of the study was 267 ± 17 g (Mean ± S.D., n = 120). All animals gained a significant amount of weight over the course of the study (Figure 3.4). Body weight was greater in all ovariectomized groups as compared to the intact control, indicating the influence of estrogen-deprivation on animal growth. Additionally, we observed a further increase in body weight for the 3 mg/day S-4 dose group as compared to other groups in the study. In intact animals, DHT treatment resulted in further increases in body weight when compared with intact controls. However, S-4 administration to intact animals resulted a significant decrease in body weight when compared to both OVX and intact controls.

Percent fat mass (FM) at day 120 was measured by DEXA and the results are shown in Figure 3.5. The OVX control group showed a significantly higher FM than that observed in intact controls. We observed a dose-dependent decrease in FM with S-4 therapy, with 3 mg/day S-4 treatment returning FM to the level of intact controls. Co-administration of bicalutamide prevented the decrease in FM observed with S-4 treatment alone. DHT treatment in both intact and OVX animals increased FM to values higher than those observed in intact controls but lower than those observed in OVX controls. Intact animals receiving S-4 showed a decrease in FM compared to intact controls. Corresponding changes in percentage lean mass were observed in all groups.

3.3.2 *Ex Vivo* DEXA Analysis

Figure 3.6 summarizes the results of the DEXA analysis of the excised L5-L6 vertebra. OVX animals receiving vehicle alone lost a significant amount of BMD over the course of the study. We observed a dose-dependent bone-sparing effect with S-4 treatment. The 3 mg/day dose of S-4 completely prevented bone loss caused by OVX. The 0.5 and 1 mg/day doses of S-4 partially prevented the bone loss in the L5-L6 region. We observed positive trends in the data from the 0.1, 0.3, and 0.75 mg/day doses, but statistical significance was not reached. Co-administration of bicalutamide with S-4 partially abolished the effects seen with S-4 alone. DHT treatment in intact animals resulted in a significant decrease in BMD to a level not different from OVX controls. DHT treatment in OVX animals did not prevent bone loss in the L5-L6 vertebra. BMD in intact animals receiving S-4 was not different from intact controls.

Femoral BMD in region 4 was analyzed by DEXA at day 120 and the results are shown in Figure 3.7. Femoral BMD was decreased in animals following ovariectomy. S-4 maintained femoral BMD in a dose-dependent manner. Doses of 0.1, 1, and 3 mg/day S-4 in OVX animals fully prevented the decrease in femoral BMD. BMD in OVX animals treated with DHT was not different from OVX controls. DHT treatment in intact animals caused a non-significant decrease in this parameter. S-4 treatment in intact animals resulted in a decrease in femoral BMD.

3.3.3 Femoral pQCT Analysis and Biomechanical Testing

Cortical thickness (CT) at the femoral mid-shaft was determined by pQCT analysis and the results are presented in Figure 3.8. DHT and S-4 prevented the decrease in CT following OVX. However, CT in S-4 treated groups was greater than that observed with DHT treatment. Additionally, intact animals (1 mg/day) and OVX animals (3 mg/day) receiving S-4 showed significant increases in CT above the level of intact controls.

Cortical content (CC) measured by pQCT at the mid-shaft of the femur is reported in Figure 3.9. We observed a significant loss in CC following OVX, with values of 10.3 and 8.8 mg/mm observed in intact and OVX animals, respectively. DHT only partially prevented the loss in CC. S-4 completely blocked the loss in CC at the femoral mid-shaft following OVX. The 3 mg/day dose of S-4 caused a non-significant increase in CC over intact control levels.

We measured the periosteal circumference (PC) of the femoral mid-shaft by pQCT. The results are presented in Figure 3.10. S-4 treatment in OVX animals completely prevented the decrease in PC observed between intact and OVX control groups. Although CT was increased in intact animals receiving S-4, PC was decreased in these animals. The DHT treated animals were not different from either intact or OVX control animals.

Cortical bone mineral density (CD) of the femoral mid-shaft was measured by pQCT. S-4 completely prevented the loss in CD caused by OVX (Figure 3.11), while

DHT only partially prevented the loss in CD. Intact animals receiving S-4 (1 mg/day) showed an increased CD compared to OVX and intact control animals.

Trabecular BMD was measured by pQCT at the distal femur. Figure 3.12 shows the results from these analyses. Profound trabecular bone loss was evident in the distal femur following OVX, 735 and 609 mg/cm^3 in intact and OVX animals, respectively. S-4 and DHT partially prevented the loss of trabecular bone in the distal femur. Additionally, S-4 treatment in intact animals resulted in an increase of trabecular BMD to a level significantly higher than intact controls, indicating an anabolic action of S-4 in trabecular bone.

Biomechanical strength of the femur was determined by three-point bending analysis. Results from biomechanical strength testing are shown in Figure 3.13. S-4 treatment in OVX animals completely prevented the loss of femoral biomechanical strength that was observed in OVX control animals. DHT also prevented the decrease in femoral biomechanical strength. Intact animals treated with S-4 were not different from intact controls.

3.3.4 Vertebral Biomechanical Testing

Biomechanical strength of the L5 vertebra was determined by vertebral crush testing, and the results are shown in Figure 3.14. We did not observe any differences between intact and OVX vehicle control groups. However, the L5 vertebra in intact animals receiving S-4 (1 mg/day) was significantly stronger than that observed in OVX control animals. OVX animals receiving S-4 (3 mg/day) demonstrated an increase in

biomechanical strength as compared to OVX control animals, but these differences did not reach significance.

3.3.5 Urine and Serum Markers

Urinary levels of DPD were markedly increased following OVX (Figure 3.15). Although the 1 mg/day S-4 dose group showed a further increase in DPD excretion, the 3 mg/day S-4 and DHT dose groups were unchanged when compared to OVX controls.

Osteocalcin was measured in serum samples drawn immediately prior to sacrifice. OVX control animals had higher osteocalcin levels, and drug treatment with S-4 and DHT returned the levels to that observed in intact controls. Results from osteocalcin analysis are presented in Figure 3.16.

We observed an apparent dose-dependent increase in IGF-1 levels with S-4 treatment with significance being reached following the 3 mg/day S-4 treatment (Figure 3.17). However, no significant differences were noted between the intact, OVX, DHT, or 1 mg/day S-4 treated groups.

3.4 Discussion

Previous studies in our laboratory thoroughly characterized the pharmacokinetics [117], anabolic, androgenic, and tissue-selective effects of S-4 in rats [19], as well as, the lack of cross-reactivity with the other steroid hormone receptors *in vitro* [17]. Since androgens are known to exert skeletal effects [11, 31, 47, 52, 54, 55, 57, 58, 59, 61, 65,

68, 70, 72, 74, 75, 76, 83, 86, 87, 89, 90, 91, 92, 95, 96, 104, 118, 119, 120, 121, 122, 123, 124, 125, 126, 127, 128], we hypothesized that a nonsteroidal SARM would reduce bone loss in the ovariectomized rat. To this end, we evaluated the therapeutic potential and efficacy of S-4 in an animal model of post-menopausal bone loss. We chose to investigate the effects of S-4 in the rat model because every clinically used therapy that has been shown to modulate bone loss (e.g., estrogens, bisphosphonates, PTH, etc.) either partially or completely prevented OVX-induced bone loss in this model [41]. Additionally older animals (23 wks) were used to minimize the confounding effects of skeletal growth during the study [129, 130]. Finally, we chose to dose on a mg/day basis rather than a mg/kg basis to simplify dose preparation and minimize animal handling. Further, as observed in DHT-treated intact animals, androgens significantly increase body weight. Therefore, dosing on a mg/kg basis would result in an escalation of the daily dose throughout the study making comparisons between dosing groups more difficult to interpret. In addition, clinically used drugs are not generally given on a mg/kg basis but rather a mg/dosing interval basis. Therefore, we believe that this dosing regimen is more appropriate for this study since the animals in different treatment groups exhibit different changes in body weight over the course of the study, and it is more clinically relevant.

Our studies clearly show that OVX-induced changes in whole body BMD, body weight, percent fat mass, L5-L6 BMD, femoral BMD, femoral CT, femoral CC, femoral PC, trabecular density, biomechanical strength, and biological markers of bone resorption and formation are modulated by a nonsteroidal SARM. We observed positive therapeutic outcomes in nearly all of the parameters that were examined. Taken together, these data

suggest that S-4 could provide a novel pharmacological intervention in the prevention of bone loss in postmenopausal women.

As a whole, most of the parameters we measured appeared to respond in a dose-dependent manner. However, some of the whole body DEXA measurements showed variability between similar doses. The variability could be a result of all doses producing maximal effect in the measured parameter, pharmacokinetic variability, or DEXA variability. However, we did not measure S-4 plasma concentrations or perform more stringent analyses on the excised bones of each group. Therefore, we are unable to speculate as to the contributions of the factors listed above.

We measured serum and urine markers of bone turnover, as a secondary endpoint and to gain insight into the mechanism by which S-4 acts in bone. Some of the results reached statistical significance. However, we observed a great deal of variation in these parameters, and based on our primary endpoints, it is unlikely that these differences were of clinical relevance. The variation in these parameters may have been due to the limited number of animals tested in each group (n=5) or the sensitivity of the assays.

The primary circulating and the most significant biologically active androgen in women is testosterone [131]. However, aromatization to estradiol makes it difficult to delineate the androgenic versus estrogenic action of testosterone. Therefore, we included DHT, which cannot be aromatized, as a positive control group for the AR mediated actions in this model. While DHT partially prevented some of the OVX-induced changes, DHT treatment in intact animals caused some detrimental effects. These effects were most likely due to the ability of DHT to inhibit luteinizing hormone (LH) and follicle stimulating hormone (FSH) release from the pituitary. Therefore, DHT indirectly

inhibited production of ovarian hormones, in effect, pharmacologically ovariectomizing the intact animals. However, we did not measure the estrogen levels in these animals. Other studies in our laboratory have shown that S-4 does not affect LH or FSH levels (data not shown), highlighting an important difference between steroidal AR agonists and S-4.

Our results show that S-4 decreases the percentage of fat mass in OVX animals. Therefore, the percentage of lean body mass is increased in OVX animals. Lean mass is important to fracture risk for two reasons. First, increases in muscle mass are indirectly responsible for increases in BMD [20]. Secondly, increasing muscle mass may improve balance and muscle strength thereby, reducing the risk of falling [132], which is a primary cause of fracture in the elderly. The primary endpoints in this study were focused on BMD and biomechanical strength. However, S-4 may exert additive effects in reducing fracture risk through increasing both BMD and muscle mass. More detailed studies focused on delineating the effects of SARMs on muscle mass and muscle strength are currently underway in our laboratory.

DEXA is currently the "gold-standard" for measuring bone mineral density in human populations [133]. However, there are several factors to consider when utilizing DEXA in small animals. Since DEXA measures an areal bone mineral density, body positioning for small animals, <500 g, is very important (i.e., small changes in bone orientation can affect measured parameters). Additionally, the animals in this study are very close to the limit of quantitation for DEXA, which may increase the variability of the measurements. Therefore, we chose to validate our DEXA results by more rigorous analysis of excised bones using pQCT and biomechanical strength testing. With the

excised bones, we were able to more precisely position the bones and more clearly define regions of interest such as the L5-L6 vertebra. We chose pQCT analysis of select groups because the resolution for pQCT (~70 μm) is approximately two fold greater than that observed with DEXA. Biomechanical testing was employed to verify that the changes in bone parameters measured by DEXA and pQCT were physiologically relevant to bone quality.

We subjected the excised bones to biomechanical strength testing and a more stringent analysis of BMD. These findings further support our hypothesis that SARMs inhibit bone loss. The L5-L6 BMD and the distal femur trabecular BMD data suggest that S-4 is an inhibitor of trabecular bone loss. We showed that the 0.5, 1.0, and 3.0 mg/day doses of S-4 were able to significantly increase BMD in the L5-L6 region and both 1.0 and 3.0 mg/day dose groups exhibited higher BMD in the distal femur. Skeletch Inc. also performed vertebral crush testing of the L5 vertebra. We observed trends in these data indicating beneficial effects of S-4 on vertebral strength (i.e., both the intact group receiving S-4 and the 3.0 mg/day group were higher than intact controls), but the variability of the crush testing obscured significance in these measurements (Figure 3.14). The variability in these measurements was likely caused by the difficulty in obtaining core vertebral samples without cortical bone interference (e.g., the amount of cortical bone included in the core sample may vary). Our data are in agreement with previous studies published by Lea *et al*. [115, 134] and Tobias *et al.* [71], which have shown that androgens reduce cancellous bone loss in OVX rats. Recent studies reported by Hanada *et al*. [70] failed to observe significant anti-resorptive effects in the cancellous bone of the distal femur with S-40503, a tetrahydroquinolin-based SARM. Differences in

study duration and method of BMD detection may explain the apparent contradictory results.

pQCT was used to analyze the cortical bone at the mid-shaft of the femur. These results demonstrated a dose-dependent effect of S-4 on CT, CC, and PC. BMD was completely maintained by S-4 although we did not observe dose-dependent effects. Three point bending analysis showed that the increases in bone parameters observed by pQCT were important to bone quality. DHT and S-4 significantly increased the maximum load required to break the femur compared to OVX controls. Further, S-4 treated groups showed a non-significant increase over DHT treated controls. The effects of S-4 treatment on cortical bone are similar to those reported by Hanada *et al*. [70] during their evaluation of the anabolic effects of S-40503, a nonsteroidal SARM, in a rat model of osteoporosis. They concluded that S-40503 was anabolic in cortical bone (30 mg/kg dose). Although direct comparisons with our study are not possible due to the differences in study design, their data supports our conclusions that nonsteroidal SARMs exert protective effects in cortical bone. However, the dose at which they observed significant bone effects was approximately 3-fold higher than our highest dose. These data, in addition to the data that we have previously published, demonstrate that S-4 is more potent than S-40503 in bone and levator ani muscle and more tissue selective (i.e., S-4 fully restored levator ani muscle weight at a dose that only restored the prostate to 34% of intact [19]).

Based on the pQCT and biomechanical strength data, we speculate that the primary mechanism of action of S-4 is anabolic. We observed increased trabecular density at the distal femur in S-4 treated intact animals. CC, CT, BMD, and ML at the

femoral mid-shaft were higher in S-4 treated OVX animals than intact animals, but trabecular density in S-4 treated OVX animals was only partially maintained. These data suggest that while S-4 may exert some anti-resorptive action, the bone-sparing effects observed in this study were primarily due to anabolic actions. We would have expected to observe a greater protective effect in trabecular bone if the primary mechanism of action were anti-resorptive. However, we did not perform histomorphometry on these bones, and are therefore unable to quantify the contributions of anti-resorptive versus anabolic effects of S-4. Nevertheless, we showed that S-4 exerts a protective effect on the skeleton following OVX. At equivalent doses, S-4 performed as well or better than DHT in each of the indices we examined, suggesting that S-4 is a more potent modulator of bone quality than DHT. Co-administration of bicalutamide either partially or completely blocked the effects of S-4 indicating the AR mediates the skeletal effects of S-4.

Although S-4 is not as effective for preventing bone resorption as estradiol and bisphosphonates [135, 136, 137], the anabolic actions of S-4 make it a good candidate for combination therapy with anti-resorptive agents. We observed positive effects on biomechanical strength and bone parameters in intact animals receiving S-4. These data suggest that S-4 can increase bone quality even in the presence of estrogen.

These studies showed that S-4 is a promising candidate for further development as a treatment for osteoporosis. Ongoing studies in our laboratory are investigating the anabolic effects of S-4 in rats that are allowed to become osteopenic before drug therapy begins and are of similar design to the study reported herein. These studies will provide support for the mechanism of action (i.e., anti-resorptive versus anabolic) of S-4 in bone.

Separation of the anabolic and androgenic effects of AR ligands may provide a unique mechanism by which clinicians could exploit the anabolic potential of androgens in muscle and bone without the virilizing side effects of current clinically available androgens. Many studies have attempted to delineate the androgenic versus estrogenic regulation of the skeleton. However, steroidal AR ligands, even in the presence of an aromatase inhibitor, exhibit some cross reactivity with other steroid hormone receptors and feedback at the level of the pituitary complicating the interpretation of the results. Since S-4 cannot be aromatized to an estrogen, does not affect the pituitary hormone release, and shows no cross-reactivity with any of the other steroid hormone receptors, it may also be used as a model compound to elucidate the debated effects of androgens in bone.

These studies are the first to show that an orally bioavailable SARM [117], S-4, can improve body composition, increase BMD, and enhance bone quality in an ovariectomized rat model of post-menopausal osteoporosis.

Group Number	Gonadal Status	S-4 (mg/day)	DHT (mg/day)	Bicalutamide (mg/day)
1	OVX	0.1	--	--
2	OVX	0.3	--	--
3	OVX	0.5	--	--
4	OVX	0.75	--	--
5	OVX	1.0	--	--
6	OVX	3.0	--	--
7	OVX	--	1.0	--
8	OVX	0.5	--	1.0
9	OVX	--	--	--
10	Intact	1.0	--	--
11	Intact	--	1.0	--
12	Intact	--	--	--

Table 3.1: Summary of the dosing groups.

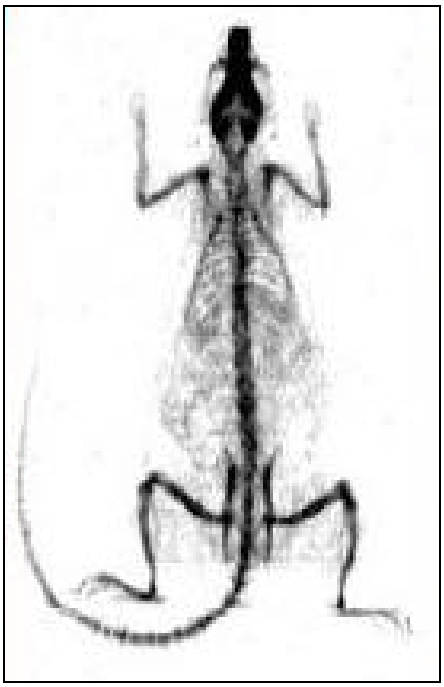

Figure 3.1: Animal positioning for DEXA scan.

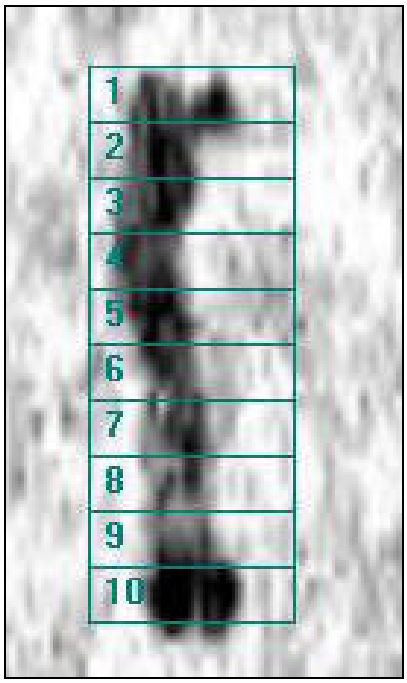

Figure 3.2: Regional divisions of the excised femur.

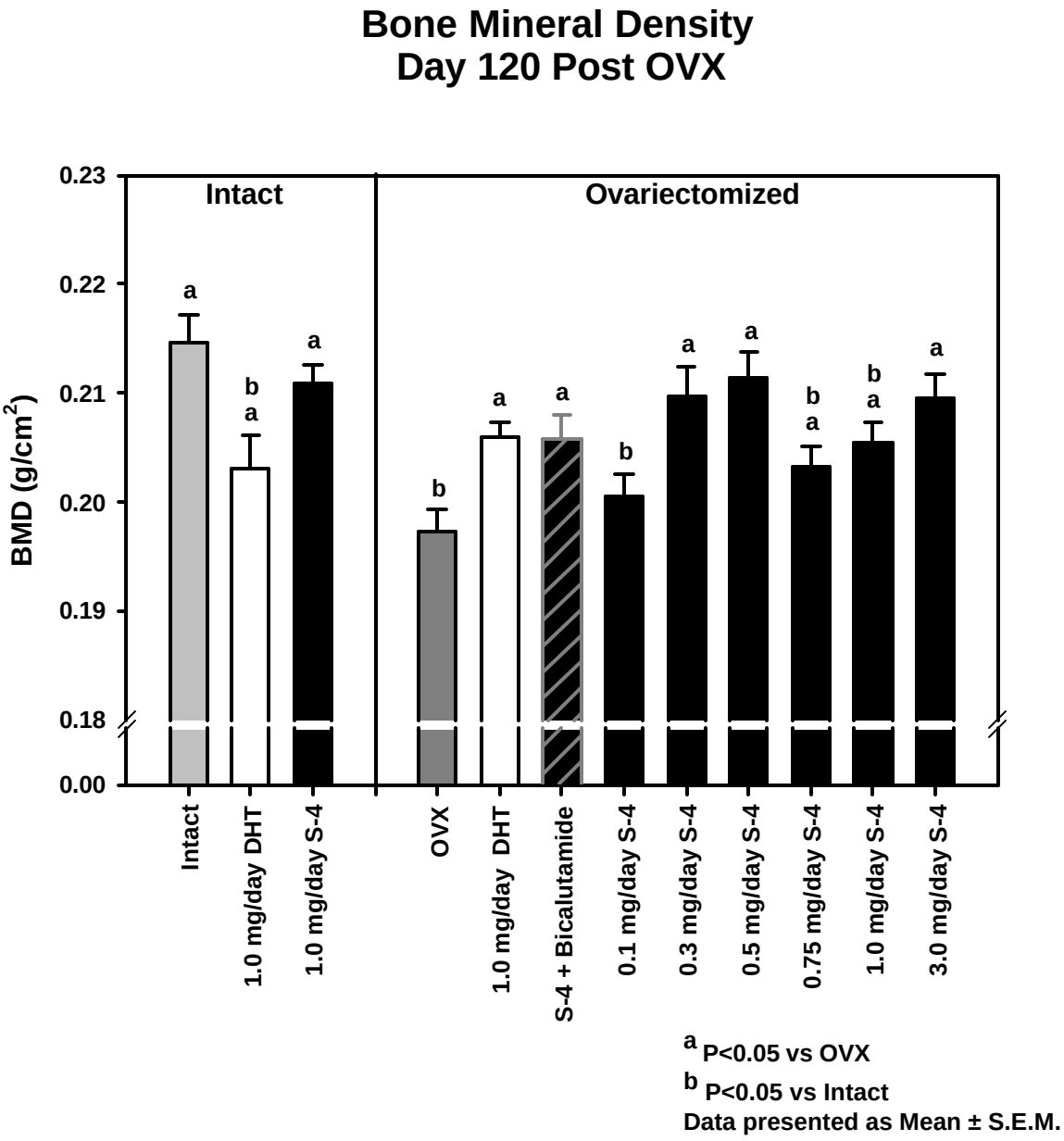

Figure 3.3: Whole body BMD at day 120 (DEXA). Data for individual animals is summarized in Table B.1 of Appendix B.

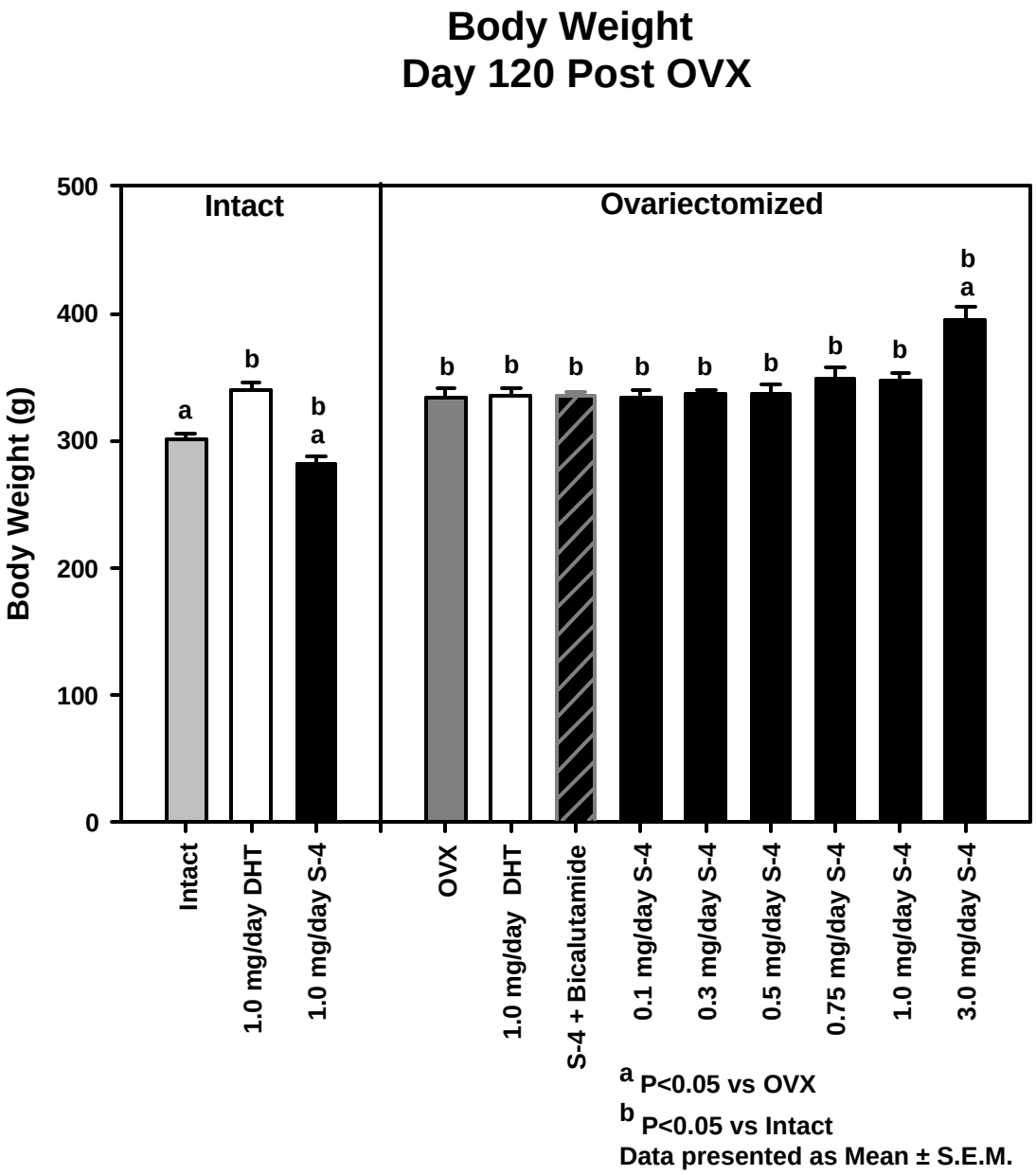

Figure 3.4: Body weight at day 120 (DEXA). Data for individual animals is summarized in Table B.2 of Appendix B.

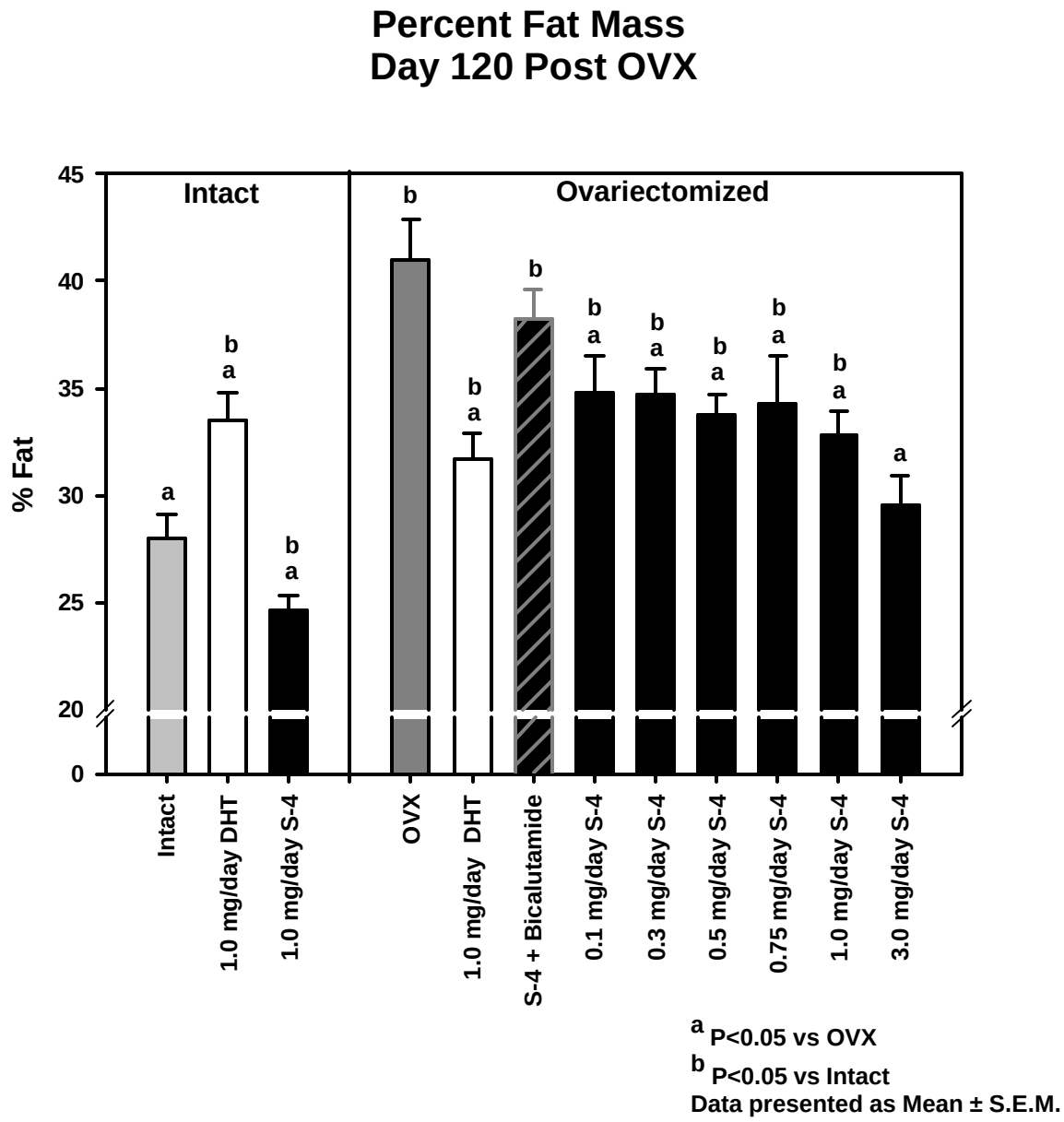

Figure 3.5: Percent fat mass at day 120 (DEXA). Data for individual animals is summarized in Table B.3 of Appendix B.

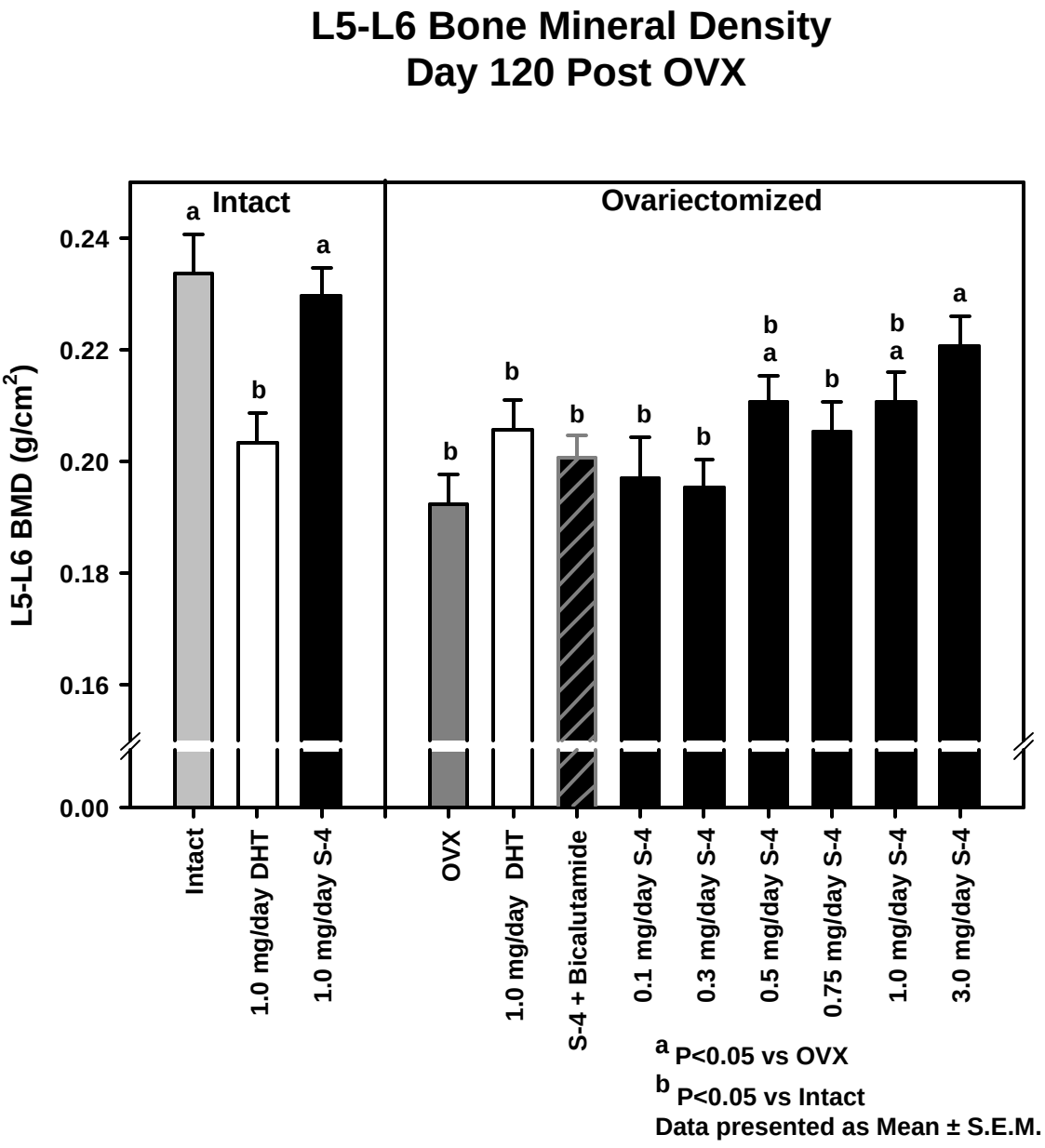

Figure 3.6: L5-L6 BMD at day 120 (DEXA). Data for individual animals is summarized in Table B.4 of Appendix B.

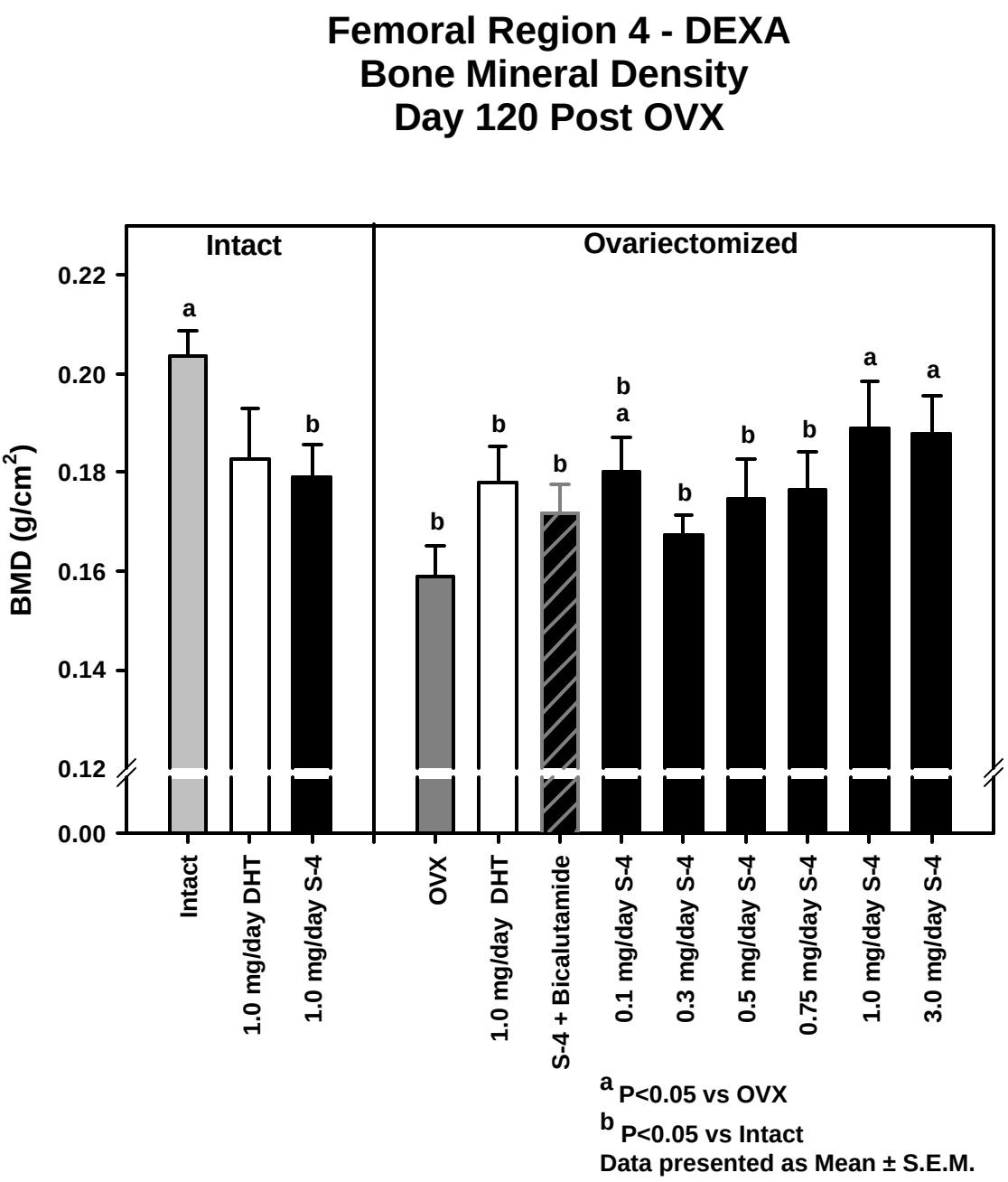

Figure 3.7: Femoral region 4 BMD at day 120 (DEXA). Data for individual animals is summarized in Table B.5 of Appendix B.

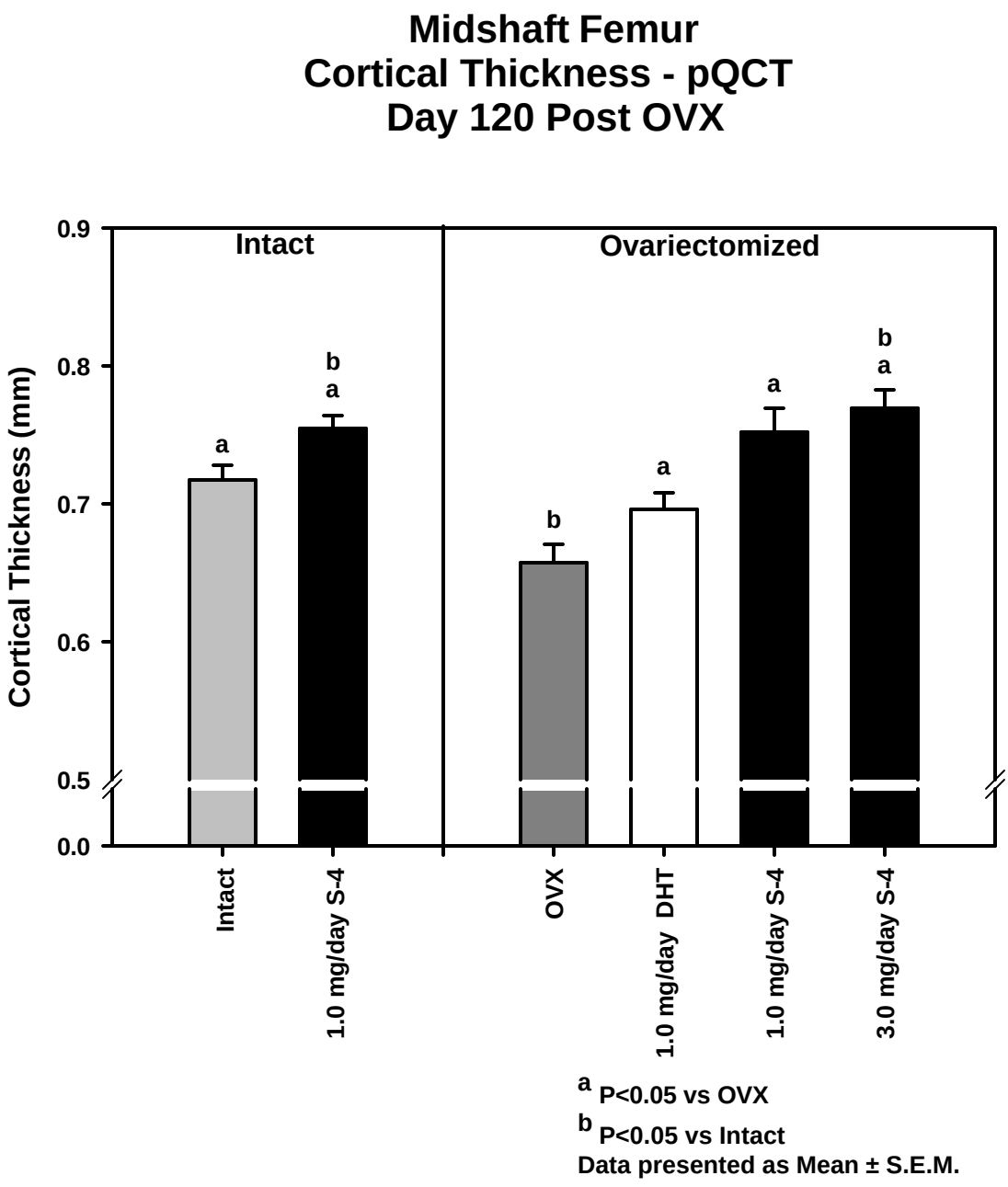

Figure 3.8: Cortical thickness of the mid-shaft femur at day 120 (pQCT). Data for individual animals is summarized in Table B.6 of Appendix B.

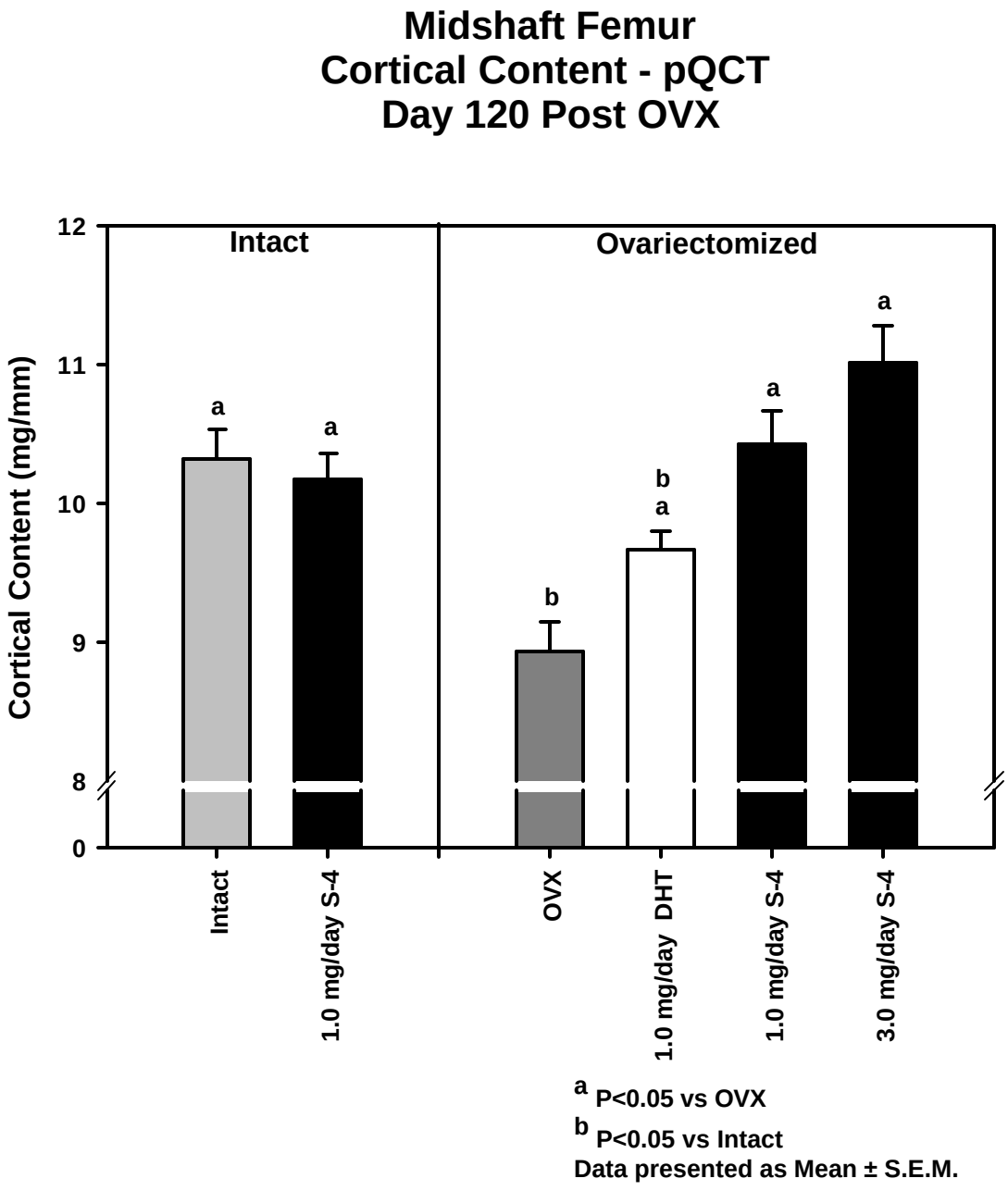

Figure 3.9: Cortical content of the mid-shaft femur at day 120 (pQCT). Data for individual animals is summarized in Table B.7 of Appendix B.

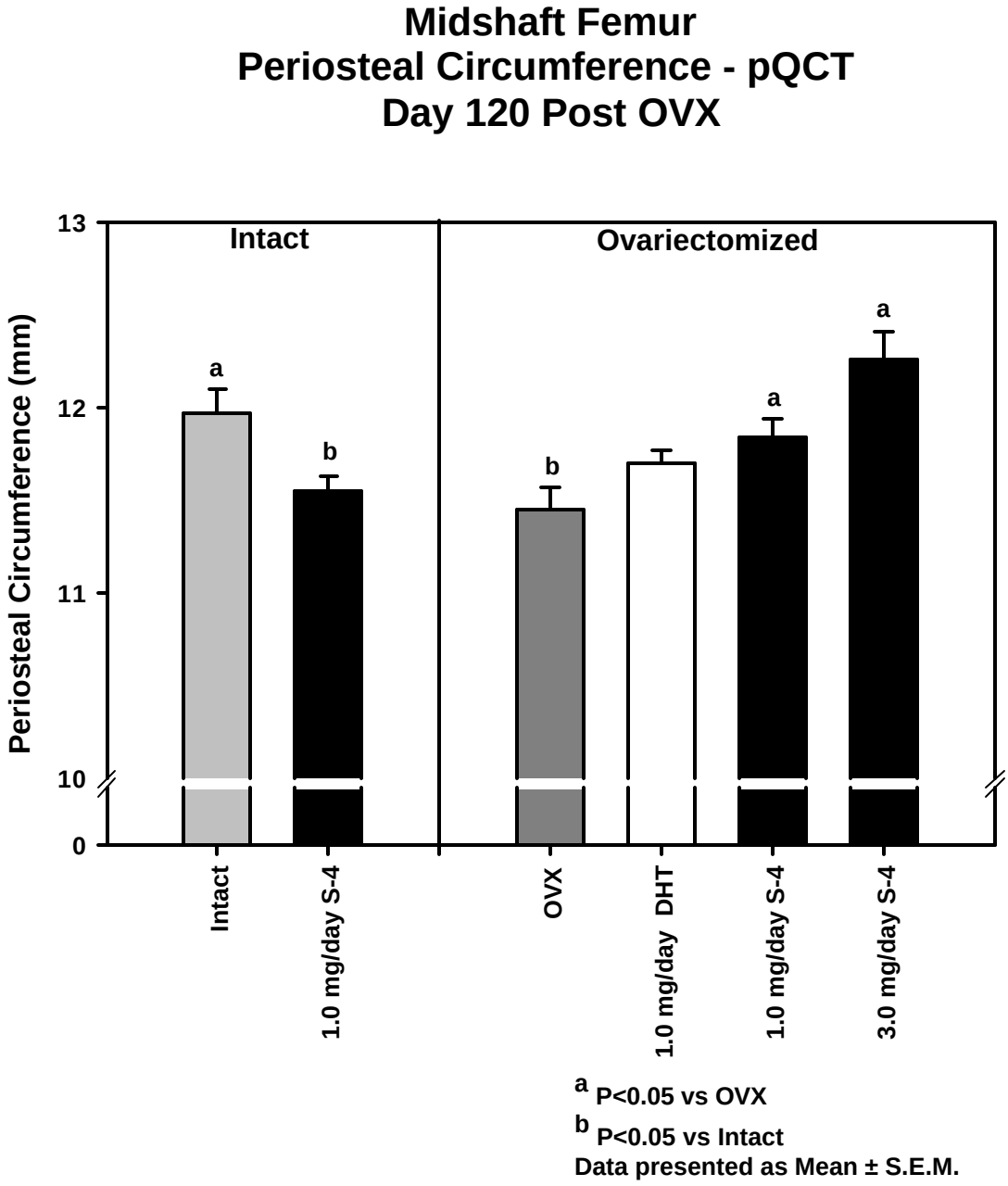

Figure 3.10: Periosteal circumference of the mid-shaft femur at day 120 (pQCT). Data for individual animals is summarized in Table B.8 of Appendix B.

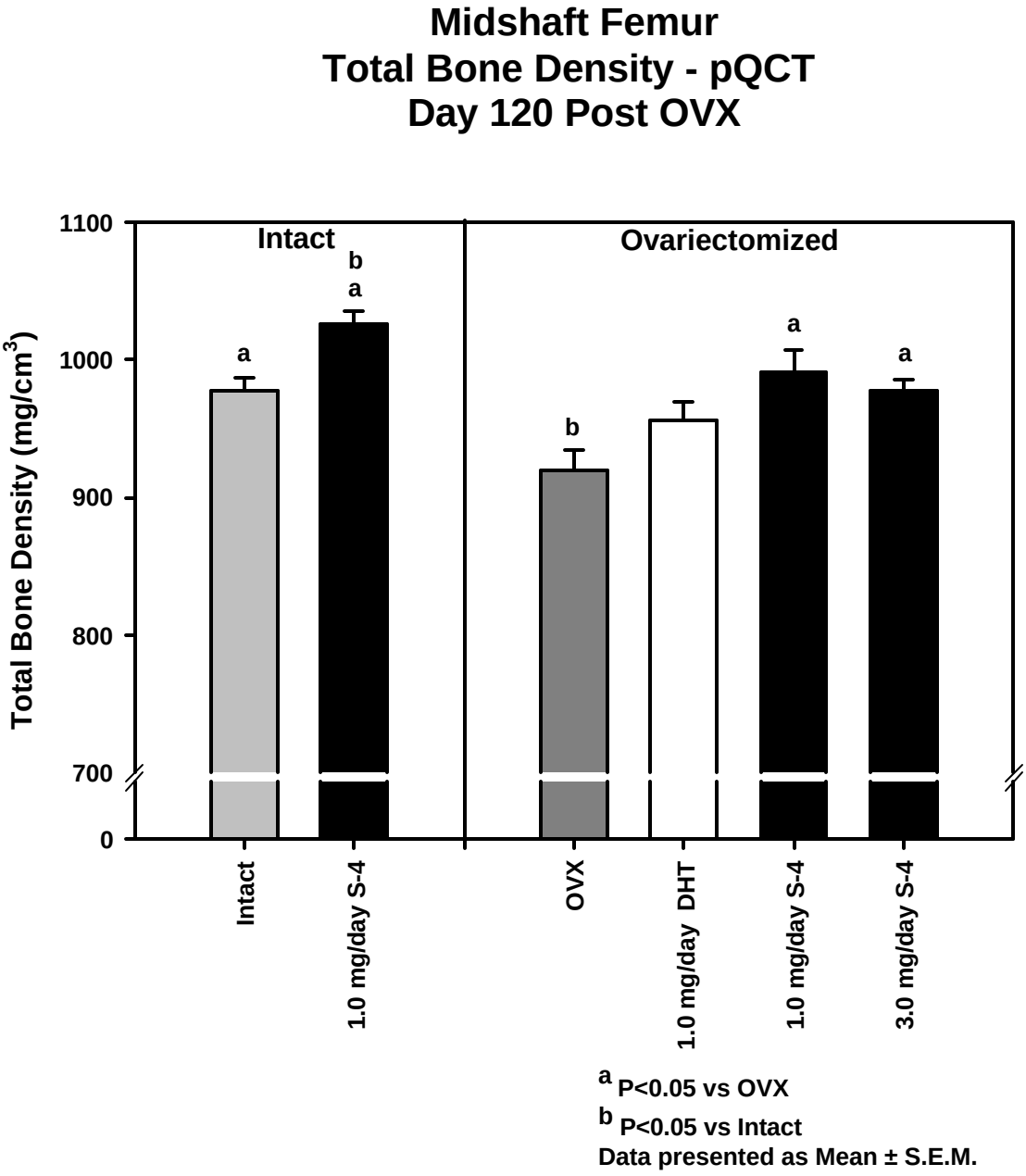

Figure 3.11: Total bone mineral density of the mid-shaft femur at day 120 (pQCT). Data for individual animals is summarized in Table B.9 of Appendix B.

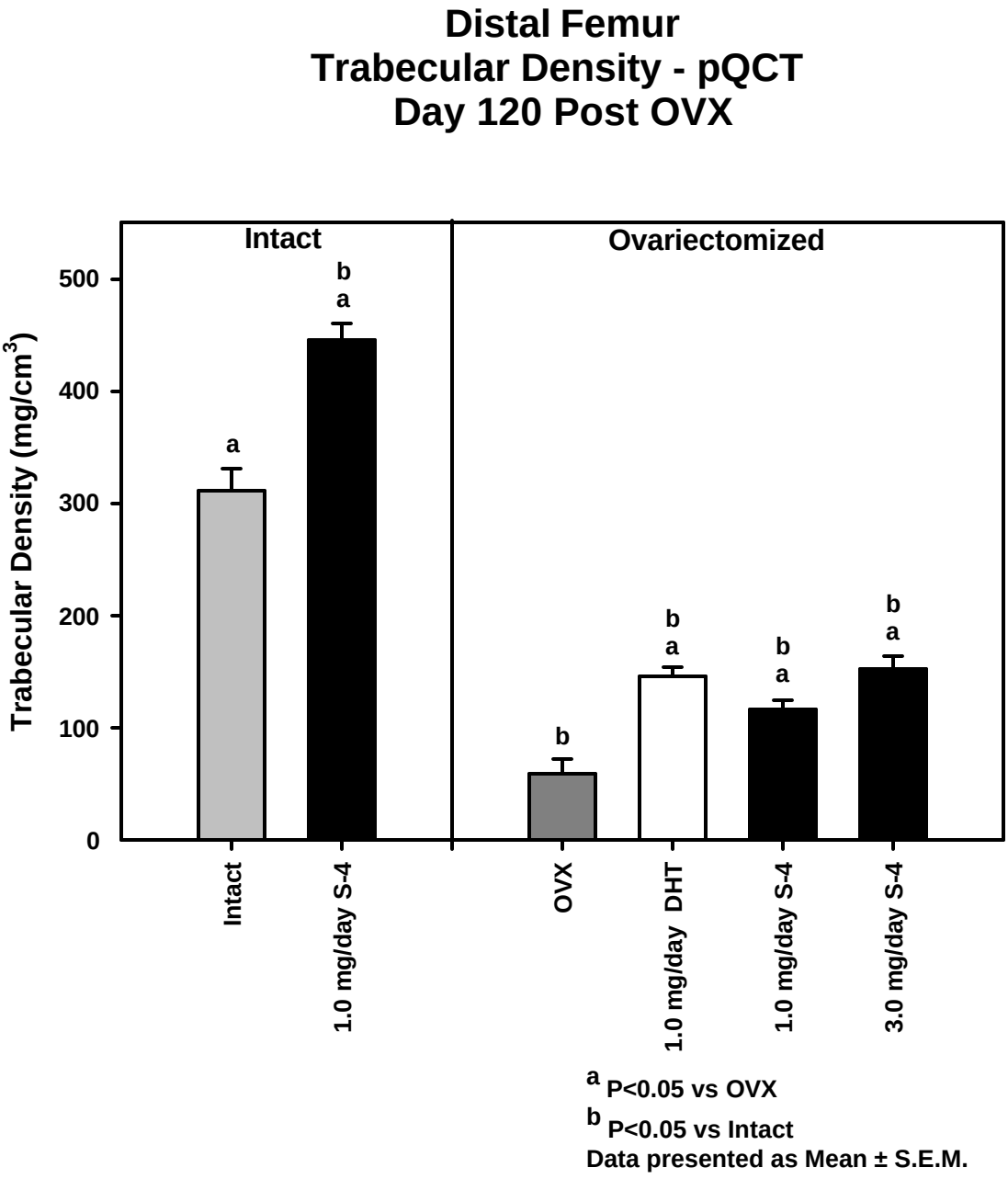

Figure 3.12: Distal femur trabecular bone density (pQCT). Data for individual animals is summarized in Table B.10 of Appendix B.

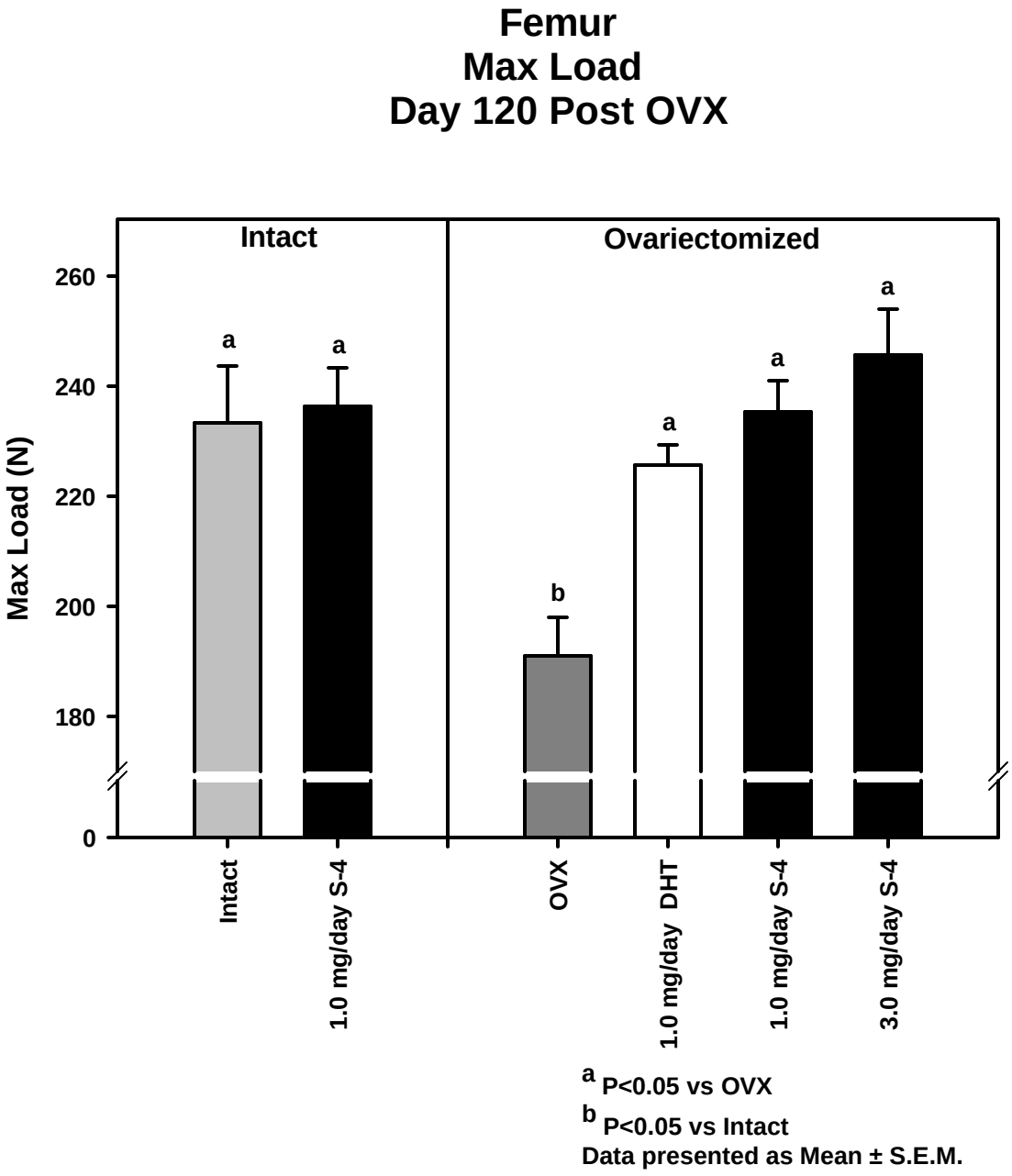

Figure 3.13: Femoral biomechanical testing of maximum load at day 120. Data for individual animals is summarized in Table B.11 of Appendix B.

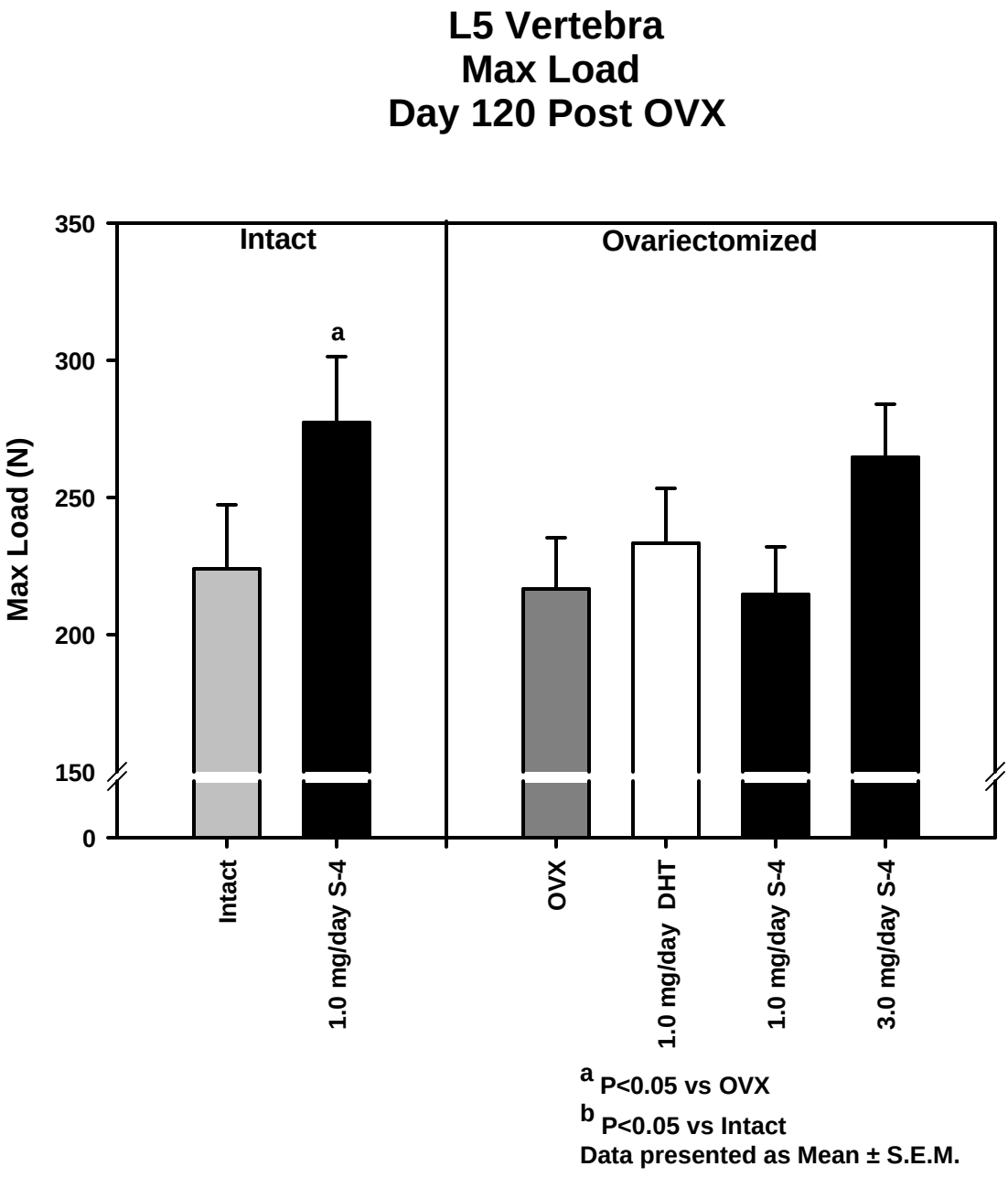

Figure 3.14: L5 Vertebra biomechanical testing of maximum load at day 120. Data for individual animals is summarized in Table B.12 of Appendix B.

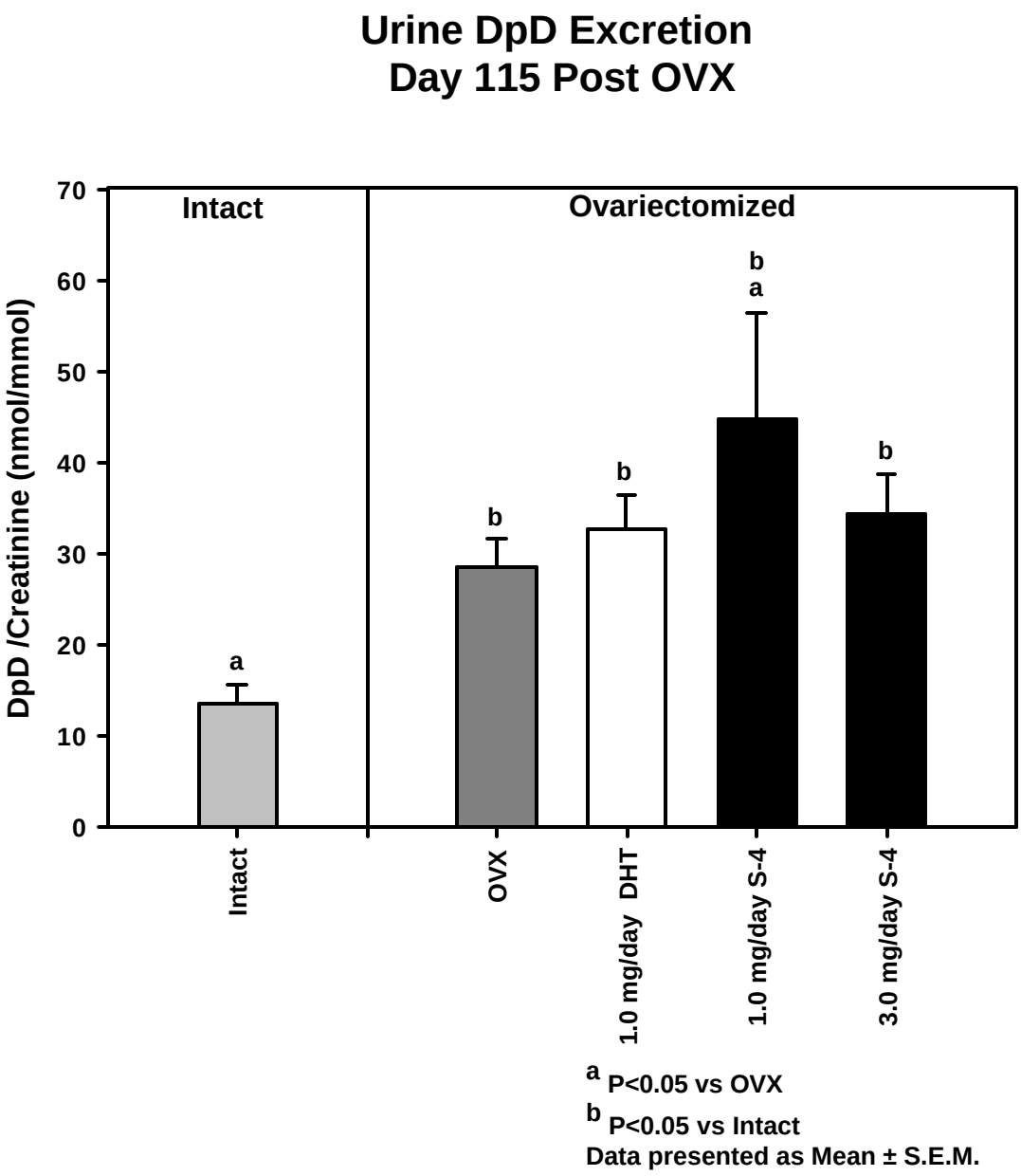

Figure 3.15: Deoxypyridinoline excretion at day 115. Data for individual animals is summarized in Table B.13 of Appendix B.

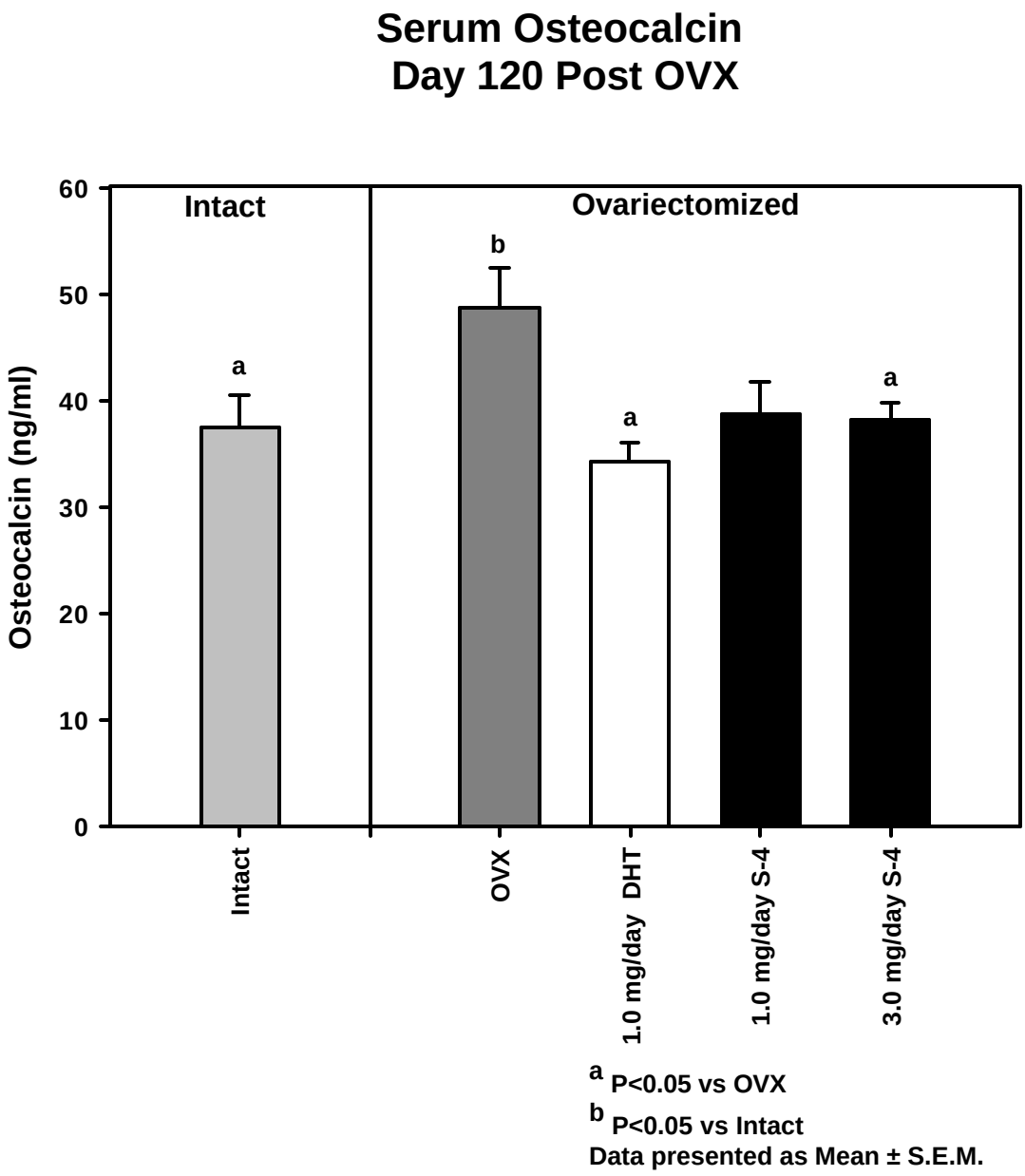

Figure 3.16: Serum levels of osteocalcin at day 120. Data for individual animals is summarized in Table B.14 of Appendix B.

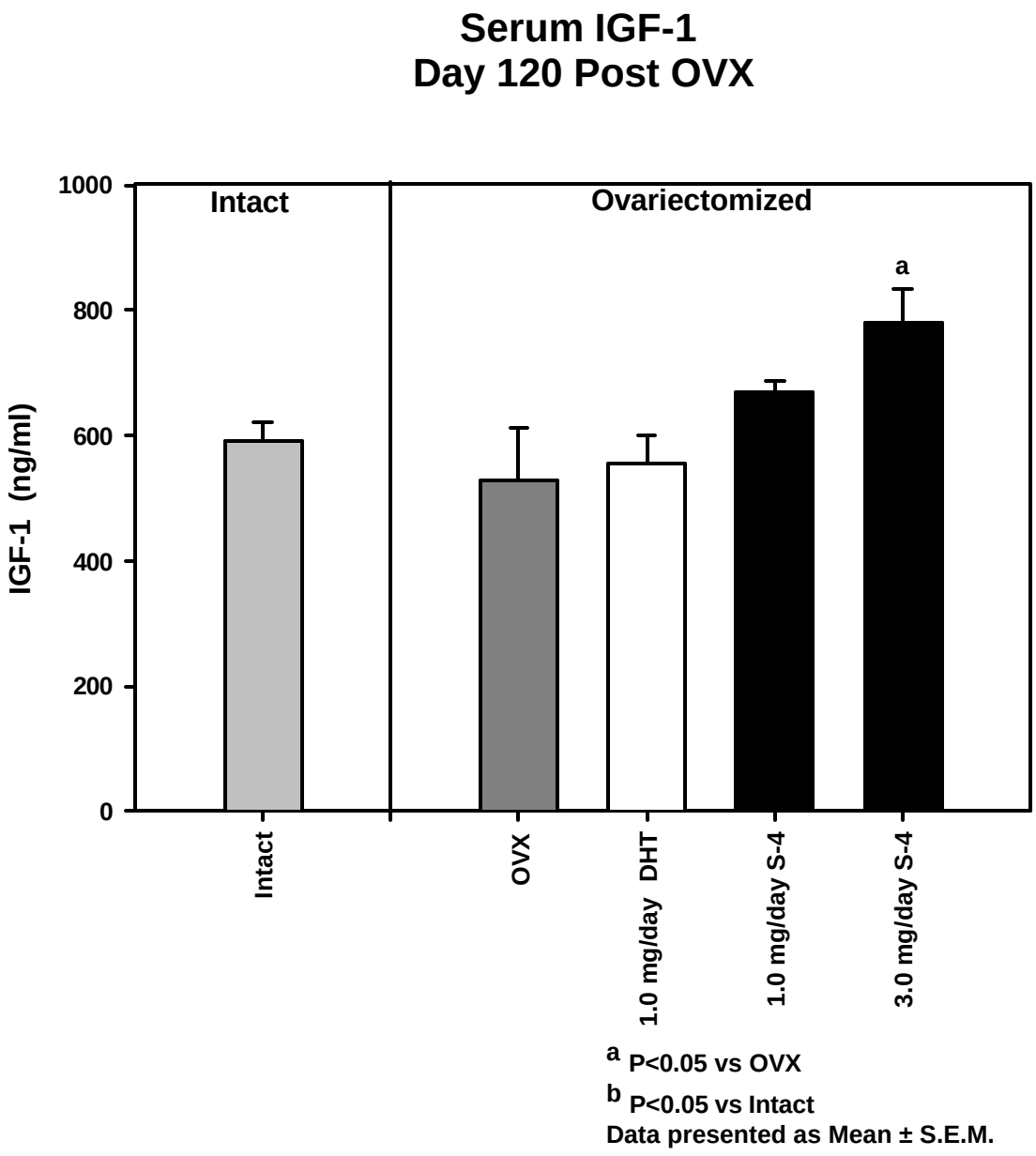

Figure 3.17: Serum levels of IGF-1 at day 120. Data for individual animals is summarized in Table B.15 of Appendix B.

CHAPTER 4

Anabolic Activity of S-3-(4-acetylamino-phenoxy)-2-hydroxy-2-methyl-N-(4-nitro-3-trifluoromethyl-phenyl)-propionamide on the Skeleton of Ovariectomized Rats

4.1 Introduction

Osteoporosis is a major clinical problem in elderly populations and the incidence increases with age. Since the primary reason for diagnosis of osteoporosis is a fracture, it is considered a "silent" disease. Unfortunately, this means that therapeutic intervention is not begun until after a significant amount of bone has already been lost, and the majority of current treatments focus on preventing resorption of existing bone [138]. Therapies such as estrogen, selective estrogen receptor modulators (SERMs), and bisphosphonates work through inhibiting bone loss and thereby reduce bone turnover. This action results in an increase in bone mass since resorption is inhibited while bone formation is not altered. Since the mechanism of action of these therapeutic agents is anti-resorptive, there is a limit to their ability to increase bone mineral density [138]. Anabolic agents act directly on the osteoblast, and therefore, have the potential to increase bone density to a

much greater degree than anti-resorptive therapies. Thus, anabolic therapies for osteoporosis would offer many significant advantages over currently available options. Fluoride, growth hormone, insulin-like growth factor, strontium, statins, tibolone, and parathyroid hormone (PTH) have all been examined for anabolic skeletal effects. Currently, PTH is the most promising, but many questions regarding anabolic effects on cortical bone, fracture risk reduction, and development of drug delivery systems remain to be answered [138]. There is increasing evidence to support an anabolic role for androgens in bone [70, 71, 115, 126]. Recent studies by Hanada *et al.* [70] showed that a tetrahydroquinoline-derived SARM (S-40503) exhibits anabolic effects in an orchidectomized rat model of bone loss. They showed that S-40503 was able to maintain cancellous bone in a gonadectomized male rat, but not in an ovariectomized female model. However, S-40503 increased cortical bone mineral density (BMD) in both models. These studies provide evidence that a SARM can modulate bone mass. Tobias *et al*. showed that DHT partially restored cancellous bone in ovariectomized female rats [71]. They found that DHT increased both trabecular number and thickness. However, they concluded that increases in trabecular thickness appeared to be the primary mechanism for the increases seen in cancellous bone volume. DHT effects were also noted in cortical bone, but these results did not reach statistical significance. The authors concluded that the study duration might have been too short for significant alterations in cortical bone to occur. Additionally, previous studies in our laboratory suggest that S-4 is anabolic in bone. We observed increases in whole body BMD, regional BMD, cortical thickness (CT), and trabecular density (TD) following ovariectomy (OVX). Although androgens are anabolic in bone, aromatization, virilizing side effects, and lack of

adequate dosage formulations have slowed the development of androgen therapies for osteoporosis. There is a great need for a therapeutic agent capable of building new bone. S-4, an AR-specific, tissue-selective anabolic agent [19], is an ideal pharmacologic tool to explore the anabolic effects of androgens in bone. S-4 binds tightly and specifically to the androgen receptor (AR) [19], is orally bioavailable [117], and not converted to estrogenic metabolites. We hypothesized that a nonsteroidal SARM would be anabolic in the skeleton of ovariectomized rats. As such, we evaluated the anabolic effects of S-4 in both cortical and cancellous bone.

4.2 Materials and Methods

4.2.1 Animals

One hundred twenty female Sprague-Dawley rats were purchased from Harlan (Indianapolis, IN). The animals were housed three per cage and were allowed free access to tap water and commercial rat chow (Harlan Teklad 22/5 rodent diet - 8640). During the course of the study, the animals were maintained on a 12 hr light:dark cycle. This study was reviewed and approved by the Institutional Laboratory Care and Use Committee of The Ohio State University. At 23 weeks of age, the animals were ovariectomized (OVX) or sham-operated and then assigned to one of 12 treatment groups of 10 animals as follows: (1) OVX+S-4 (0.1 mg/day); (2) OVX+S-4 (0.3 mg/day); (3) OVX+S-4 (0.5 mg/day); (4) OVX+S-4 (0.75 mg/day); (5) OVX+S-4 (1.0 mg/day); (6) OVX+S-4 (3.0 mg/day); (7) OVX+DHT (1 mg/day); (8) OVX+S-4+Antiandrogen (0.5 +

1.0 mg/day); (9) OVX+Vehicle; (10) intact+S-4 (1 mg/day); (11) intact+DHT (1 mg/day); (12) intact+Vehicle. Table 4.1 summarizes the dosing groups. The doses of S-4 were chosen based on a pilot study and prior pharmacodynamic studies performed in our laboratory [19]. Since DHT cannot be aromatized to estradiol, DHT treatment was included in both intact and ovariectomized animals to serve as a positive control group to evaluate the skeletal effects of a pure androgen. Intact and ovariectomized animals receiving vehicle alone served as negative controls. Another control group received an antiandrogen along with S-4 in an effort to delineate the AR mediated versus AR independent effects of S-4. Four animals died during the course of the study. Therefore, groups 5, 7, 8, and 11 consisted of nine animals each. Dosing solutions were prepared daily by dissolving drug in dimethyl sulfoxide (DMSO) and diluting in polyethylene glycol 300 (PEG 300). Compounds of interest were administered beginning at day 90 and continued for 120 days via daily subcutaneous injections in a volume of 0.20 ml.

4.2.2 Whole Body DEXA Analysis

Total body bone mineral density (BMD), percent fat mass (FM), and body weight (BW), bone mineral content (BMC), bone mineral area (BMA), and lean mass (LM) were determined by dual energy x-ray absorptiometry (DEXA) (GE, Lunar Prodigy™) using the small animal software (Lunar enCORE, version 6.60.041) on days 90 and 210. Since the purpose of this study was to evaluate the anabolic activity of S-4, the OVX control group measurements were taken on day 90 (*in vivo* measurements) or 120 (*ex vivo* measurements) to serve as baseline controls. The ex vivo measurements could not be

made until day 120 because the OVX control group served as a control group in another experiment. Animal BW was also determined by standard gravimetric methods using a 700 series Ohaus triple beam animal balance (Florham Park, NJ). For scanning, the animals were anesthetized with ketamine:xylazine (87:13 mg/kg) and positioned in a prone position as demonstrated in Figure 4.1. Total body data was obtained by selecting an area encompassing the entire animal as the region of interest during data processing. The parameters determined to be the most sensitive to estrogen withdrawal (i.e., largest differences between intact and OVX control groups) were reported herein.

4.2.3 *Ex Vivo* DEXA Analysis

Immediately following the whole body DEXA scan on day 210, animals were sacrificed, and the lumbar vertebrae, femurs, and tibia were excised and cleared of soft tissue. The excised bones from the OVX control group were analyzed immediately following sacrifice on day 120. The excised bones were scanned through a 3 in. deep room temperature water bath to simulate soft tissue. The L5-L6 vertebrae were selected as a region of interest and analyzed for BMD by DEXA. The femur images were also subdivided into ten equal regions of interest, as shown in Figure 4.2, from proximal (region 1) to distal (region 10), and the BMD of each region was determined by the Lunar enCORE small animal software. We observed the greatest difference in BMD between the intact and OVX groups in femoral region 4. Therefore, femoral analysis between all groups was performed in region 4.

4.2.4 Femoral pQCT Analysis and Biomechanical Testing

pQCT analysis and biomechanical testing of the right femurs from the OVX + 1.0 mg/day S-4 (Group 5), OVX + 3.0 mg/day S-4 (Group 6), OVX + 1.0 mg/day DHT (Group 7), OVX control (Group 9), and intact control (Group 12) groups were performed by Skeletech, Inc. (Bothell, WA). The femur was subjected to pQCT scan using a Stratec XCT RM and associated software (Stratec Medizintechnik GmbH, Pforzheim, Germany. Software version 5.40 C). The femur was analyzed at both the mid-shaft and distal regions. The length of the femur was determined using scout scan views, and the mid-shaft region was chosen at 50% of the length of the femur. The distal region was chosen at 20% of the length of the femur starting at the distal end. One 0.5 mm slice perpendicular to the long axis of the femur was used for analysis. Total bone mineral content, total bone area, total bone mineral density, cortical bone mineral content, cortical bone area, cortical bone mineral density, cortical thickness, periosteal perimeter (circumference) and endosteal perimeter were determined at the mid-shaft of the femur. At the distal femur total bone mineral content, total bone area, total bone mineral density, trabecular bone mineral content, trabecular bone area and trabecular bone mineral density were determined. After pQCT analysis, the de-fleshed whole femur was used in the three-point bending test. The anterior to posterior diameter (APD) (unit:mm) at the midpoint of the femoral shaft was measured with an electronic caliper. The femur was placed on the lower supports of a three-point bending fixture with the anterior side of the femur facing downward in an Instron Mechanical Testing Machine (Instron 4465 retrofitted to 5500)(Canton, MA). The length (L) between the lower supports was set to

14 mm. The upper loading device was aligned to the center of the femoral shaft. The load was applied at a constant displacement rate of 6 mm/min until the femur broke. The mechanical testing machine directly measured the maximum load (F_u) (unit:N), stiffness (S) (units:N/mm), and energy absorbed (W) (unit:mJ). The axial area moment of inertia (I) (unit:mm^4) was calculated by the software during the pQCT analysis of the femoral mid-shaft. Stress (σ) (units:N/mm^2), elastic modulus (E) (unit:Mpa), and toughness (T) (units:mJ/m^3) were calculated by the following formulas: stress: $\sigma = (F_u * L *(a/2)) / (4* I)$; elastic modulus: $E = S*L^3/(48*I)$; and toughness: $T = 3*W*(APD/2)^2/(L*I)$. The parameters determined to be the most sensitive to estrogen withdrawal are reported herein.

4.2.5 Statistical Analysis

Statistical analysis was performed by single factor analysis of variance (ANOVA). P-values of less than 0.05 were considered as statistically significant differences. Raw data is presented in tabular form in Appendix C.

4.3 Results

4.3.1 Whole Body DEXA Analysis

The results of the whole body BMD DEXA analysis are presented in Figure 4.3. The vehicle-treated OVX control group had a lower whole body BMD (0.197 g/cm^2) than the intact control group (0.212 g/cm^2). BMD in the 0.3, 0.5, 0.75, 1.0, and 3.0 mg/day S-4 dose groups increased to 0.204, 0.209, 0.206, 0.205, 0.205, and 0.206 g/cm^2, respectively. DHT (1 mg/day) was unable to restore the BMD in OVX animals during the treatment period. Neither DHT nor S-4 increased BMD in intact animals. However, DHT-treated animals trended lower (0.205 g/cm^2) while S-4 treated animals trended higher (0.214 g/cm^2) than intact controls. Animals receiving co-administration of bicalutamide with S-4 (0.204 g/cm^2) were not different from animals receiving S-4 alone (0.209 g/cm^2).

We observed a dose-dependent increase in body weight in OVX animals receiving S-4 (Figure 4.4). Body weight in OVX groups treated with S-4 averaged 350 and 381 g following doses of 0.1 and 3.0 mg/day, respectively. Intact control animals had an average body weight of 308 g, and OVX resulted in an increase in body weight to 336 g. DHT treatment in intact animals resulted in an increase in body weight to 357 g. Body weight of intact animals treated with S-4 (312 g) was not different from intact controls. BW in animals treated with bicalutamide and S-4 averaged 347 g, and were not significantly different from those observed in OVX controls.

Body composition data were determined using DEXA. Results from the FM analysis by DEXA are presented in Figure 4.5. FM in the OVX control group increased to 41% from 29% in the intact control group, illustrating the profound effect of estrogen deprivation on body composition. S-4 treatment resulted in a 2% decrease while DHT caused an 8% increase in intact animals compared to intact controls. FM was maximal depressed to 34% following the 0.75 mg/day S-4 dose group. Significant decreases were also observed in the 0.5 and 3.0 mg/day S-4 dose groups resulting in a FM of 35 and 36%, respectively. Although not all differences reached significance, S-4 treatment in all dose groups resulted in lower FM than the OVX control group, indicating that S-4 decreased FM and increased LM with prolonged treatment. Co-administration of bicalutamide with S-4 partially abrogated the positive effects on FM seen with S-4 treatment alone. DHT treatment in OVX animals resulted in a 4% decrease in FM.

4.3.2 *Ex Vivo* DEXA Analysis

OVX negatively affected the BMD in the L5-L6 vertebra causing a decrease from 0.234 in intact animals to 0.192 g/cm^2 in OVX controls. Data from the L5-L6 DEXA BMD analysis is presented in Figure 4.6. The 3.0 mg/day S-4 dose completely restored the L5-L6 BMD in OVX animals, and significant increases in L5-L6 BMD were observed in the 0.3 mg/day dose group. Although we observed positive trends in L5-L6 BMD following S-4 treatment at all other dose levels, these differences did not reach significance. DHT treatment in intact animals resulted in a significant decrease in BMD to a level not different from OVX controls, while S-4 had no effect on L5-L6 BMD in

intact animals. DHT treatment in OVX animals partially restored the L5-L6 BMD. We failed to observe bicalutamide effects in L5-L6 BMD.

Femoral BMD in region 4 ranged from 0.197 to 0.212 g/cm^2 in OVX and intact controls, respectively. No differences were noted in intact animals receiving S-4 or DHT (Figure 4.7). S-4 treatment resulted in higher BMD in all treatment groups. Significant increases were observed in the 0.1, 0.75, and 3.0 mg/day dose groups returning these animals back to the level of intact controls. Co-administration of bicalutamide resulted in a decrease in BMD. OVX animals treated with DHT showed a slight increase in BMD. Data for the femoral BMD is summarized in Figure 4.7.

4.3.3 Femoral pQCT Analysis and Biomechanical Testing

CT at the femoral mid-shaft was determined by pQCT and the results are presented in Figure 4.8. CT decreased from 0.72 mm in intact animals to 0.66 mm following OVX. We failed to observe significant differences in CT between drug-treated groups and the OVX control group. However, we observed significant differences in CC after drug therapy (Figure 4.9). CC in intact control animals was 10.3 mg/mm. OVX resulted in a loss of CC to 8.9 mg/mm. The 1.0 mg/day dose of S-4 partially restored the CC to 9.6 mg/mm and the 3.0 mg/day dose of S-4 fully restored the CC to 10.1 mg/mm. DHT fully restored the CC to 9.9 mg/mm.

Trabecular BMD was measured by pQCT at the distal femur. Figure 4.10 shows the results from these analyses. Trabecular bone loss was evident in the distal femur following OVX. We observed positive trends in trabecular bone density following S-4

treatment. However, neither DHT nor S-4 fully restored trabecular BMD, suggesting androgens primarily increase trabecular BMD by increasing trabecular thickness as opposed to trabecular number.

Biomechanical strength of the femur was determined by three-point bending. Results from biomechanical strength testing are shown in Figure 4.11. OVX caused a reduction in the ML required to break the femur from 233 N in intact controls to 191 N in vehicle-treated OVX controls. S-4 treatment resulted in an increase in ML for both the 1.0 and 3.0 mg/day dose groups restoring them to 217 and 215 N, respectively. These values were not significantly different from that of intact controls. DHT treatment increased the femoral ML to 214 N.

4.4 Discussion

The vast majority of current treatments for osteoporosis act through an anti-resorptive mechanism. Thus, increases in BMD are due to prolongation of mineralization and reduction of remodeling space [138]. Anabolic mediators of bone formation would act through a completely different mechanism, and have the potential to increase BMD to a greater degree than agents that only inhibit bone resorption [138]. In this study, female rats with established bone loss were used to evaluate the anabolic activity of S-4. This study demonstrates that S-4 is anabolic in an osteopenic rat model. Many lines of evidence support this conclusion. Examination of whole body and regional BMD as well as biomechanical indices of bone quality clearly showed that S-4 exerts anabolic activity in bone. Whole body BMD was fully restored in animals receiving > 0.1 mg/day S-4.

Regional analysis of the L5-L6 and the femur by DEXA showed that S-4 completely restored BMD. pQCT results confirmed anabolic effects on the cortical bone in the femur, but trabecular density in the distal femur was unchanged with drug treatment. Results showing increased femoral breaking strength further supports this conclusion. In the parameters measured by DEXA, we observed variability between similar dose groups. This variability could be a result of all doses producing maximal effect in the measured parameter, pharmacokinetic variability, or DEXA variability. However, we did not measure S-4 plasma concentrations or perform more stringent analyses on the excised bones of each group. Therefore, we are unable to speculate as to the contributions of the factors listed above. Previous studies in our laboratory to examine the protective skeletal effects of S-4 in an acute post-ovariectomized model of postmenopausal bone loss showed that S-4 prevented bone loss following OVX. Since bone loss prevention would result from either increased bone formation or decreased bone resorption, we could only hypothesize as to the primary mechanism by which S-4 prevented bone loss. However, S-4 only partially maintained the trabecular density of the distal femur. Known anti-resorptive agents such as estrogen and bisphosphonates fully maintain trabecular density. As a whole, these data suggest the mechanism of action of S-4 is primarily anabolic as opposed to anti-resorptive.

It is well documented that following OVX rats lose a significant amount of BMD. In aged female rats, there is a rapid decline of BMD for a period of about 90 days whereupon bone turnover stabilizes [139]. In order to evaluate the anabolic effects of S-4, we withheld drug therapy for 90 days following OVX to allow bone loss to occur and then treated the animals for 120 days with the compounds of interest. The OVX

control group also served as a control group for a previous study in which we evaluated the protective effects of S-4 in an acute post-OVX model of accelerated bone loss. For this reason, the excised bone parameters for the OVX control group were collected on day 120 as opposed to day 90, which would be a true baseline measurement. Since, there is little change in the bone parameters of OVX animals between days 90 and 120 [139], these samples were used for baseline comparisons. However, the whole body parameters measured by DEXA (i.e. whole body BMD, body weight, and percent fat mass) were collected at day 90 for the OVX control group.

Although S-4 treatment resulted in an increased body weight, these animals exhibited a lower FM than the OVX control animals. These results were similar to those observed in our previous study. As discussed in our previous study, increases in lean mass are beneficial to the skeleton in two ways. Firstly, lean mass may indirectly increase BMD due to increasing skeletal stresses, which stimulate bone formation [20]. Secondly, increased muscle mass and strength may reduce the risk of falling and thereby reduce the risk of fracture [132]. Therefore, S-4 may be more advantageous for clinical used than other purely bone anabolic agents. Interestingly, DHT treatment in intact animals resulted in an 8% increase in FM compared to intact controls. This is likely due to the DHT-inhibition of luteinizing hormone and follicle stimulating hormone release from the pituitary causing a decrease in estrogen levels.

In an effort to delineate androgen effects in cortical versus cancellous bone, we analyzed the mid-shaft and distal femur by pQCT. Although we did not observe differences in cortical thickness between the OVX groups, the drug treated groups exhibited increased cortical content and biomechanical strength. S-4 fully restored CC at

the 3 mg/day dose level and partially restored CC at the 1 mg/day dose level. However, biomechanical strength was fully restored by both 1 and 3 mg/day doses. These data show that S-4 and DHT are both anabolic in cortical bone. The lack of effects in trabecular bone was likely due to the loss of pre-existing architecture on which to rebuild lost bone. In cortical bone, our results are in agreement with those reported by Hanada *et al*., which showed increases in cortical BMD with androgens [70]. Additionally, we have shown that the androgenic effect in cortical bone translates directly to biomechanical strength (Figure 4.11). In trabecular bone, we observed positive trends in S-4 treated groups. Although the differences did not reach significance, S-4 treated animals had a higher average trabecular BMD. Our DHT control group showed significant differences from OVX controls. Studies by Tobias *et al*. found that DHT was able to partially restore cancellous bone in OVX rats [71]. They noted that DHT primarily increased trabecular thickness as opposed to trabecular number at the distal femur. Since the trabecular effects of androgens are due to increasing trabecular thickness instead of stimulating the formation of new trabeculae, we did not expect androgens to fully restore trabecular BMD.

PTH has been shown to fully restore both cancellous and cortical bone in ovariectomized rats [140, 141, 142]. In some cases, PTH increased BMD in OVX animals to a level greater than that observed in sham-operated intact controls [140, 141, 142]. Although S-4 is not quite as efficacious as PTH in bone, S-4 fully restored whole body BMD, L5-L6 BMD, mid-shaft femoral BMD, CC, and femur biomechanical strength.

As a whole, these data suggest that S-4 is likely to significantly reduce the fracture risk in patients with osteoporosis through direct anabolic action on both muscle and bone. S-4 performed as well or better than DHT in these assays. As S-4 is anabolic in bone, orally bioavailable [117], tissue-selective [19], and does not cross-react with other steroid hormone receptors [17], it offers significant advantages over currently available therapies for osteoporosis.

Group Number	Gonadal Status	S-4 (mg/day)	DHT (mg/day)	Bicalutamide (mg/day)
1	OVX	0.1	--	--
2	OVX	0.3	--	--
3	OVX	0.5	--	--
4	OVX	0.75	--	--
5	OVX	1.0	--	--
6	OVX	3.0	--	--
7	OVX	--	1.0	--
8	OVX	0.5	--	1.0
9	OVX	--	--	--
10	Intact	1.0	--	--
11	Intact	--	1.0	--
12	Intact	--	--	--

Table 4.1: Summary of dosing groups.

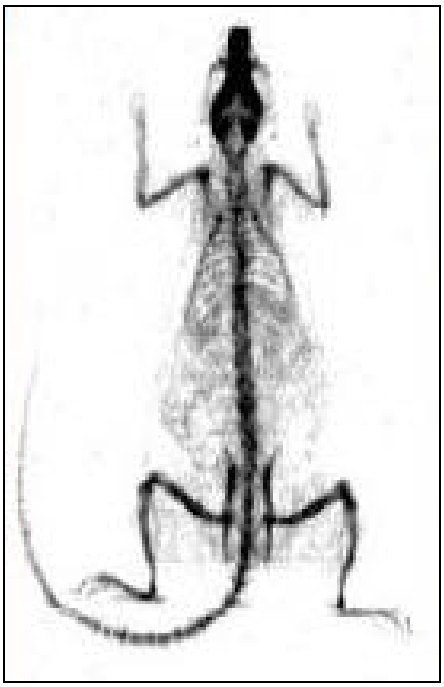

Figure 4.1: Animal positioning for DEXA scan.

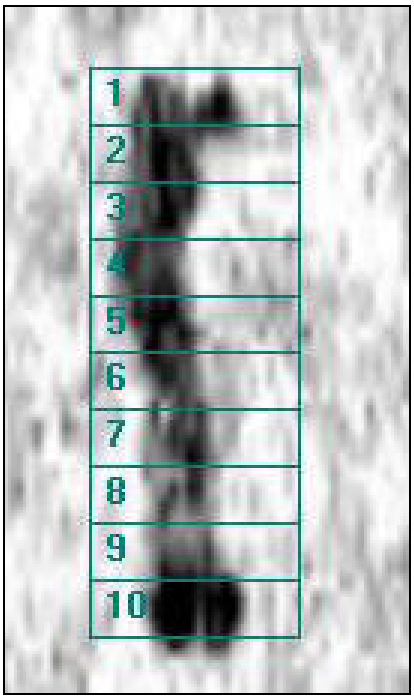

Figure 4.2: Regional divisions of the excised femur.

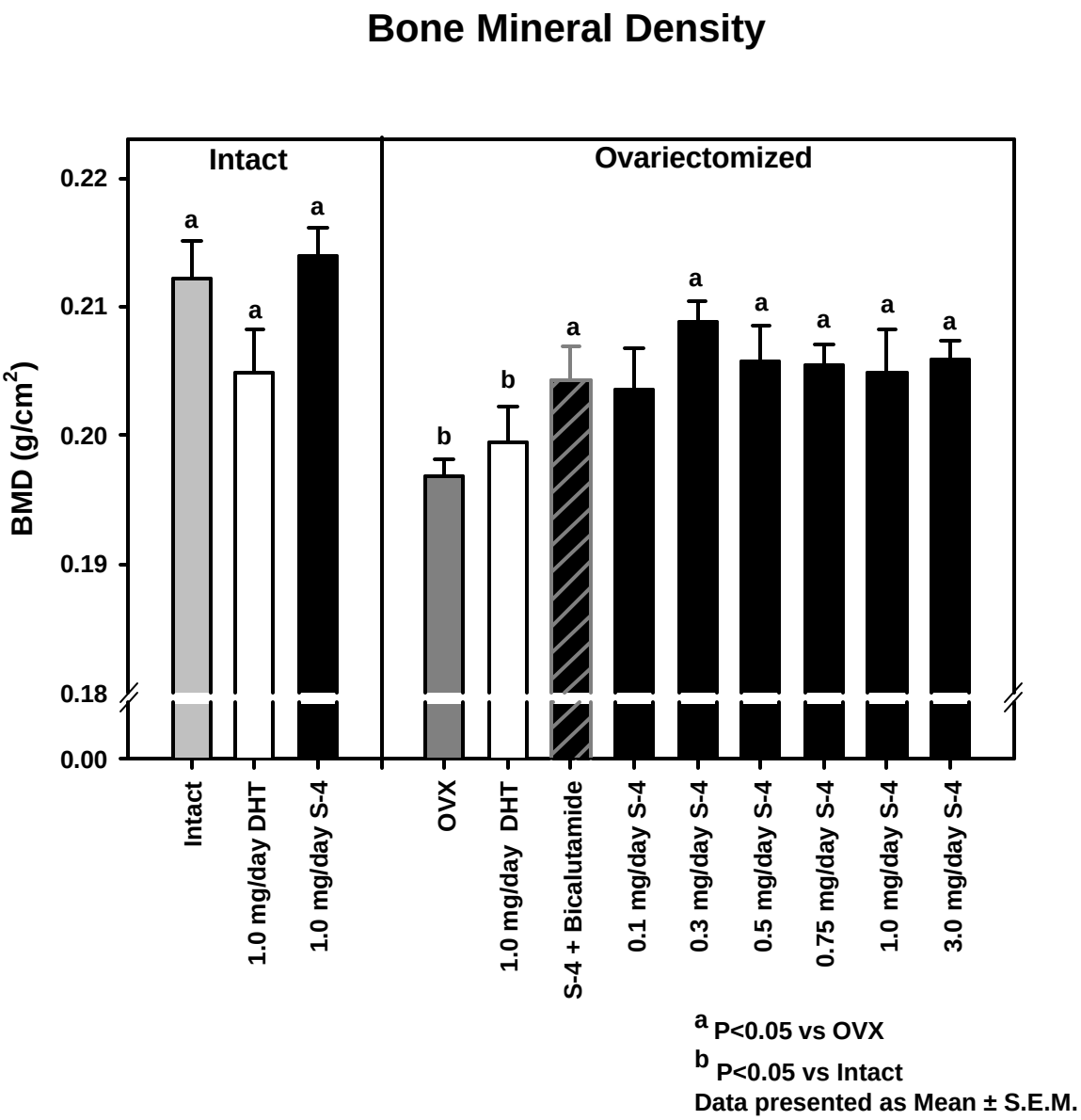

Figure 4.3: Whole body BMD (DEXA). Data for individual animals is summarized in Table C.1 of Appendix C.

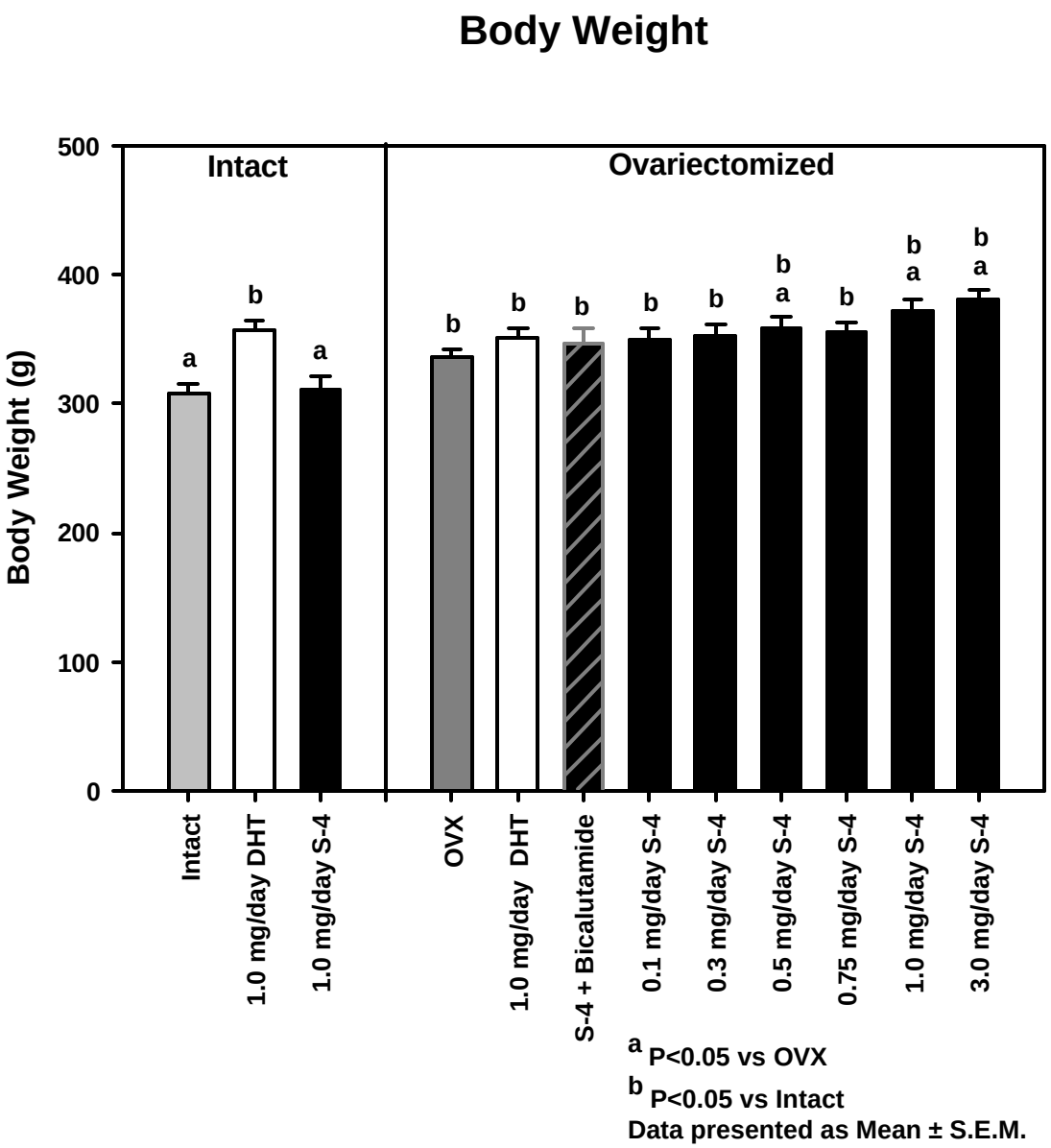

Figure 4.4: Body weight (DEXA). Data for individual animals is summarized in Table C.2 of Appendix C.

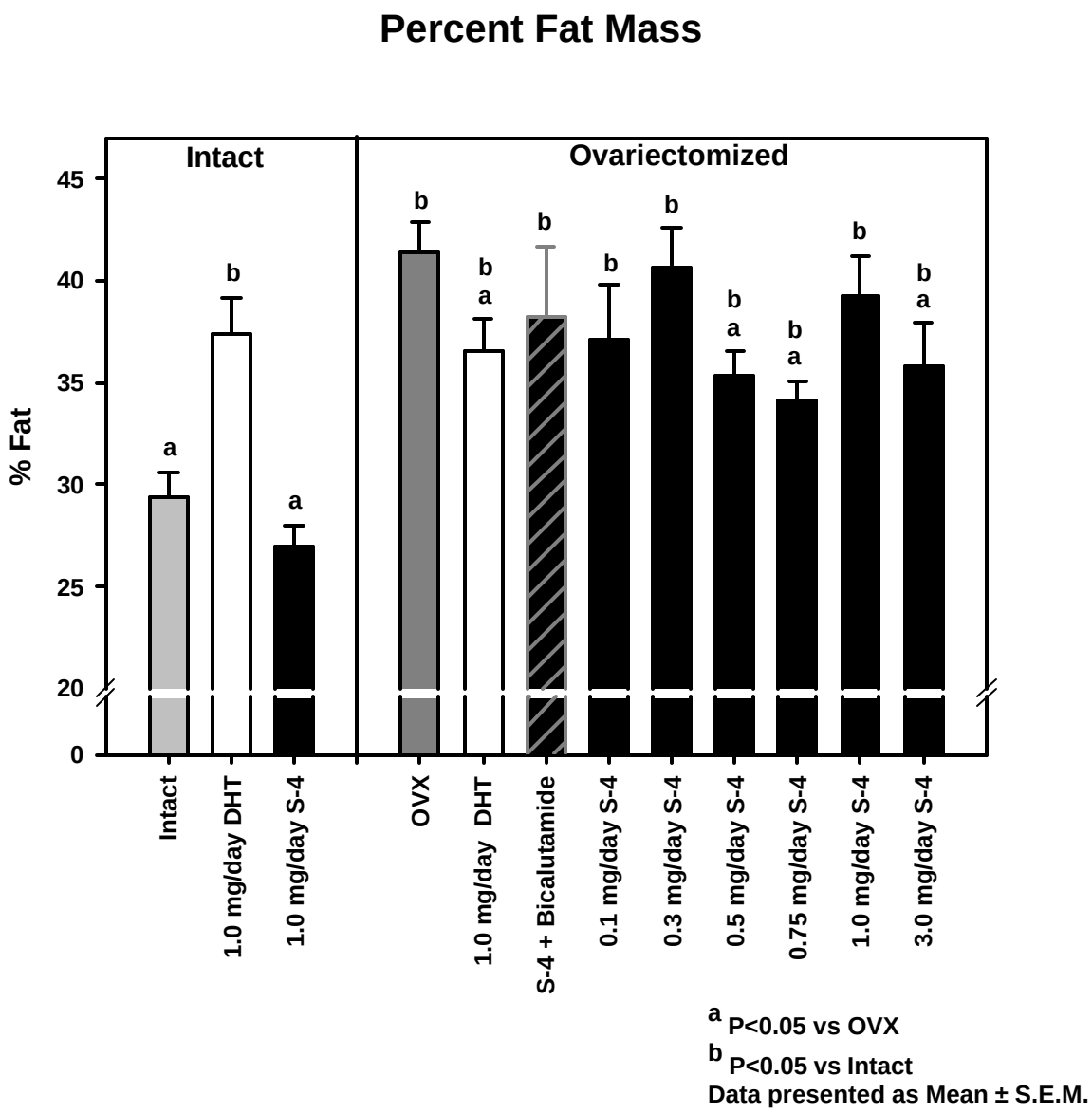

Figure 4.5: Percent fat mass (DEXA). Data for individual animals is summarized in Table C.3 of Appendix C.

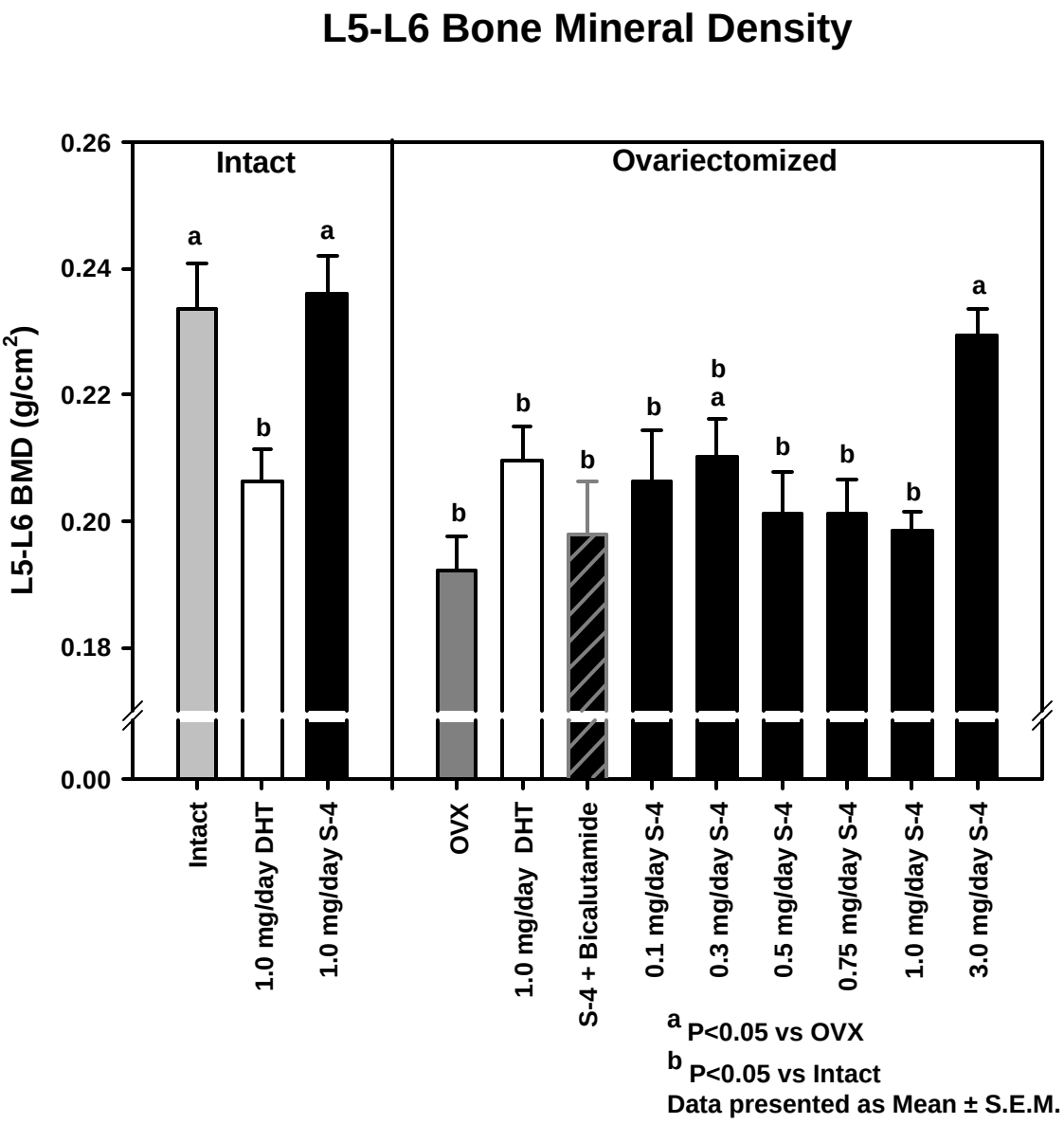

Figure 4.6: L5-L6 BMD (DEXA). Data for individual animals is summarized in Table C.4 of Appendix C.

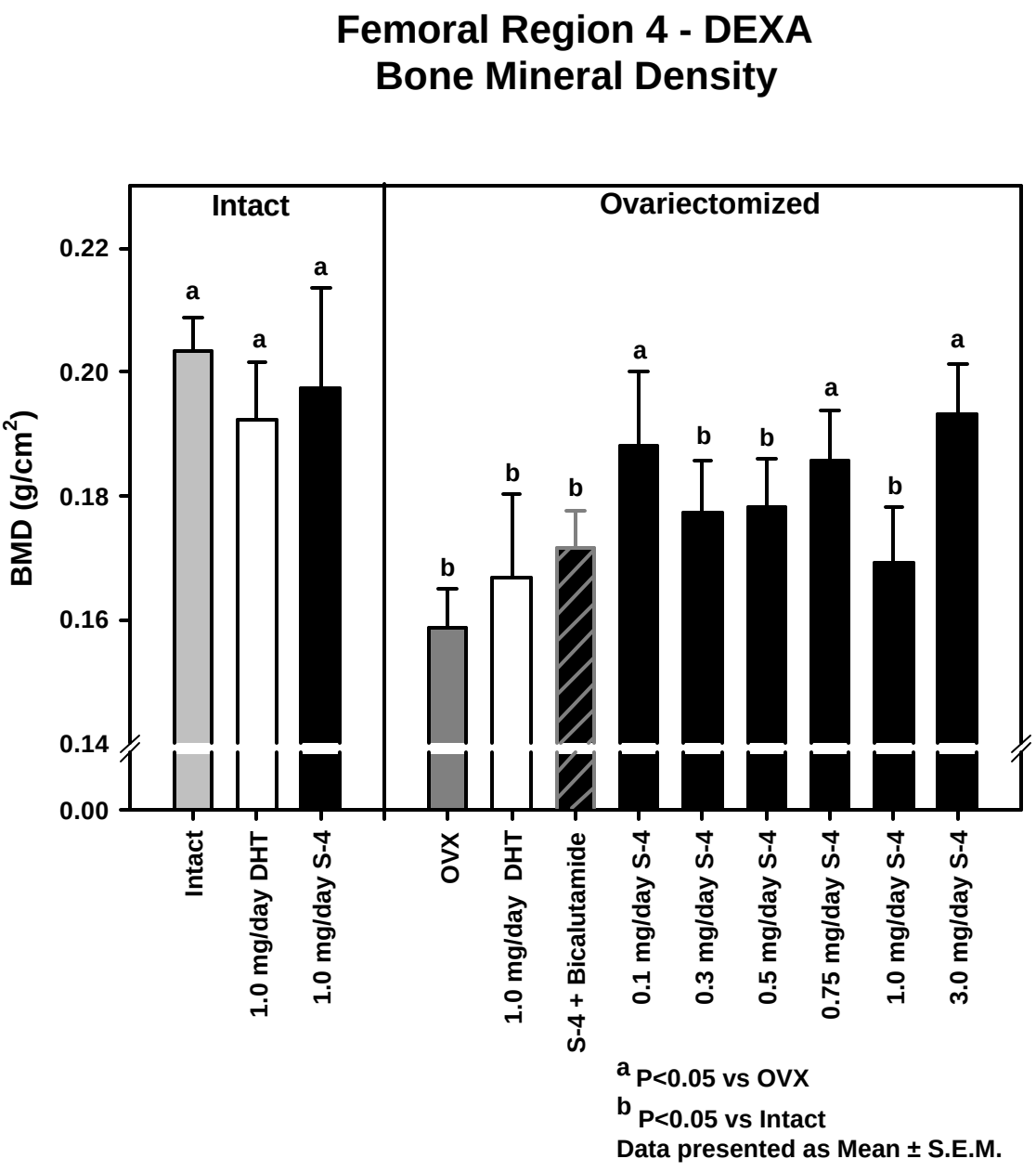

Figure 4.7: Femoral region 4 BMD (DEXA). Data for individual animals is summarized in Table C.5 of Appendix C.

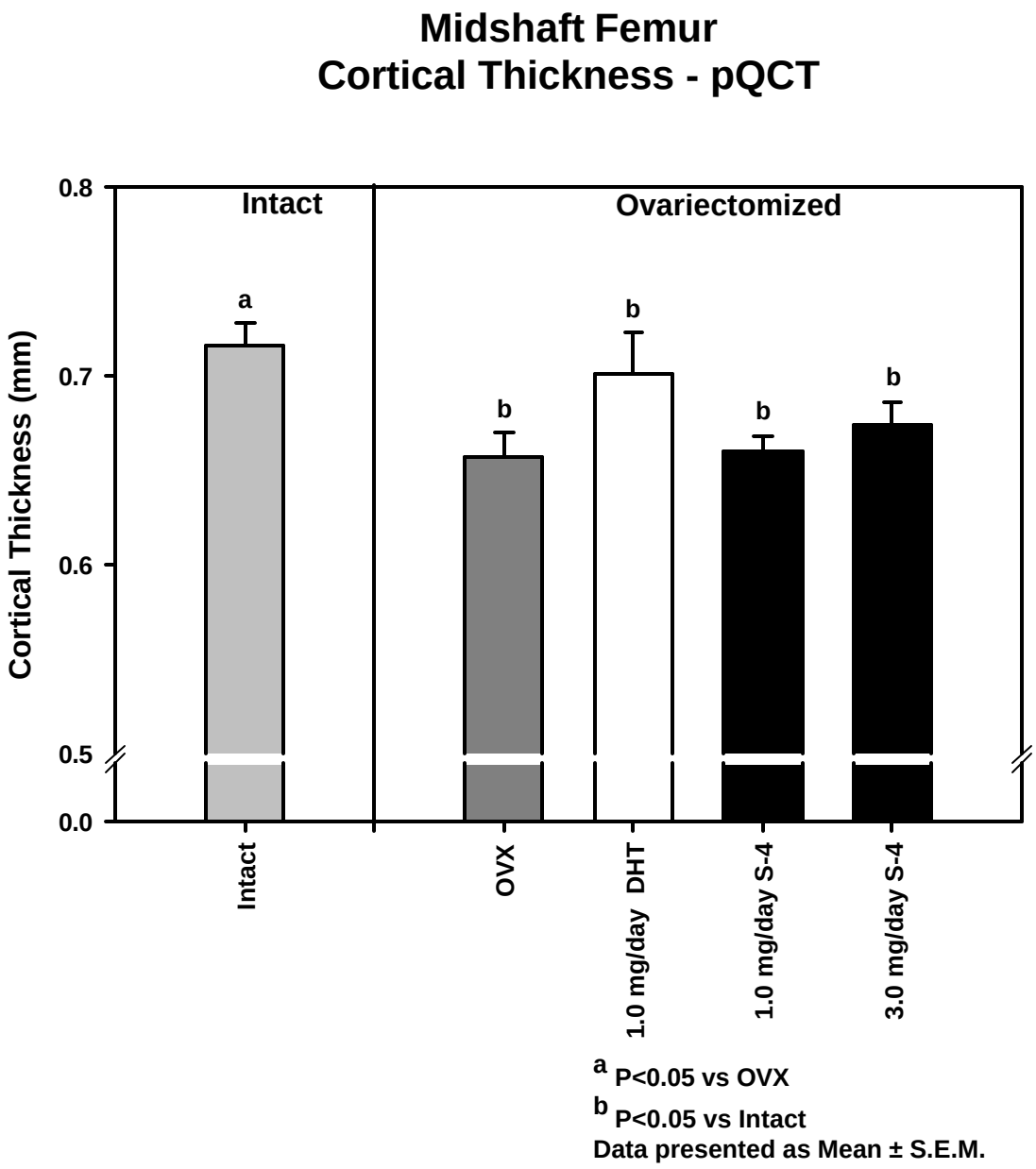

Figure 4.8: Cortical thickness of the mid-shaft femur (pQCT). Data for individual animals is summarized in Table C.6 of Appendix C.

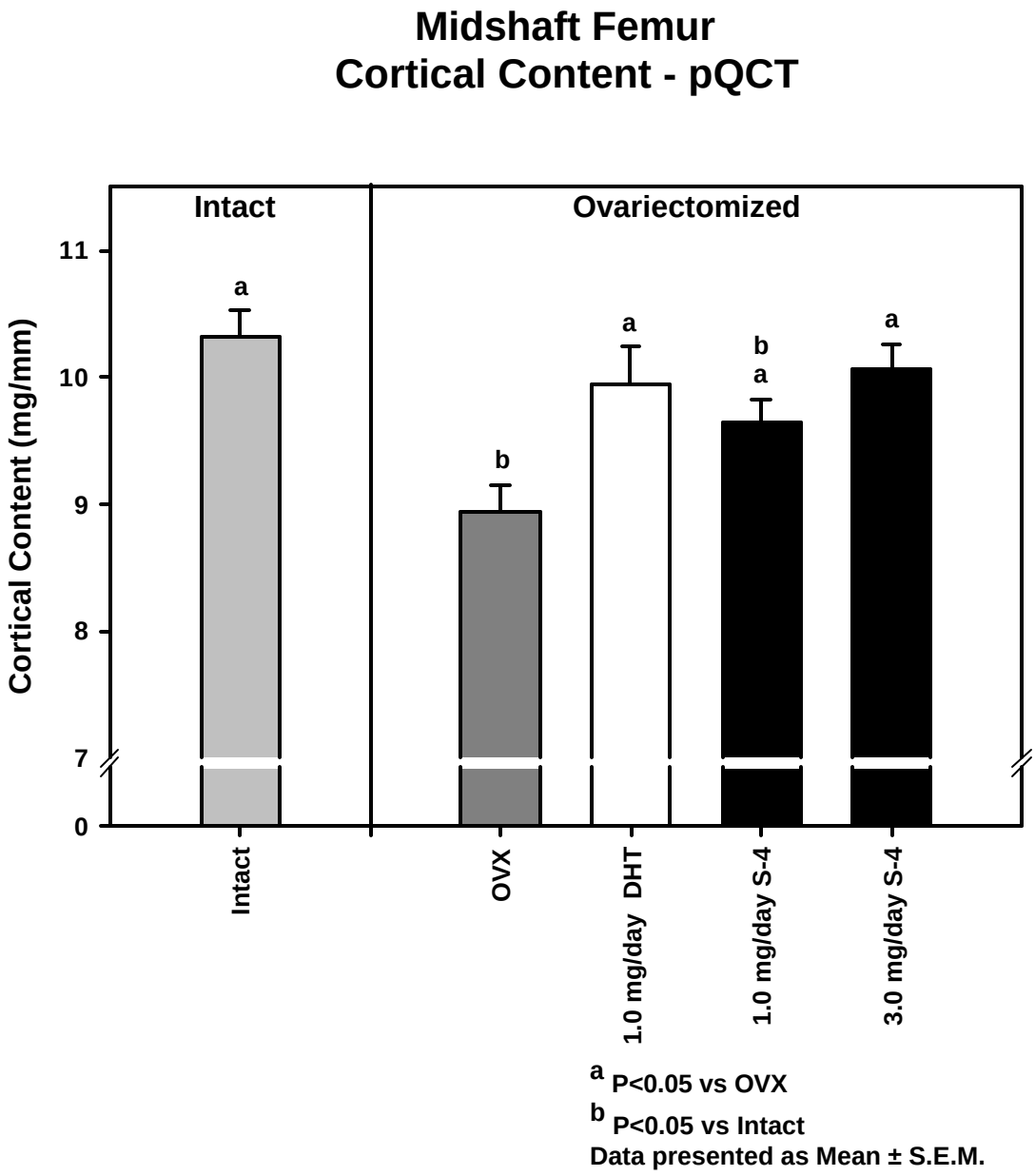

Figure 4.9: Cortical content at the mid-shaft femur (pQCT). Data for individual animals is summarized in Table C.7 of Appendix C.

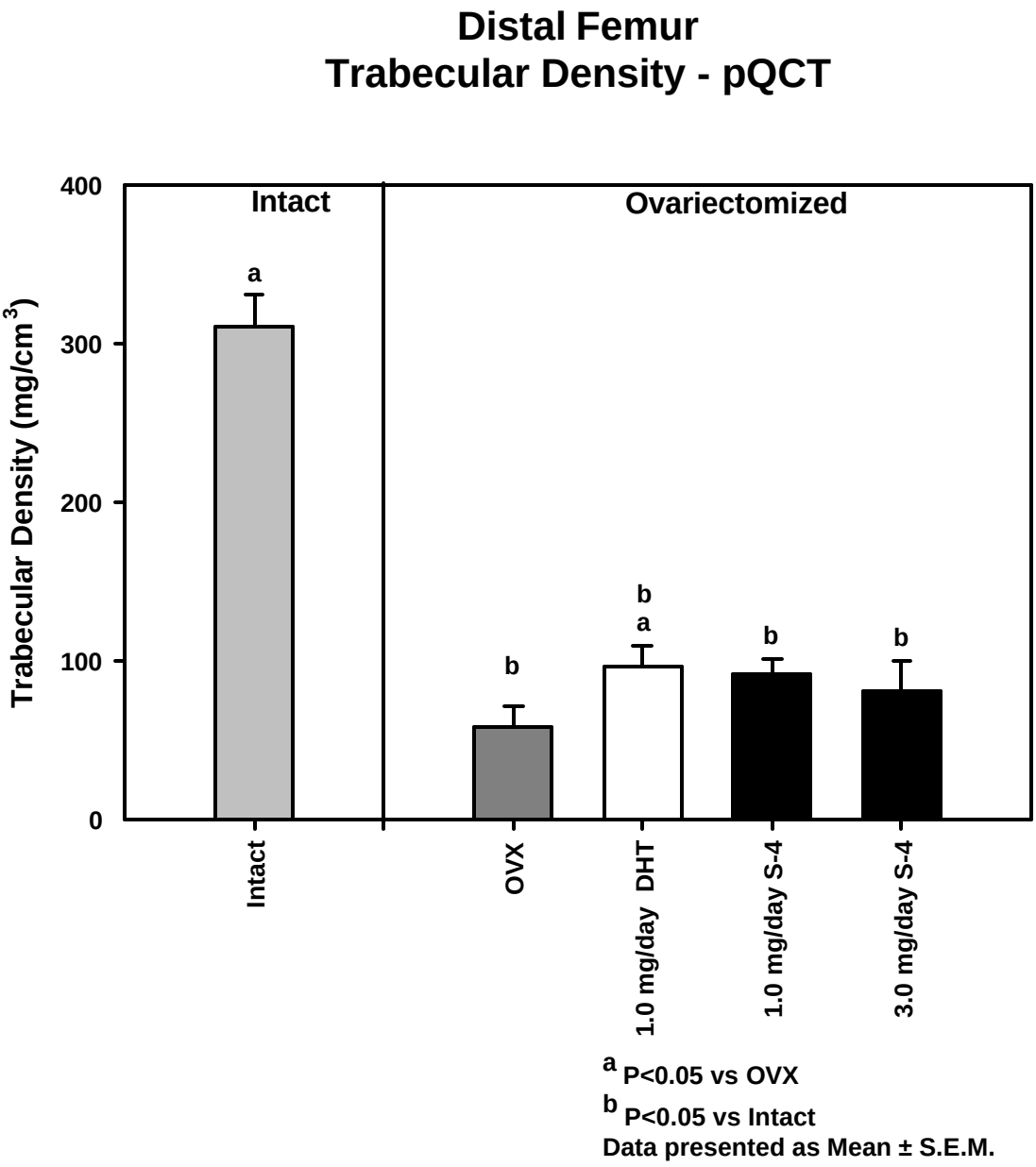

Figure 4.10: Distal femur trabecular bone density (pQCT). Data for individual animals is summarized in Table C.8 of Appendix C.

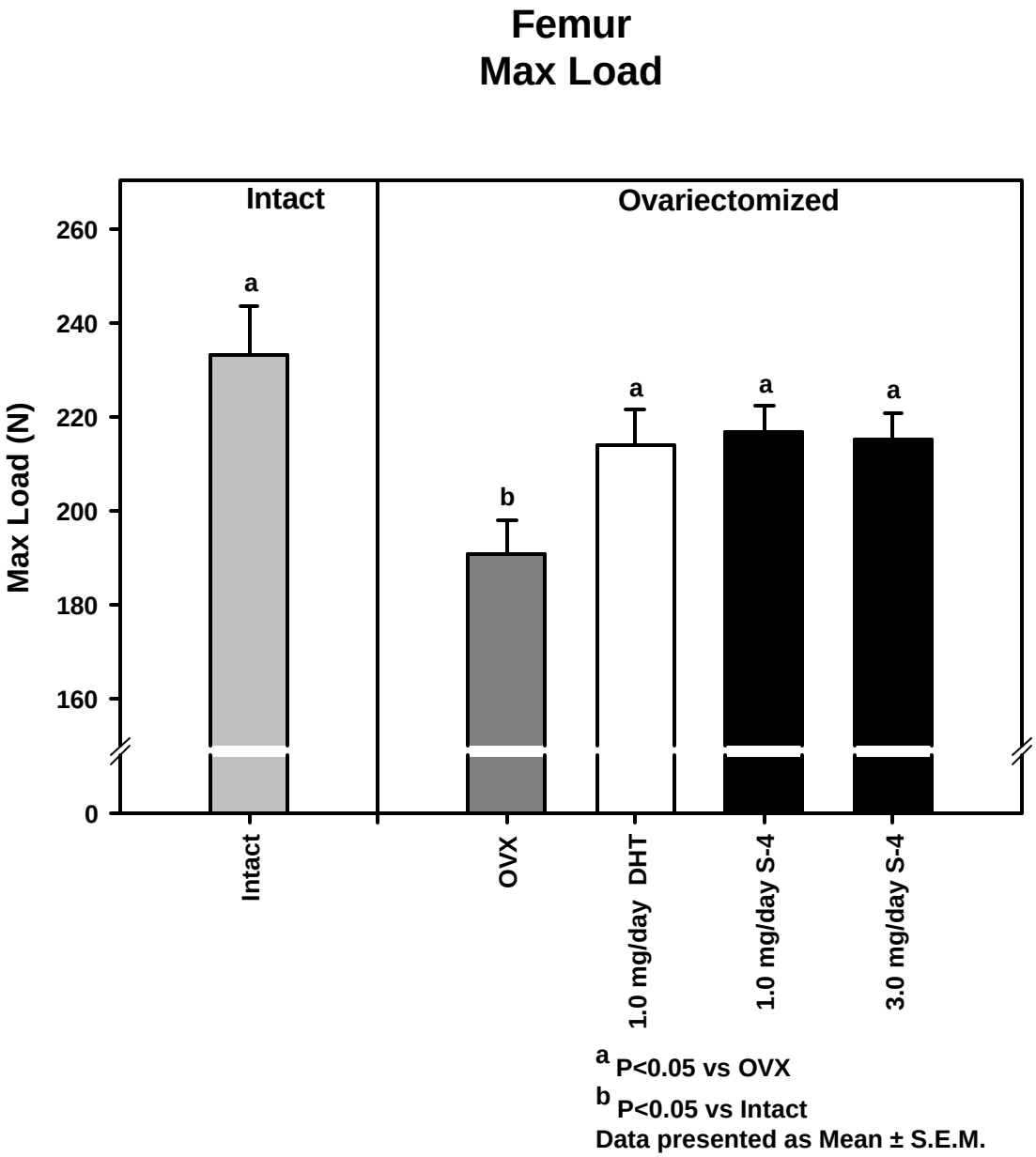

Figure 4.11: Femoral biomechanical testing of maximum load. Data for individual animals is summarized in Table C.9 of Appendix C.

CHAPTER 5

Summary and Conclusions

Androgens play a pivotal role in bone biology. However, side effect profiles and poor oral bioavailability limit the application of currently available androgen formulations. The discovery of nonsteroidal AR agonists with tissue selective pharmacologic effects provides a unique opportunity to more clearly define the role of androgens in skeletal growth and maintenance, as well as explore these new compounds for the treatment of osteoporosis. This novel class of therapeutic agents offers many potential advantages over steroidal androgens in regards to pharmacokinetic properties and tissue selectivity. During preclinical pharmacokinetic and pharmacodynamic characterization of several series of selective androgen receptor modulators, S-3-(4-acetylamino-phenoxy)-2-hydroxy-2-methyl-N-(4-nitro-3-trifluoromethyl-phenyl)-propionamide (S-4) emerged as our lead compound [19]. We employed a rational experimental design to test the hypothesis that treatment of ovariectomy-induced osteoporosis in animal models with an orally bioavailable nonsteroidal agonist for the AR, S-4, would exert a protective and proliferative effect on the skeleton.

The specific aims of this project were to: evaluate the therapeutic potential of S-4 based on its pharmacokinetic parameters in rats and delineate the protective and/or proliferative effects of SARMs on bone *in vivo.* To this end, we conducted pharmacokinetic studies in rats, skeletal pharmacology studies in a rat model of accelerated bone loss, and skeletal pharmacology studies in an osteopenic rat model.

We hypothesized that S-4 would be rapidly and completely absorbed after oral administration and avoid some of the historical drawbacks of testosterone administration due to its nonsteroidal structure. As expected, we observed decreased metabolic clearance and enhanced oral bioavailability compared to testosterone. S-4 demonstrates complete bioavailability, short time to peak plasma concentration, and relatively slow metabolic clearance at doses capable of eliciting maximal pharmacologic effect [19]. These properties favor the continued development of S-4 as an orally bioavailable nonsteroidal SARM.

In order to examine the protective effects of S-4 on bone loss, we evaluated the pharmacologic activity of S-4 in a rat model of accelerated bone loss. Our studies clearly show that OVX-induced changes in whole body BMD, body weight, percent fat mass, L5-L6 BMD, femoral BMD, femoral CT, femoral CC, femoral PC, trabecular density, biomechanical strength, and biological markers of bone resorption and formation are modulated by a nonsteroidal SARM. S-4 fully restored whole body BMD, L5-L6 BMD, femoral BMD, cortical content, and biomechanical strength in ovariectomized animals. Taken together, these data suggest that S-4 could provide a novel pharmacological intervention in the prevention of bone loss in postmenopausal women.

Finally, we assessed the anabolic activity of S-4 in an osteopenic rat model. Whole body BMD was fully restored in animals receiving > 0.1 mg/day S-4. Regional analysis of the L5-L6 vertebra and the femur by DEXA showed that S-4 completely restored BMD. pQCT results confirmed anabolic effects on the cortical bone in the femur, but trabecular density in the distal femur was unchanged with drug treatment. The lack of effect in trabecular bone was likely due to the lack of preexisting architecture upon which to rebuild lost bone. Complete restoration of the biomechanical strength in the femur further supports our conclusion that S-4 is anabolic in bone. These data suggest that S-4 is likely to significantly reduce the fracture risk in patients with osteoporosis through direct anabolic action on both muscle and bone. S-4 performed as well or better than DHT in these assays. As S-4 is anabolic in bone, orally bioavailable [117], tissue-selective [19], and does not cross-react with other steroid hormone receptors [17], it offers significant advantages over currently available therapies for osteoporosis.

These studies are the first to show that an orally bioavailable SARM can protect against bone loss, improve body composition, and rebuild lost bone. There are many antiresorptive therapies available, but parathyroid hormone (PTH) is the only FDA approved bone anabolic agent. However, PTH must be administered by daily subcutaneous injection, and is only indicated in high fracture risk patients. Therefore, patients with low bone mass are only placed on antiresorptive therapy to prevent further bone loss. Our results suggest that we may be able to exploit the bioavailability, selectivity, and anabolic activity of S-4 and offer a favorable anabolic option to patients with low bone mineral density.

While a great deal is known about estrogenic regulation of the skeleton, relatively little is known about androgenic skeletal regulation. Androgenic skeletal effects have been difficult to delineate due the lack of specific and selective AR agonist. Steroidal AR ligands, even in the presence of an aromatase inhibitor, exhibit some cross reactivity with other steroid hormone receptors and feedback at the level of the pituitary complicating the interpretation of the results. Further studies are needed to determine the mechanism of action for S-4 in bone. It will be important to determine if S-4 modulates gene expression in osteoblast cultures in the same manner as endogenous androgens. We believe S-4 is an ideal model compound to elucidate the debated effects of androgens in bone, since it cannot be aromatized to an estrogen, does not affect the pituitary hormone release, and shows no cross-reactivity with any of the other steroid hormone receptors. As our data suggests that S-4 is anabolic as opposed to antiresorptive in bone, it may be beneficial to examine combination therapies with S-4 and known antiresorptive agents. Overall, S-4 is a promising candidate for further development as an anabolic treatment for osteoporosis.

BIBLIOGRAPHY

1. Mooradian, A.D., J.E. Morley, and S.G. Korenman, Biological actions of androgens. *Endocr Rev*, 1987. 8(1): p. 1-28.

2. Davison, S.L. and S.R. Davis, Androgens in women. *J Steroid Biochem Mol Biol*, 2003. 85(2-5): p. 363-6.

3. Baniahmad, A., T.P. Burris, and M.-J. Tsai, The Nuclear Hormone Receptor Superfamily, in *Mechanism of steroid hormone regulation of gene transcription*, M.-J. Tsai and B.W. O'Malley, Editors. 1994, R.G. Landes Co.: Austin, Tex. p. 1-24.

4. Cooney, A.J. and S.Y. Tsai, Nuclear Receptor - DNA Interactions, in *Mechanism of steroid hormone regulation of gene transcription*, M.-J. Tsai and B.W. O'Malley, Editors. 1994, R.G. Landes Co.: Austin, Tex. p. 25-59.

5. Culig, Z., A. Hobisch, M.V. Cronauer, A. Hittmair, C. Radmayr, G. Bartsch, and H. Klocker, Activation of the androgen receptor by polypeptide growth factors and cellular regulators. *World J Urol*, 1995. 13(5): p. 285-9.

6. Culig, Z., A. Hobisch, M.V. Cronauer, C. Radmayr, J. Trapman, A. Hittmair, G. Bartsch, and H. Klocker, Androgen receptor activation in prostatic tumor cell lines by insulin-like growth factor-I, keratinocyte growth factor, and epidermal growth factor. *Cancer Res*, 1994. 54(20): p. 5474-8.

7. Weigel, N.L., Steroid hormone receptors and their regulation by phosphorylation. *Biochem J*, 1996. 319 (Pt 3): p. 657-67.

8. Judd, H.L., G.E. Judd, W.E. Lucas, and S.S. Yen, Endocrine function of the postmenopausal ovary: concentration of androgens and estrogens in ovarian and peripheral vein blood. *J Clin Endocrinol Metab*, 1974. 39(6): p. 1020-4.

9. Bachmann, G., J. Bancroft, G. Braunstein, H. Burger, S. Davis, L. Dennerstein, I. Goldstein, A. Guay, S. Leiblum, R. Lobo, M. Notelovitz, R. Rosen, P. Sarrel, B. Sherwin, J. Simon, E. Simpson, J. Shifren, R. Spark, and A. Traish, Female

androgen insufficiency: the Princeton consensus statement on definition, classification, and assessment. *Fertil Steril*, 2002. 77(4): p. 660-5.

10. Schneider, H.P., Androgens and antiandrogens. *Ann N Y Acad Sci*, 2003. 997: p. 292-306.

11. Gruenewald, D.A. and A.M. Matsumoto, Testosterone supplementation therapy for older men: potential benefits and risks. *J Am Geriatr Soc*, 2003. 51(1): p. 101-15; discussion 115.

12. MacIndoe, J.H., The challenges of testosterone deficiency. Uncovering the problem, evaluating the role of therapy. *Postgrad Med*, 2003. 114(4): p. 51-3, 57-8, 61-2.

13. Padero, M.C., S. Bhasin, and T.C. Friedman, Androgen supplementation in older women: too much hype, not enough data. *J Am Geriatr Soc*, 2002. 50(6): p. 1131-40.

14. Negro-Vilar, A., Selective androgen receptor modulators (SARMs): a novel approach to androgen therapy for the new millennium. *J Clin Endocrinol Metab*, 1999. 84(10): p. 3459-62.

15. Dalton, J.T., A. Mukherjee, Z. Zhu, L. Kirkovsky, and D.D. Miller, Discovery of nonsteroidal androgens. *Biochemical and Biophysical Research Communications*, 1998. 244(1): p. 1-4.

16. He, Y., D. Yin, M. Perera, L. Kirkovsky, N. Stourman, W. Li, J.T. Dalton, and D.D. Miller, Novel nonsteroidal ligands with high binding affinity and potent functional activity for the androgen receptor. *Eur J Med Chem*, 2002. 37(8): p. 619-34.

17. Yin, D., Y. He, M.A. Perera, S.S. Hong, C. Marhefka, N. Stourman, L. Kirkovsky, D.D. Miller, and J.T. Dalton, Key structural features of nonsteroidal ligands for binding and activation of the androgen receptor. *Mol Pharmacol*, 2003. 63(1): p. 211-23.

18. Yin, D., H. Xu, Y. He, L.I. Kirkovsky, D.D. Miller, and J.T. Dalton, Pharmacology, pharmacokinetics, and metabolism of acetothiolutamide, a novel nonsteroidal agonist for the androgen receptor. *Journal of Pharmacology and Experimental Therapeutics*, 2003. 304(3): p. 1323-33.

19. Yin, D., W. Gao, J.D. Kearbey, H. Xu, K. Chung, Y. He, C.A. Marhefka, K.A. Veverka, D.D. Miller, and J.T. Dalton, Pharmacodynamics of selective androgen receptor modulators. *Journal of Pharmacology and Experimental Therapeutics*, 2003. 304(3): p. 1334-40.

20. Ott, S., Osteoporosis and Bone Physiology. 1998. *http://courses.washington.edu/bonephys/opmale.html*.

21. Avioli, L.V. and M. Kleerekoper, Osteoporosis: The Clinical Problem, in *Bone Densitometry and Osteoporosis*, H.K. Genant, G. Guglielmi, and M. Jergas, Editors. 1998, Springer: Berlin. p. 1-20.

22. Francis, R.M., Pathogenesis of Osteoporosis, in *Osteoporosis: Pathogenesis and Management*, R.M. Francis, Editor. 1990, Kluwer: Lancaster. p. 51-80.

23. Melton, L.J., 3rd, E.A. Chrischilles, C. Cooper, A.W. Lane, and B.L. Riggs, Perspective. How many women have osteoporosis? *J Bone Miner Res*, 1992. 7(9): p. 1005-10.

24. Riggs, B.L. and L.J. Melton, 3rd, Involutional osteoporosis. *N Engl J Med*, 1986. 314(26): p. 1676-86.

25. Schneider, E.L. and J.M. Guralnik, The aging of America. Impact on health care costs. *Jama*, 1990. 263(17): p. 2335-40.

26. Cummings, S.R., S.M. Rubin, and D. Black, The future of hip fractures in the United States. Numbers, costs, and potential effects of postmenopausal estrogen. *Clin Orthop*, 1990(252): p. 163-6.

27. Poor, G., E.J. Atkinson, D.G. Lewallen, W.M. O'Fallon, and L.J. Melton, 3rd, Age-related hip fractures in men: clinical spectrum and short-term outcomes. *Osteoporos Int*, 1995. 5(6): p. 419-26.

28. Poor, G., E.J. Atkinson, W.M. O'Fallon, and L.J. Melton, 3rd, Determinants of reduced survival following hip fractures in men. *Clin Orthop*, 1995(319): p. 260-5.

29. Sernbo, I. and O. Johnell, Consequences of a hip fracture: a prospective study over 1 year. *Osteoporos Int*, 1993. 3(3): p. 148-53.

30. Martin, T.J. and D.W. Dempster, Bone Structure and Cellular Activity, in *Osteoporosis*, J.C. Stevenson and R. Lindsay, Editors. 1998, Champman & Hall: London. p. 1-28.

31. Beresford, J.N., J.A. Gallagher, J.W. Poser, and R.G. Russell, Production of osteocalcin by human bone cells in vitro. Effects of 1,25(OH)2D3, 24,25(OH)2D3, parathyroid hormone, and glucocorticoids. *Metab Bone Dis Relat Res*, 1984. 5(5): p. 229-34.

32. Robey, P.G. and J.D. Termine, Human bone cells in vitro. *Calcif Tissue Int*, 1985. 37(5): p. 453-60.

33. Peck, W.A., J.K. Burks, J. Wilkins, S.B. Rodan, and G.A. Rodan, Evidence for preferential effects of parathyroid hormone, calcitonin and adenosine on bone and periosteum. *Endocrinology*, 1977. 100(5): p. 1357-64.

34. Martin, T.J., K.W. Ng, N.C. Partridge, and S.A. Livesey, Hormonal influences on bone cells. *Methods Enzymol*, 1987. 145: p. 324-36.

35. Franceschi, R.T., W.M. James, and G. Zerlauth, 1 alpha, 25-dihydroxyvitamin D3 specific regulation of growth, morphology, and fibronectin in a human osteosarcoma cell line. *J Cell Physiol*, 1985. 123(3): p. 401-9.

36. Heldin, C.H., A. Johnsson, S. Wennergren, C. Wernstedt, C. Betsholtz, and B. Westermark, A human osteosarcoma cell line secretes a growth factor structurally related to a homodimer of PDGF A-chains. *Nature*, 1986. 319(6053): p. 511-4.

37. Rodan, S.B., Y. Imai, M.A. Thiede, G. Wesolowski, D. Thompson, Z. Bar-Shavit, S. Shull, K. Mann, and G.A. Rodan, Characterization of a human osteosarcoma cell line (Saos-2) with osteoblastic properties. *Cancer Res*, 1987. 47(18): p. 4961-6.

38. Gallagher, A., Human osteoblast culture, in *Bone research protocols*, M.H. Helfrich and S. Ralston, Editors. 2003, Humana Press: Totowa, N.J. p. 3-18.

39. Scutt, A., L. Reading, N. Scutt, and K. Still, Mineralizing fibroblast-colony-forming assays, in *Bone research protocols*, M.H. Helfrich and S. Ralston, Editors. 2003, Humana Press: Totowa, N.J. p. 29-39.

40. Thompson, D.D., H.A. Simmons, C.M. Pirie, and H.Z. Ke, FDA Guidelines and animal models for osteoporosis. *Bone*, 1995. 17(4 Suppl): p. 125S-133S.

41. Kalu, D.N., The ovariectomized rat model of postmenopausal bone loss. *Bone Miner*, 1991. 15(3): p. 175-91.

42. Yamauchi, H., K. Kushida, K. Yamazaki, and T. Inoue, Assessment of spine bone mineral density in ovariectomized rats using DXA. *J Bone Miner Res*, 1995. 10(7): p. 1033-9.

43. Jowsey, J., Studies of Haversian systems in man and some animals. *J Anat*, 1966. 100(4): p. 857-64.

44. Ziambaras, K. and R. Civitelli, Biochemical markers of bone turnover, in *Bone Densitometry and Osteoporosis*, H.K. Genant, G. Guglielmi, and M. Jergas, Editors. 1998, Springer: Berlin. p. 95-125.

45. Robins, S.P., Biochemical markers of bone turnover, in *Methods in Bone Biology*, T.R. Arnett and B. Henderson, Editors. 1997, Chapman and Hall: London. p. 229-250.

46. Ross, P.D., A. Lombardi, and D. Freedholm, The assesment of bone mass in men, in *Osteoporosis in men*, E.S. Orwoll, Editor. 1999, Academic Press: San Diego. p. 505-525.

47. Colvard, D.S., E.F. Eriksen, P.E. Keeting, E.M. Wilson, D.B. Lubahn, F.S. French, B.L. Riggs, and T.C. Spelsberg, Identification of androgen receptors in normal human osteoblast-like cells. *Proc Natl Acad Sci U S A*, 1989. 86(3): p. 854-7.

48. Liesegang, P., G. Romalo, M. Sudmann, L. Wolf, and H.U. Schweikert, Human osteoblast-like cells contain specific, saturable, high-affinity glucocorticoid, androgen, estrogen, and 1 alpha,25- dihydroxycholecalciferol receptors. *J Androl*, 1994. 15(3): p. 194-9.

49. Nakano, Y., I. Morimoto, O. Ishida, T. Fujihira, A. Mizokami, A. Tanimoto, N. Yanagihara, F. Izumi, and S. Eto, The receptor, metabolism and effects of androgen in osteoblastic MC3T3- E1 cells. *Bone Miner*, 1994. 26(3): p. 245-59.

50. Takeuchi, M., H. Kakushi, and M. Tohkin, Androgens directly stimulate mineralization and increase androgen receptors in human osteoblast-like osteosarcoma cells. *Biochem Biophys Res Commun*, 1994. 204(2): p. 905-11.

51. Zhuang, Y.H., M. Blauer, A. Pekki, and P. Tuohimaa, Subcellular location of androgen receptor in rat prostate, seminal vesicle and human osteosarcoma MG-63 cells. *J Steroid Biochem Mol Biol*, 1992. 41(3-8): p. 693-6.

52. Orwoll, E.S., L. Stribrska, E.E. Ramsey, and E.J. Keenan, Androgen receptors in osteoblast-like cell lines. *Calcif Tissue Int*, 1991. 49(3): p. 183-7.

53. Mizuno, Y., T. Hosoi, S. Inoue, A. Ikegami, M. Kaneki, Y. Akedo, T. Nakamura, Y. Ouchi, C. Chang, and H. Orimo, Immunocytochemical identification of androgen receptor in mouse osteoclast-like multinucleated cells. *Calcif Tissue Int*, 1994. 54(4): p. 325-6.

54. Bellido, T., R.L. Jilka, B.F. Boyce, G. Girasole, H. Broxmeyer, S.A. Dalrymple, R. Murray, and S.C. Manolagas, Regulation of interleukin-6, osteoclastogenesis,

and bone mass by androgens. The role of the androgen receptor. *J Clin Invest*, 1995. 95(6): p. 2886-95.

55. Abu, E.O., A. Horner, V. Kusec, J.T. Triffitt, and J.E. Compston, The localization of androgen receptors in human bone. *J Clin Endocrinol Metab*, 1997. 82(10): p. 3493-7.

56. Eriksen, E.F., D.S. Colvard, N.J. Berg, M.L. Graham, K.G. Mann, T.C. Spelsberg, and B.L. Riggs, Evidence of estrogen receptors in normal human osteoblast-like cells. *Science*, 1988. 241(4861): p. 84-6.

57. Fukayama, S. and A.H. Tashjian, Jr., Direct modulation by androgens of the response of human bone cells (SaOS-2) to human parathyroid hormone (PTH) and PTH-related protein. *Endocrinology*, 1989. 125(4): p. 1789-94.

58. Kasperk, C., R. Fitzsimmons, D. Strong, S. Mohan, J. Jennings, J. Wergedal, and D. Baylink, Studies of the mechanism by which androgens enhance mitogenesis and differentiation in bone cells. *J Clin Endocrinol Metab*, 1990. 71(5): p. 1322-9.

59. Weinstein, R.S., R.L. Jilka, A.M. Parfitt, and S.C. Manolagas, The effects of androgen deficiency on murine bone remodeling and bone mineral density are mediated via cells of the osteoblastic lineage. *Endocrinology*, 1997. 138(9): p. 4013-21.

60. Wiren, K.M., X. Zhang, C. Chang, E. Keenan, and E.S. Orwoll, Transcriptional up-regulation of the human androgen receptor by androgen in bone cells. *Endocrinology*, 1997. 138(6): p. 2291-300.

61. Kasperk, C.H., J.E. Wergedal, J.R. Farley, T.A. Linkhart, R.T. Turner, and D.J. Baylink, Androgens directly stimulate proliferation of bone cells in vitro. *Endocrinology*, 1989. 124(3): p. 1576-8.

62. Hofbauer, L.C., R.M. Ten, and S. Khosla, The anti-androgen hydroxyflutamide and androgens inhibit interleukin-6 production by an androgen-responsive human osteoblastic cell line. *J Bone Miner Res*, 1999. 14(8): p. 1330-7.

63. Poli, V., R. Balena, E. Fattori, A. Markatos, M. Yamamoto, H. Tanaka, G. Ciliberto, G.A. Rodan, and F. Costantini, Interleukin-6 deficient mice are protected from bone loss caused by estrogen depletion. *Embo J*, 1994. 13(5): p. 1189-96.

64. Jilka, R.L., G. Hangoc, G. Girasole, G. Passeri, D.C. Williams, J.S. Abrams, B. Boyce, H. Broxmeyer, and S.C. Manolagas, Increased osteoclast development after estrogen loss: mediation by interleukin-6. *Science*, 1992. 257(5066): p. 88-91.

65. Gori, F., L.C. Hofbauer, C.A. Conover, and S. Khosla, Effects of androgens on the insulin-like growth factor system in an androgen-responsive human osteoblastic cell line. *Endocrinology*, 1999. 140(12): p. 5579-86.

66. Yakar, S., C.J. Rosen, W.G. Beamer, C.L. Ackert-Bicknell, Y. Wu, J.L. Liu, G.T. Ooi, J. Setser, J. Frystyk, Y.R. Boisclair, and D. LeRoith, Circulating levels of IGF-1 directly regulate bone growth and density. *J Clin Invest*, 2002. 110(6): p. 771-81.

67. Delany, A.M., J.M. Pash, and E. Canalis, Cellular and clinical perspectives on skeletal insulin-like growth factor I. *J Cell Biochem*, 1994. 55(3): p. 328-33.

68. Vanderschueren, D., Androgens and their role in skeletal homeostasis. *Horm Res*, 1996. 46(2): p. 95-8.

69. Turner, R.T., G.K. Wakley, and K.S. Hannon, Differential effects of androgens on cortical bone histomorphometry in gonadectomized male and female rats. *J Orthop Res*, 1990. 8(4): p. 612-7.

70. Hanada, K., K. Furuya, N. Yamamoto, H. Nejishima, K. Ichikawa, T. Nakamura, M. Miyakawa, S. Amano, Y. Sumita, and N. Oguro, Bone anabolic effects of S-40503, a novel nonsteroidal selective androgen receptor modulator (SARM), in rat models of osteoporosis. *Biol Pharm Bull*, 2003. 26(11): p. 1563-9.

71. Tobias, J.H., A. Gallagher, and T.J. Chambers, 5 alpha-Dihydrotestosterone partially restores cancellous bone volume in osteopenic ovariectomized rats. *Am J Physiol*, 1994. 267(6 Pt 1): p. E853-9.

72. Gallagher, A.C., T.J. Chambers, and J.H. Tobias, Androgens contribute to the stimulation of cancellous bone formation by ovarian hormones in female rats. *Am J Physiol*, 1996. 270(3 Pt 1): p. E407-12.

73. Soule, S.G., G. Conway, G.M. Prelevic, M. Prentice, J. Ginsburg, and H.S. Jacobs, Osteopenia as a feature of the androgen insensitivity syndrome. *Clin Endocrinol (Oxf)*, 1995. 43(6): p. 671-5.

74. Munoz-Torres, M., E. Jodar, M. Quesada, and F. Escobar-Jimenez, Bone mass in androgen-insensitivity syndrome: response to hormonal replacement therapy. *Calcif Tissue Int*, 1995. 57(2): p. 94-6.

75. Finkelstein, J.S., A. Klibanski, R.M. Neer, S.L. Greenspan, D.I. Rosenthal, and W.F. Crowley, Jr., Osteoporosis in men with idiopathic hypogonadotropic hypogonadism. *Ann Intern Med*, 1987. 106(3): p. 354-61.

76. Arisaka, O., M. Arisaka, A. Hosaka, N. Shimura, and K. Yabuta, Effect of testosterone on radial bone mineral density in adolescent male hypogonadism. *Acta Paediatr Scand*, 1991. 80(3): p. 378-80.

77. Devogelaer, J.P., S. De Cooman, and C. Nagant de Deuxchaisnes, Low bone mass in hypogonadal males. Effect of testosterone substitution therapy, a densitometric study. *Maturitas*, 1992. 15(1): p. 17-23.

78. Stanhope, R., C.R. Buchanan, G.C. Fenn, and M.A. Preece, Double blind placebo controlled trial of low dose oxandrolone in the treatment of boys with constitutional delay of growth and puberty. *Arch Dis Child*, 1988. 63(5): p. 501-5.

79. Keenan, B.S., G.E. Richards, S.W. Ponder, J.S. Dallas, M. Nagamani, and E.R. Smith, Androgen-stimulated pubertal growth: the effects of testosterone and dihydrotestosterone on growth hormone and insulin-like growth factor-I in the treatment of short stature and delayed puberty. *J Clin Endocrinol Metab*, 1993. 76(4): p. 996-1001.

80. Martin, B., Aging and strength of bone as a structural material. *Calcif Tissue Int*, 1993. 53(Suppl 1): p. S34-9; discussion S39-40.

81. Bonjour, J.P., G. Theintz, F. Law, D. Slosman, and R. Rizzoli, Peak bone mass. *Osteoporos Int*, 1994. 4(Suppl 1): p. 7-13.

82. van der Meulen, M.C., M.W. Ashford, Jr., B.J. Kiratli, L.K. Bachrach, and D.R. Carter, Determinants of femoral geometry and structure during adolescent growth. *J Orthop Res*, 1996. 14(1): p. 22-9.

83. Baran, D.T., M.A. Bergfeld, S.L. Teitelbaum, and L.V. Avioli, Effect of testosterone therapy on bone formation in an osteoporotic hypogonadal male. *Calcif Tissue Res*, 1978. 26(2): p. 103-6.

84. Morita, R., I. Yamamoto, M. Fukunaga, S. Dokoh, J. Konishi, T. Kousaka, K. Nakajima, K. Torizuka, T. Aso, and T. Motohashi, Changes in sex hormones and calcium regulating hormones with reference to bone mass associated with aging. *Endocrinol Jpn*, 1979. 26(Suppl): p. 15-22.

85. Foresta, C., B. Busnardo, G. Ruzza, G. Zanatta, and R. Mioni, Lower calcitonin levels in young hypogonadic men with osteoporosis. *Horm Metab Res*, 1983. 15(4): p. 206-7.

86. Foresta, C., G. Ruzza, R. Mioni, A. Meneghello, and C. Baccichetti, Testosterone and bone loss in Klinefelter syndrome. *Horm Metab Res*, 1983. 15(1): p. 56-7.

87. Foresta, C., G. Ruzza, R. Mioni, G. Guarneri, R. Gribaldo, A. Meneghello, and I. Mastrogiacomo, Osteoporosis and decline of gonadal function in the elderly male. *Horm Res*, 1984. 19(1): p. 18-22.

88. Baille, S.P., C.E. Davison, F.J. Johnson, and R.M. Francis, Pathogenesis of vertebral crush fractures in men. *Age Ageing*, 1992. 21: p. 139-41.

89. Leifke, E., H.C. Korner, T.M. Link, H.M. Behre, P.E. Peters, and E. Nieschlag, Effects of testosterone replacement therapy on cortical and trabecular bone mineral density, vertebral body area and paraspinal muscle area in hypogonadal men. *Eur J Endocrinol*, 1998. 138(1): p. 51-8.

90. Behre, H.M., S. Kliesch, E. Leifke, T.M. Link, and E. Nieschlag, Long-term effect of testosterone therapy on bone mineral density in hypogonadal men. *J Clin Endocrinol Metab*, 1997. 82(8): p. 2386-90.

91. Katznelson, L., J.S. Finkelstein, D.A. Schoenfeld, D.I. Rosenthal, E.J. Anderson, and A. Klibanski, Increase in bone density and lean body mass during testosterone administration in men with acquired hypogonadism. *J Clin Endocrinol Metab*, 1996. 81(12): p. 4358-65.

92. Isaia, G., M. Mussetta, F. Pecchio, A. Sciolla, M. di Stefano, and G.M. Molinatti, Effect of testosterone on bone in hypogonadal males. *Maturitas*, 1992. 15(1): p. 47-51.

93. Devogelaer, J.P., S. De Cooman, and C. Nagant de Deuxchaisnes, Low bone mass in hypogonadal males. Effect of testosterone substitution therapy, a densitometric study. *Maturitas*, 1992. 15(1): p. 17-23.

94. Reid, I.R., D.J. Wattie, M.C. Evans, and J.P. Stapleton, Testosterone therapy in glucocorticoid-treated men. *Arch Intern Med*, 1996. 156(11): p. 1173-7.

95. Anderson, F.H., R.M. Francis, and K. Faulkner, Androgen supplementation in eugonadal men with osteoporosis-effects of 6 months of treatment on bone mineral density and cardiovascular risk factors. *Bone*, 1996. 18(2): p. 171-7.

96. Finkelstein, J.S., A. Klibanski, R.M. Neer, S.H. Doppelt, D.I. Rosenthal, G.V. Segre, and W.F. Crowley, Jr., Increases in bone density during treatment of men with idiopathic hypogonadotropic hypogonadism. *J Clin Endocrinol Metab*, 1989. 69(4): p. 776-83.

97. Wu, F.C., Testicular steroidogenesis and androgen use and abuse. *Baillieres Clin Endocrinol Metab*, 1992. 6(2): p. 373-403.

98. Bhasin, S. and W.J. Bremner, Clinical review 85: Emerging issues in androgen replacement therapy. *J Clin Endocrinol Metab*, 1997. 82(1): p. 3-8.

99. Handelsman, D.J., A.J. Conway, and L.M. Boylan, Pharmacokinetics and pharmacodynamics of testosterone pellets in man. *J Clin Endocrinol Metab*, 1990. 71(1): p. 216-22.

100. Wilson, J.D., Androgens, in *The Pharmacological Basis of Therapeutics*, J.G. Hardman, L.E. Limbird, P.B. Molinoff, R.W. Ruddon, and A.G. Gilman, Editors. 1996, McGraw-Hill: New York. p. 1441-1458.

101. Rhoden, E.L. and A. Morgentaler, Risks of testosterone-replacement therapy and recommendations for monitoring. *N Engl J Med*, 2004. 350(5): p. 482-92.

102. Heywood, R., H. Chesterman, S.A. Ball, and P.F. Wadsworth, Toxicity of methyl testosterone in the beagle dog. *Toxicology*, 1977. 7(3): p. 357-65.

103. Ishak, K.G. and H.J. Zimmerman, Hepatotoxic effects of the anabolic/androgenic steroids. *Semin Liver Dis*, 1987. 7(3): p. 230-6.

104. Velazquez, E. and G. Bellabarba Arata, Testosterone replacement therapy. *Arch Androl*, 1998. 41(2): p. 79-90.

105. Wang, C., R.S. Swedloff, A. Iranmanesh, A. Dobs, P.J. Snyder, G. Cunningham, A.M. Matsumoto, T. Weber, and N. Berman, Transdermal testosterone gel improves sexual function, mood, muscle strength, and body composition parameters in hypogonadal men. Testosterone Gel Study Group. *J Clin Endocrinol Metab*, 2000. 85(8): p. 2839-53.

106. Wilson, J.D., J. Aiman, and P.C. MacDonald, The pathogenesis of gynecomastia. *Adv Intern Med*, 1980. 25: p. 1-32.

107. Marhefka, C.A., W. Gao, K. Chung, J. Kim, Y. He, D. Yin, C. Bohl, J.T. Dalton, and D.D. Miller, Design, synthesis, and biological characterization of metabolically stable selective androgen receptor modulators. *J Med Chem*, 2004. 47(4): p. 993-8.

108. Davies, B. and T. Morris, Physiological parameters in laboratory animals and humans. *Pharm Res*, 1993. 10(7): p. 1093-5.

109. Boyle, G.W., D. McKillop, P.J. Phillips, J.R. Harding, R. Pickford, and A.D. McCormick, Metabolism of Casodex in laboratory animals. *Xenobiotica*, 1993. 23(7): p. 781-98.

110. Kearbey, J.D., W. Gao, D.D. Miller, and J.T. Dalton, Selective androgen receptor modulators inhibit bone resorption in rats. *AAPS Pharm Sci*, 2003. 5(S1).

111. Mukherjee, A., L.I. Kirkovsky, Y. Kimura, M.M. Marvel, D.D. Miller, and J.T. Dalton, Affinity labeling of the androgen receptor with nonsteroidal chemoaffinity ligands. *Biochem Pharmacol*, 1999. 58(8): p. 1259-67.

112. Wang, D.Y., R.D. Bulbrook, A. Sneddon, and T. Hamilton, The metabolic clearance rates of dehydroepiandrosterone, testosterone and their sulphate esters in man, rat and rabbit. *J Endocrinol*, 1967. 38(3): p. 307-18.

113. Goulding, A. and E. Gold, Flutamide-mediated androgen blockade evokes osteopenia in the female rat. *J Bone Miner Res*, 1993. 8(6): p. 763-9.

114. Lea, C., N. Kendall, and A.M. Flanagan, Casodex (a nonsteroidal antiandrogen) reduces cancellous, endosteal, and periosteal bone formation in estrogen-replete female rats. *Calcif Tissue Int*, 1996. 58(4): p. 268-72.

115. Lea, C.K. and A.M. Flanagan, Physiological plasma levels of androgens reduce bone loss in the ovariectomized rat. *Am J Physiol*, 1998. 274(2 Pt 1): p. E328-35.

116. Lea, C.K., V. Moxham, M.J. Reed, and A.M. Flanagan, Androstenedione treatment reduces loss of cancellous bone volume in ovariectomised rats in a dose-responsive manner and the effect is not mediated by oestrogen. *J Endocrinol*, 1998. 156(2): p. 331-9.

117. Kearbey, J.D., D. Wu, W. Gao, D.D. Miller, and J.T. Dalton, Pharmacokinetics of S-3-(4-acetylamino-phenoxy)-2-hydroxy-2-methyl-N-(4-nitro-3-trifluoromethyl-phenyl)-propionamide, a nonsteroidal selective androgen receptor modulator. *Xenobiotica*, 2004. 34(3): p. 273-280.

118. Davey, R.A., C.N. Hahn, B.K. May, and H.A. Morris, Osteoblast gene expression in rat long bones: effects of ovariectomy and dihydrotestosterone on mRNA levels. *Calcif Tissue Int*, 2000. 67(1): p. 75-9.

119. Erben, R.G., J. Eberle, K. Stahr, and M. Goldberg, Androgen deficiency induces high turnover osteopenia in aged male rats: a sequential histomorphometric study. *J Bone Miner Res*, 2000. 15(6): p. 1085-98.

120. Hofbauer, L.C., K.C. Hicok, and S. Khosla, Effects of gonadal and adrenal androgens in a novel androgen-responsive human osteoblastic cell line. *J Cell Biochem*, 1998. 71(1): p. 96-108.

121. Hofbauer, L.C. and S. Khosla, Androgen effects on bone metabolism: recent progress and controversies. *Eur J Endocrinol*, 1999. 140(4): p. 271-86.

122. Kasra, M. and M.D. Grynpas, The effects of androgens on the mechanical properties of primate bone. *Bone*, 1995. 17(3): p. 265-70.

123. Khosla, S., The effects of androgens on osteoblast function in vitro. *Mayo Clin Proc*, 2000. 75 Suppl: p. S51-4.

124. Pederson, L., M. Kremer, J. Judd, D. Pascoe, T.C. Spelsberg, B.L. Riggs, and M.J. Oursler, Androgens regulate bone resorption activity of isolated osteoclasts in vitro. *Proc Natl Acad Sci U S A*, 1999. 96(2): p. 505-10.

125. Vandenput, L., A.G. Ederveen, R.G. Erben, K. Stahr, J.V. Swinnen, E. Van Herck, A. Verstuyf, S. Boonen, R. Bouillon, and D. Vanderschueren, Testosterone prevents orchidectomy-induced bone loss in estrogen receptor-alpha knockout mice. *Biochem Biophys Res Commun*, 2001. 285(1): p. 70-6.

126. Vanderschueren, D. and L. Vandenput, Androgens and osteoporosis. *Andrologia*, 2000. 32(3): p. 125-30.

127. Vanderschueren, D., E. Van Herck, A.M. Suiker, W.J. Visser, L.P. Schot, and R. Bouillon, Bone and mineral metabolism in aged male rats: short and long term effects of androgen deficiency. *Endocrinology*, 1992. 130(5): p. 2906-16.

128. Vanderschueren, D., L. Vandenput, S. Boonen, E. Van Herck, J.V. Swinnen, and R. Bouillon, An aged rat model of partial androgen deficiency: prevention of both loss of bone and lean body mass by low-dose androgen replacement. *Endocrinology*, 2000. 141(5): p. 1642-7.

129. Kalu, D.N., Evaluation of the pathogenesis of skeletal changes in ovariectomized rats. *Endocrinology*, 1984. 115(2): p. 507-12.

130. Kalu, D.N. and R.R. Hardin, Evaluation of the role of calcitonin deficiency in ovariectomy-induced osteopenia. *Life Sci*, 1984. 34(24): p. 2393-8.

131. Burger, H.G. and S.R. Davis, The role of androgen therapy. *Best Pract Res Clin Obstet Gynaecol*, 2002. 16(3): p. 383-93.

132. Lipsitz, L.A., I. Nakajima, M. Gagnon, T. Hirayama, C.M. Connelly, and H. Izumo, Muscle strength and fall rates among residents of Japanese and American nursing homes: an International Cross-Cultural Study. *J Am Geriatr Soc*, 1994. 42(9): p. 953-9.

133. Newton, J.L., R.A. Kenny, R. Frearson, and R.M. Francis, A prospective evaluation of bone mineral density measurement in females who have fallen. *Age Ageing*, 2003. 32(5): p. 497-502.

134. Lea, C.K. and A.M. Flanagan, Ovarian androgens protect against bone loss in rats made oestrogen deficient by treatment with ICI 182,780. *J Endocrinol*, 1999. 160(1): p. 111-7.

135. Bauss, F., S. Lalla, R. Endele, and L.A. Hothorn, Effects of treatment with ibandronate on bone mass, architecture, biomechanical properties, and bone concentration of ibandronate in ovariectomized aged rats. *J Rheumatol*, 2002. 29(10): p. 2200-8.

136. Kalu, D.N., C.C. Liu, E. Salerno, B. Hollis, R. Echon, and M. Ray, Skeletal response of ovariectomized rats to low and high doses of 17 beta-estradiol. *Bone Miner*, 1991. 14(3): p. 175-87.

137. Osterman, T., L. Lauren, P. Kuurtamo, R. Hannuniemi, P. Isaksson, K. Kippo, Z. Peng, H.K. Vaananen, and R. Sellman, The effect of orally administered clodronate on bone mineral density and bone geometry in ovariectomized rats. *J Pharmacol Exp Ther*, 1998. 284(1): p. 312-6.

138. Rubin, M.R. and J.P. Bilezikian, New anabolic therapies in osteoporosis. *Endocrinol Metab Clin North Am*, 2003. 32(1): p. 285-307.

139. Wronski, T.J., M. Cintron, and L.M. Dann, Temporal relationship between bone loss and increased bone turnover in ovariectomized rats. *Calcif Tissue Int*, 1988. 43(3): p. 179-83.

140. Samnegard, E., M.P. Akhter, and R.R. Recker, Maintenance of vertebral body bone mass and strength created by human parathyroid hormone treatment in ovariectomized rats. *Bone*, 2001. 28(4): p. 414-22.

141. Samnegard, E., U.T. Iwaniec, D.M. Cullen, D.B. Kimmel, and R.R. Recker, Maintenance of cortical bone in human parathyroid hormone (1-84)-treated ovariectomized rats. *Bone*, 2001. 28(3): p. 251-60.

142. Iwaniec, U.T., E. Samnegard, D.M. Cullen, and D.B. Kimmel, Maintenance of cancellous bone in ovariectomized, human parathyroid hormone [hPTH(1-84)]-treated rats by estrogen, risedronate, or reduced hPTH. *Bone*, 2001. 29(4): p. 352-60.

APPENDIX A

DATA RELEVANT TO CHAPTER 2

	Plasma Concentration (µg/ml)				
Time (min)	Animal 1	Animal 2	Animal 3	Animal 4	Animal 5
5	1.337	1.247	1.411	1.417	1.327
10	1.620	1.138	1.355	1.135	1.121
20	0.946	1.179	1.185	1.038	0.807
30	0.950	1.031	0.959	0.882	1.290
60	0.654	0.866	0.759	0.765	0.568
120	0.516	0.585	0.492	0.574	0.476
240	0.291	0.353	0.286	0.383	0.191
480	0.100	0.060	0.094	0.165	0.255
720	0.053	0.017	0.032	0.109	0.020
1440	0.003	0.001	0.002	0.001	0.001

Table A.1: Concentration time data for 0.5 mg/kg intravenous dose group.

	Plasma Concentration (µg/ml)				
Time (min)	Animal 1	Animal 2	Animal 3	Animal 4	Animal 5
5	1.999	2.368	1.819	1.872	1.824
10	2.097	1.758	1.814	1.567	2.191
20	1.755	1.668	1.584	1.863	1.525
30	1.611	1.303	1.634	1.403	1.583
60	1.164	1.324	1.245	1.172	1.127
120	1.387	1.275	0.924	0.794	0.730
240	1.413	0.756	0.489	0.417	0.559
480	0.338	0.302	0.189	0.078	0.134
720	0.189	0.227	0.076	0.046	0.043
1440	0.005	0.006	0.002	0.006	0.005

Table A.2: Concentration time data for 1 mg/kg intravenous dose group.

	Plasma Concentration (µg/ml)				
Time (min)	Animal 1	Animal 2	Animal 3	Animal 4	Animal 5
5	23.810	25.540	26.820	25.340	20.870
10	20.160	25.030	21.690	19.970	21.480
20	19.470	20.590	17.620	19.510	20.140
30	18.330	17.620	18.920	18.830	18.590
60	15.630	16.900	16.940	13.610	17.310
120	12.640	11.830	12.900	11.990	12.540
240	9.720	8.070	7.350	6.980	9.160
480	3.910	4.010	3.630	3.570	4.640
720	2.960	2.110	1.520	1.730	1.900
1080	0.900				0.540

Table A.3: Concentration time data for 10 mg/kg intravenous dose group.

	Plasma Concentration (µg/ml)				
Time (min)	Animal 1	Animal 2	Animal 3	Animal 4	Animal 5
20	122.980	107.540	121.060	133.590	124.550
40	75.380	86.720	97.090	95.350	93.440
60	77.210	87.490	68.050	77.280	48.000
90	41.570	41.630	51.430	55.680	40.320
120	36.950	35.710	31.850	43.460	37.610
240	19.310	27.120	28.860	33.690	23.500
360	18.860	19.940	21.560	21.320	20.980
480	16.580	14.110	15.150	17.840	17.210
720	8.180	8.450	12.130	8.780	14.540
1440	1.050	3.290	1.160	1.190	5.680

Table A.4: Concentration time data for 30 mg/kg intravenous dose group.

	Plasma Concentration (µg/ml)				
Time (min)	Animal 1	Animal 2	Animal 3	Animal 4	Animal 5
30	2.266	0.521	0.796	0.977	1.127
60	1.495	1.169	1.259	1.130	1.069
90	1.728	1.115	1.211	0.999	0.974
180	1.380	0.841	0.862	0.647	0.808
240	0.992	0.676	0.685	0.747	0.801
360	0.305	0.572	0.723	0.652	0.575
480	0.562	0.544	0.167	0.387	0.469
720	0.270	0.153	0.171	0.270	0.253
1440	0.015	0.037	0.008	0.013	0.012
1800	0.005	0.013	0.001	0.003	XX[1]
2160	0.003	0.002	0.002	0.001	0.001

Table A.5: Concentration time data for 1 mg/kg oral dose group.

[1] Sample missing

	Plasma Concentration (µg/ml)				
Time (min)	Animal 1	Animal 2	Animal 3	Animal 4	Animal 5
30	3.937	10.461	8.860	12.527	9.161
60	5.532	11.701	8.643	11.648	7.328
90	7.866	17.234	8.619	9.936	9.784
180	8.220	8.379	7.249	11.852	7.120
240	5.793	8.262	7.668	10.877	8.286
360	4.651	6.170	5.278	7.967	7.831
480	4.432	5.327	4.459	7.607	5.942
720	2.352	2.665	1.794	4.998	4.383
1440	0.187	0.158	0.026	0.543	0.223
1800	0.014	0.066	0.009	0.135	0.043
2160	0.004	0.020	0.004	0.004	0.014

Table A.6: Concentration time data for 10 mg/kg oral dose group.

	Plasma Concentration (µg/ml)				
Time (min)	Animal 1	Animal 2	Animal 3	Animal 4	Animal 5
20	4.350	3.261	1.511	24.243	2.599
40	6.826	XX[2]	4.134	32.010	3.221
60	8.249	9.614	6.577	34.481	4.256
90	9.401	9.597	9.424	31.571	4.052
120	8.438	9.347	8.993	39.610	4.501
240	13.371	11.521	18.084	33.305	10.281
360	13.561	14.810	16.670	28.462	10.520
480	15.293	14.769	14.048	20.837	12.367
720	12.121	13.612	9.978	15.749	9.860
1440	1.912	1.439	1.006	1.635	1.238

Table A.7: Concentration time data for 30 mg/kg oral dose group.

[2] Sample missing

Parameter	Units	Animal 1	Animal 2	Animal 3	Animal 4	Animal 5
Dosing_time	min	0	0	0	0	0
Rsq		0.9974	0.9977	0.9996	0.9681	0.9669
Rsq(adjusted)		0.9967	0.9954	0.9992	0.9641	0.9627
Corr(x:y)		-0.9987	-0.9988	-0.9998	-0.9839	-0.9833
Tmax	min	10	0	0	0	0
Cmax	ug/mL	1.62	1.37	1.47	1.77	1.57
No._points_Lambda_z		6	3	3	10	10
Tlast	min	1440	1440	1440	1440	1440
Clast	ug/mL	0.0028	0.0008	0.0016	0.0008	0.0006
AUClast	min*ug/mL	229	228	220	295	227
Lambda_z	1/min	0.0039	0.0045	0.0042	0.0047	0.0051
Lambda_z_lower	min	60	480	480	5	5
Lambda_z_upper	min	1440	1440	1440	1440	1440
t1/2_Lambda_z	min	177	155	164	147	135
AUCall	min*ug/mL	229	228	220	295	227
AUCINF(observed)	min*ug/mL	230	229	221	295	227
AUCINF(observed)/D	min*ug/mL/mg	2025	2005	1944	2535	1971
AUC_%Extrap(obs.)	%	0.3061	0.0758	0.1699	0.0591	0.0521
Vz(observed)	mL	126	112	122	83	99
Cl(observed)	mL/min	0.4938	0.4987	0.5144	0.3944	0.5073
AUCINF(predicted)	min*ug/mL	230	229	221	295	227
AUCINF(predicted)/D	min*ug/mL/mg	2025	2005	1944	2536	1971
AUC_%Back_Ext(obs.)	%	2.9089	2.8599	3.2624	2.6971	3.196
AUC_%Back_Ext(pred.)	%	2.9089	2.86	3.2624	2.696	3.1959
AUC_%Extrap(pred.)	%	0.3062	0.0736	0.1679	0.0994	0.0564
Vz(predicted)	mL	126	112	122	83	99
Cl(predicted)	mL/min	0.4938	0.4987	0.5144	0.3943	0.5073
AUMClast	min*min*ug/mL	51967	37934	43287	82700	52530
AUMCINF(observed)	min*min*ug/mL	53160	38222	43915	82989	52723
AUMC_%Extrap(obs.)	%	2.2432	0.7547	1.4305	0.3477	0.3662
AUMCINF(predicted)	min*min*ug/mL	53160	38214	43908	83185	52739
AUMC_%Extrap(pred.)	%	2.2442	0.7327	1.4145	0.5831	0.3962
MRTlast	min	227	166	197	280	232
MRTINF(observed)	min	231	167	199	281	233
Vss(observed)	mL	114	83	102	111	118
MRTINF(predicted)	min	231	167	199	282	233
Vss(predicted)	mL	114	83	102	111	118

Table A.8: Pharmacokinetic parameters for 0.5 mg/kg intravenous dose group determined by noncompartmental analysis.

Parameter	Units	Animal 1	Animal 2	Animal 3	Animal 4	Animal 5
Dosing_time	min	0	0	0	0	0
Rsq		0.9916	0.9791	0.9981	0.9975	0.9891
Rsq(adjusted)		0.9874	0.9762	0.9978	0.9951	0.9782
Corr(x:y)		-0.9958	-0.9895	-0.9991	-0.9988	-0.9945
Tmax	min	10	0	0	0	10
Cmax	ug/mL	2.10	3.19	1.82	2.24	2.19
No._points_Lambda_z		4	9	8	3	3
Tlast	min	1440	1440	1440	1440	1440
Clast	ug/mL	0.0048	0.006	0.0024	0.0056	0.0049
AUClast	min*ug/mL	685	570	386	315	349
Lambda_z	1/min	0.0046	0.0038	0.0045	0.0028	0.0033
Lambda_z_lower	min	240	10	20	480	480
Lambda_z_upper	min	1440	1440	1440	1440	1440
t1/2_Lambda_z	min	149	184	154	250	208
AUCall	min*ug/mL	685	570	386	315	349
AUCINF(observed)	min*ug/mL	686	571	386	317	350
AUCINF(observed)/D	min*ug/mL/mg	2896	2632	1831	1391	1496
AUC_%Extrap(obs.)	%	0.1521	0.276	0.1399	0.6355	0.4223
Vz(observed)	mL	74	101	121	259	200
Cl(observed)	mL/min	0.3453	0.3799	0.5462	0.7188	0.6684
AUCINF(predicted)	min*ug/mL	686	572	386	317	350
AUCINF(predicted)/D	min*ug/mL/mg	2896	2635	1831	1391	1496
AUC_%Back_Ext(obs.)	%	1.4559	2.4331	2.3581	3.2392	2.6046
AUC_%Back_Ext(pred.)	%	1.4557	2.4307	2.358	3.2388	2.6051
AUC_%Extrap(pred.)	%	0.1605	0.3743	0.1459	0.6477	0.4024
Vz(predicted)	mL	74	101	121	259	200
Cl(predicted)	mL/min	0.3453	0.3795	0.5462	0.7187	0.6685
AUMClast	min*min*ug/mL	187314	167614	85258	58711	69382
AUMCINF(observed)	min*min*ug/mL	189042	170302	86157	62339	71953
AUMC_%Extrap(obs.)	%	0.914	1.5783	1.0427	5.8208	3.574
AUMCINF(predicted)	min*min*ug/mL	189138	171262	86195	62409	71831
AUMC_%Extrap(pred.)	%	0.964	2.1305	1.0865	5.9263	3.4104
MRTlast	min	273	294	221	186	199
MRTINF(observed)	min	275	298	223	197	206
Vss(observed)	mL	95	113	122	141	137
MRTINF(predicted)	min	276	300	223	197	205
Vss(predicted)	mL	95	114	122	141	137

Table A.9: Pharmacokinetic parameters for 1 mg/kg intravenous dose group determined by noncompartmental analysis.

Parameter	Units	Animal 1	Animal 2	Animal 3	Animal 4	Animal 5
Dosing_time	min	0	0	0	0	0
Rsq		0.9738	0.9994	0.9951	0.9995	0.9997
Rsq(adjusted)		0.9607	0.9988	0.9941	0.999	0.9995
Corr(x:y)		-0.9868	-0.9997	-0.9975	-0.9998	-0.9999
Tmax	min	0	0	0	0	10
Cmax	ug/mL	28.11	26.06	33.16	32.16	21.48
No._points_Lambda_z		4	3	7	3	3
Tlast	min	1080	720	720	720	1080
Clast	ug/mL	0.8982	2.1146	1.524	1.7266	0.5401
AUClast	min*ug/mL	6482	5434	5234	4939	6231
Lambda_z	1/min	0.0027	0.0028	0.0036	0.0029	0.0036
Lambda_z_lower	min	240	240	20	240	480
Lambda_z_upper	min	1080	1080	720	720	1080
t1/2_Lambda_z	min	256	248	193	238	194
AUCall	min*ug/mL	6482	5434	5234	4939	6231
AUCINF(observed)	min*ug/mL	6814	6192	5659	5532	6381
AUCINF(observed)/D	min*ug/mL/mg	2748	2692	2450	2470	2824
AUC_%Extrap(obs.)	%	4.8728	12.2408	7.5103	10.7234	2.3652
Vz(observed)	mL	135	133	114	139	99
Cl(observed)	mL/min	0.3639	0.3714	0.4082	0.4049	0.3541
AUCINF(predicted)	min*ug/mL	6829	6185	5651	5538	6380
AUCINF(predicted)/D	min*ug/mL/mg	2754	2689	2446	2472	2823
AUC_%Back_Ext(obs.)	%	1.9045	2.0831	2.65	2.5981	1.635
AUC_%Back_Ext(pred.)	%	1.9003	2.0855	2.6537	2.5956	1.6353
AUC_%Extrap(pred.)	%	5.0827	12.1394	7.3792	10.8096	2.3466
Vz(predicted)	mL	134	133	114	139	99
Cl(predicted)	mL/min	0.3631	0.3719	0.4088	0.4045	0.3542
AUMClast	min*min*ug/mL	1881164	1184414	1069154	1045082	1646486
AUMCINF(observed)	min*min*ug/mL	2362525	2001824	1493668	1676092	1851668
AUMC_%Extrap(obs.)	%	20.3748	40.8333	28.421	37.6477	11.0809
AUMCINF(predicted)	min*min*ug/mL	2384378	1994119	1485664	1681780	1850018
AUMC_%Extrap(pred.)	%	21.1046	40.6047	28.0353	37.8586	11.0017
MRTlast	min	290	218	204	212	264
MRTINF(observed)	min	347	323	264	303	290
Vss(observed)	mL	126	120	108	123	103
MRTINF(predicted)	min	349	322	263	304	290
Vss(predicted)	mL	127	120	107	123	103

Table A.10: Pharmacokinetic parameters for 10 mg/kg intravenous dose group determined by noncompartmental analysis.

Parameter	Units	Animal 1	Animal 2	Animal 3	Animal 4	Animal 5
Dosing_time	min	0	0	0	0	0
Rsq		1	0.9874	0.9792	0.9998	0.9939
Rsq(adjusted)		0.9999	0.9748	0.9723	0.9997	0.9919
Corr(x:y)		-1	-0.9937	-0.9895	-0.9999	-0.997
Tmax	min	0	0	0	0	0
Cmax	ug/mL	200.62	133.35	150.96	187.15	166.02
No._points_Lambda_z		3	3	5	3	5
Tlast	min	1440	1440	1440	1440	1440
Clast	ug/mL	1.0523	3.2917	1.1576	1.1866	5.676
AUClast	min*ug/mL	23793	24760	26525	27767	28706
Lambda_z	1/min	0.0029	0.0015	0.0027	0.0028	0.0012
Lambda_z_lower	min	480	480	240	480	240
Lambda_z_upper	min	1440	1440	1440	1440	1440
t1/2_Lambda_z	min	242	472	261	246	587
AUCall	min*ug/mL	23793	24760	26525	27767	28706
AUCINF(observed)	min*ug/mL	24160	27002	26960	28189	33512
AUCINF(observed)/D	min*ug/mL/mg	4393	3600	3851	3759	4468
AUC_%Extrap(obs.)	%	1.5193	8.3017	1.6165	1.4963	14.3419
Vz(observed)	mL	79	189	98	95	190
Cl(observed)	mL/min	0.2277	0.2778	0.2596	0.2661	0.2238
AUCINF(predicted)	min*ug/mL	24159	26951	27010	28187	33610
AUCINF(predicted)/D	min*ug/mL/mg	4392	3593	3859	3758	4481
AUC_%Back_Ext(obs.)	%	13.3942	8.9214	10.0897	11.3782	8.6707
AUC_%Back_Ext(pred.)	%	13.3947	8.9382	10.071	11.379	8.6454
AUC_%Extrap(pred.)	%	1.5155	8.1284	1.7988	1.4892	14.5917
Vz(predicted)	mL	79	190	98	95	189
Cl(predicted)	mL/min	0.2277	0.2783	0.2592	0.2661	0.2231
AUMClast	min*min*ug/mL	6846733	8164804	8518937	7870174	11680150
AUMCINF(observed)	min*min*ug/mL	7503351	12919221	9310598	8627457	22671106
AUMC_%Extrap(obs.)	%	8.751	36.8011	8.5028	8.7776	48.48
AUMCINF(predicted)	min*min*ug/mL	7501654	12811190	9401505	8623838	22895240
AUMC_%Extrap(pred.)	%	8.7304	36.2682	9.3875	8.7393	48.9844
MRTlast	min	288	330	321	283	407
MRTINF(observed)	min	311	478	345	306	677
Vss(observed)	mL	71	133	90	81	151
MRTINF(predicted)	min	311	475	348	306	681
Vss(predicted)	mL	71	132	90	81	152

Table A.11: Pharmacokinetic parameters for 30 mg/kg intravenous dose group determined by noncompartmental analysis.

Parameter	Units	Animal 1	Animal 2	Animal 3	Animal 4	Animal 5
Dosing_time	min	0	0	0	0	0
Rsq		0.9865	0.9704	0.9413	0.9926	0.9977
Rsq(adjusted)		0.9820	0.9606	0.9217	0.9902	0.9966
Corr(x:y)		-0.9932	-0.9851	-0.9702	-0.9963	-0.9989
Tlag	min	0	0	0	0	0
Tmax	min	30	60	60	60	30
Cmax	ug/mL	2.27	1.17	1.26	1.13	1.13
No._points_Lambda_z		5	5	5	5	4
Tlast	min	2160	2160	2160	2160	2160
Clast	ug/mL	0.0027	0.0022	0.0016	0.0011	0.0009
AUClast	min*ug/mL	687	506	465	525	541
Lambda_z	1/min	0.0034	0.003	0.0033	0.0037	0.0038
Lambda_z_lower	min	480	480	480	480	480
Lambda_z_upper	min	2160	2160	2160	2160	2160
t1/2_Lambda_z	min	207	233	211	187	183
AUCall	min*ug/mL	687	506	465	525	541
AUCINF(observed)	min*ug/mL	688	507	465	525	541
AUCINF(observed)/D	min*ug/mL/mg	3042	2205	1996	2354	2353
AUC_%Extrap(obs.)	%	0.115	0.1436	0.1032	0.0558	0.0457
Vz(observed)/F	mL	98	152	152	115	112
Cl(observed)/F	mL/min	0.3287	0.4535	0.5009	0.4248	0.4250
AUCINF(predicted)	min*ug/mL	687	507	465	525	541
AUCINF(predicted)/D	min*ug/mL/mg	3041	2206	1996	2354	2353
AUC_%Extrap(pred.)	%	0.0809	0.2099	0.0566	0.0485	0.0442
Vz(predicted)/F	mL	98	152	152	115	112
Cl(predicted)/F	mL/min	0.3288	0.4532	0.5011	0.4249	0.425
AUMClast	min*min*ug/mL	224925	197087	148604	200363	202702
AUMCINF(observed)	min*min*ug/mL	226869	198905	149787	201075	203302
AUMC_%Extrap(obs.)	%	0.8567	0.9137	0.7895	0.3539	0.295
AUMCINF(predicted)	min*min*ug/mL	226293	199746	149253	200982	203282
AUMC_%Extrap(pred.)	%	0.6043	1.3311	0.4344	0.3079	0.2854
MRTlast	min	328	389	320	382	375
MRTINF(observed)	min	330	392	322	383	376
MRTINF(predicted)	min	329	394	321	383	376

Table A.12: Pharmacokinetic parameters for 1 mg/kg oral dose group determined by noncompartmental analysis.

Parameter	Units	Animal 1	Animal 2	Animal 3	Animal 4	Animal 5
Dosing_time	min	0	0	0	0	0
Rsq		0.9818	0.9956	0.9729	0.9190	0.9921
Rsq(adjusted)		0.9758	0.9941	0.9638	0.8920	0.9895
Corr(x:y)		-0.9909	-0.9978	-0.9863	-0.9586	-0.9960
Tlag	min	0	0	0	0	0
Tmax	min	180	90	30	30	90
Cmax	ug/mL	8.22	17.23	8.86	12.53	9.78
No._points_Lambda_z		5	5	5	5	5
Tlast	min	2160	2160	2160	2160	2160
Clast	ug/mL	0.0041	0.0201	0.0041	0.0039	0.0136
AUClast	min*ug/mL	4486	6162	4591	8256	6613
Lambda_z	1/min	0.0043	0.0034	0.0044	0.0041	0.0038
Lambda_z_lower	min	480	480	480	480	480
Lambda_z_upper	min	2160	2160	2160	2160	2160
t1/2_Lambda_z	min	162	205	156	167	182
AUCall	min*ug/mL	4486	6162	4591	8256	6613
AUCINF(observed)	min*ug/mL	4486	6168	4592	8257	6617
AUCINF(observed)/D	min*ug/mL/mg	1699	2391	1746	3514	2852
AUC_%Extrap(obs.)	%	0.0213	0.0967	0.0202	0.0114	0.0537
Vz(observed)/F	mL	137	124	129	69	92
Cl(observed)/F	mL/min	0.5884	0.4183	0.5727	0.2846	0.3506
AUCINF(predicted)	min*ug/mL	4487	6167	4592	8259	6616
AUCINF(predicted)/D	min*ug/mL/mg	1699	2390	1746	3514	2852
AUC_%Extrap(pred.)	%	0.0232	0.0882	0.0112	0.0362	0.0515
Vz(predicted)/F	mL	137	124	129	69	92
Cl(predicted)/F	mL/min	0.5884	0.4183	0.5728	0.2845	0.3506
AUMClast	min*min*ug/mL	1845028	2236332	1594128	3720603	2922410
AUMCINF(observed)	min*min*ug/mL	1847317	2250989	1596340	3722864	2931020
AUMC_%Extrap(obs.)	%	0.1239	0.6511	0.1386	0.0607	0.2938
AUMCINF(predicted)	min*min*ug/mL	1847520	2249696	1595353	3727783	2930661
AUMC_%Extrap(pred.)	%	0.1349	0.5941	0.0768	0.1926	0.2815
MRTlast	min	411	363	347	451	442
MRTINF(observed)	min	412	365	348	451	443
MRTINF(predicted)	min	412	365	347	451	443

Table A.13: Pharmacokinetic parameters for 10 mg/kg oral dose group determined by noncompartmental analysis.

Parameter	Units	Animal 1	Animal 2	Animal 3	Animal 4	Animal 5
Dosing_time	min	0	0	0	0	0
Rsq		0.9804	0.9559	0.9850	0.9799	0.9767
Rsq(adjusted)		0.9608	0.9117	0.9699	0.9599	0.9535
Corr(x:y)		-0.9902	-0.9777	-0.9924	-0.9899	-0.9883
Tlag	min	0	0	0	0	0
Tmax	min	480	360	240	120	480
Cmax	ug/mL	15.29	14.81	18.08	39.61	12.37
No._points_Lambda_z		3	3	3	3	3
Tlast	min	1440	1440	1440	1440	1440
Clast	ug/mL	1.9117	1.4392	1.0059	1.6351	1.2381
AUClast	min*ug/mL	13836	14293	13085	25216	10583
Lambda_z	1/min	0.0023	0.0026	0.0028	0.0028	0.0025
Lambda_z_lower	min	480	480	480	480	480
Lambda_z_upper	min	1440	1440	1440	1440	1440
t1/2_Lambda_z	min	307	268	243	251	276
AUCall	min*ug/mL	13836	14293	13085	25216	10583
AUCINF(observed)	min*ug/mL	14682	14850	13438	25807	11076
AUCINF(observed)/D	min*ug/mL/mg	1958	1980	1792	3226	1477
AUC_%Extrap(obs.)	%	5.766	3.7478	2.6281	2.2911	4.4551
Vz(observed)/F	mL	226	195	196	112	270
Cl(observed)/F	mL/min	0.5108	0.5051	0.5581	0.3100	0.6771
AUCINF(predicted)	min*ug/mL	14721	14894	13456	25841	11103
AUCINF(predicted)/D	min*ug/mL/mg	1963	1986	1794	3230	1480
AUC_%Extrap(pred.)	%	6.0111	4.0357	2.7558	2.4171	4.6892
Vz(predicted)/F	mL	226	195	196	112	269
Cl(predicted)/F	mL/min	0.5095	0.5035	0.5574	0.3096	0.6755
AUMClast	min*min*ug/mL	7593325	7830148	6544615	10808441	5930016
AUMCINF(observed)	min*min*ug/mL	9187309	8846793	7177169	11873705	6837240
AUMC_%Extrap(obs.)	%	17.3498	11.4917	8.8134	8.9716	13.2689
AUMCINF(predicted)	min*min*ug/mL	9259381	8928173	7208787	11933736	6887259
AUMC_%Extrap(pred.)	%	17.9932	12.2984	9.2134	9.4295	13.8987
MRTlast	min	549	548	500	429	560
MRTINF(observed)	min	626	596	534	460	617
MRTINF(predicted)	min	629	599	536	462	620

Table A.14: Pharmacokinetic parameters for 30 mg/kg oral dose group determined by noncompartmental analysis.

APPENDIX B

DATA RELEVANT TO CHAPTER 3

	Intact			Ovariectomized		
	Vehicle	DHT	S-4	Vehicle	DHT	S-4 + Bical
	--	1 mg/day	1 mg/day	--	1 mg/day	0.5 + 1 mg/day
Animal 1	0.2131	0.1841	0.2050	0.2014	0.2025	0.2087
Animal 2	0.2174	0.2005	0.2184	0.2001	0.2120	0.2135
Animal 3	0.2049	0.1961		0.1990	0.2071	0.1912
Animal 4	0.2178	0.2092	0.2122	0.2101	0.1996	0.2022
Animal 5	0.2120	0.1989	0.2024	0.1930	0.2140	0.2017
Animal 6	0.2231	0.1978	0.2107	0.1898	0.2016	0.2116
Animal 7	0.2231	0.2047	0.2144	0.1998	0.2070	0.2145
Animal 8	0.2212	0.2073	0.2151	0.1939	0.2051	0.2011
Animal 9	0.2160	0.2111	0.2101	0.1968	0.2045	0.2051
Animal 10	0.1973	0.2203	0.2103	0.1891	0.2066	0.2076

	Ovariectomized					
	S-4	S-4	S-4	S-4	S-4	S-4
	0.1 mg/day	0.3 mg/day	0.5 mg/day	0.75 mg/day	1 mg/day	3 mg/day
Animal 1	0.1948	0.2102	0.2118		0.2143	0.2166
Animal 2	0.1935	0.2138	0.2127		0.2021	0.2009
Animal 3	0.1979	0.222	0.2126	0.2097	0.2044	
Animal 4	0.2028	0.2154	0.2148	0.2021	0.2066	0.2172
Animal 5	0.2014	0.1979	0.2037	0.1941	0.199	0.196
Animal 6	0.1957	0.2025	0.2063	0.2005	0.2018	0.2103
Animal 7	0.2091	0.2199	0.2015	0.2044	0.2066	0.2145
Animal 8	0.1991	0.1969	0.2272	0.2004	0.1965	0.2093
Animal 9	0.2105	0.21	0.2105	0.2042	0.2137	0.209
Animal 10		0.208	0.2137	0.2106	0.2093	0.2116

Table B.1: Whole body BMD as measured by DEXA at day 120.

	Intact			Ovariectomized		
	Vehicle	DHT	S-4	Vehicle	DHT	S-4 + Bical
	--	1 mg/day	1 mg/day	--	1 mg/day	0.5 + 1 mg/day
Animal 1	265	301	282	347	343	314
Animal 2	312	335	275	338	333	345
Animal 3	308	317		356	336	341
Animal 4	308	347	275	352	300	342
Animal 5	294	345	255	333	315	346
Animal 6	313	332	295	322	343	333
Animal 7	297	347	269	342	320	344
Animal 8	311	337	316	298	335	313
Animal 9	303	370	270	308	360	338
Animal 10	302	363	297	348	367	334

	Ovariectomized					
	S-4	S-4	S-4	S-4	S-4	S-4
	0.1 mg/day	0.3 mg/day	0.5 mg/day	0.75 mg/day	1 mg/day	3 mg/day
Animal 1	302	347	334		340	424
Animal 2	325	327	351		324	334
Animal 3	337	348	317	322	342	
Animal 4	339	325	307	343	347	379
Animal 5	319	358	303	303	324	377
Animal 6	333	327	375	366	362	408
Animal 7	344	339	336	354	347	385
Animal 8	361	333	344	377	338	444
Animal 9	345	326	338	362	359	400
Animal 10		335	363	360	390	397

Table B.2: Body weight as measured by DEXA at day 120.

	Intact			Ovariectomized		
	Vehicle	DHT	S-4	Vehicle	DHT	S-4 + Bical
	--	1 mg/day	1 mg/day	--	1 mg/day	0.5 + 1 mg/day
Animal 1	23	31	23	37	33	35
Animal 2	29	27	21	52	36	48
Animal 3	28	34		48	31	44
Animal 4	23	29	26	35	28	36
Animal 5	30	38	24	33	27	38
Animal 6	27	34	27	43	36	35
Animal 7	27	37	23	40	26	35
Animal 8	35	30	25	39	36	37
Animal 9	29	36	27	40	34	38
Animal 10	29	38	26	44	30	37

	Ovariectomized					
	S-4	S-4	S-4	S-4	S-4	S-4
	0.1 mg/day	0.3 mg/day	0.5 mg/day	0.75 mg/day	1 mg/day	3 mg/day
Animal 1	30	38	37		30	22
Animal 2	44	35	38		29	33
Animal 3	39	39	37	39	35	
Animal 4	36	32	28	45	28	24
Animal 5	30	33	33	30	33	30
Animal 6	30	31	30	40	40	36
Animal 7	38	39	34	32	32	28
Animal 8	37	31	33	30	34	32
Animal 9	30	38	32	30	35	31
Animal 10		30	36	27	34	31

Table B.3: Percent fat mass as measured by DEXA at day 120.

	Intact			Ovariectomized		
	Vehicle	DHT	S-4	Vehicle	DHT	S-4 + Bical
	--	1 mg/day	1 mg/day	--	1 mg/day	0.5 + 1 mg/day
Animal 1	0.2204	0.1848	0.2443	0.1849	0.2057	0.2039
Animal 2	0.2383	0.2137	0.2211	0.1927	0.2154	0.1958
Animal 3	0.2663	0.2132		0.2003	0.1791	0.1950
Animal 4	0.2379	0.2098	0.2146	0.1857	0.2144	0.1976
Animal 5	0.2210	0.1909	0.2088	0.2041	0.2104	0.2242
Animal 6	0.2618	0.2335	0.2210	0.2049	0.1971	0.1939
Animal 7	0.2562	0.1896	0.2276	0.2086	0.2020	0.1954
Animal 8	0.1934	0.1887	0.2471	0.2092	0.1822	0.1963
Animal 9	0.2218	0.1933	0.2347	0.1765	0.2419	0.2194
Animal 10	0.2191	0.2182	0.2499	0.1559	0.2082	0.1871

	Ovariectomized					
	S-4	S-4	S-4	S-4	S-4	S-4
	0.1 mg/day	0.3 mg/day	0.5 mg/day	0.75 mg/day	1 mg/day	3 mg/day
Animal 1	0.2041	0.2023	0.2067		0.2170	0.2153
Animal 2	0.1985	0.2026	0.2050		0.2139	0.2012
Animal 3	0.1576	0.1973	0.2118	0.1868	0.1818	
Animal 4	0.2235	0.1971	0.1886	0.2070	0.2367	0.2583
Animal 5	0.2219	0.2069	0.2185	0.2088	0.1964	0.2090
Animal 6	0.1826	0.2273	0.2181	0.2155	0.2102	0.2173
Animal 7	0.2061	0.1848	0.2176	0.1836	0.2011	0.2152
Animal 8	0.1707	0.1805	0.2369	0.2115	0.2032	0.2226
Animal 9	0.2079	0.1839	0.1891	0.1856	0.2124	0.2134
Animal 10		0.1720	0.2154	0.2226	0.2355	0.2336

Table B.4: L5-L6 BMD as measured by DEXA at day 120.

	Intact			Ovariectomized		
	Vehicle	DHT	S-4	Vehicle	DHT	S-4 + Bical
	--	1 mg/day	1 mg/day	--	1 mg/day	0.5 + 1 mg/day
Animal 1	0.1787	0.2424	0.1789	0.1826	0.1573	0.1574
Animal 2	0.1698	0.2024	0.2048	0.1283	0.1432	0.1879
Animal 3	0.2106	0.1595		0.1828	0.1900	0.1981
Animal 4	0.2173	0.1946	0.1560	0.1545	0.1872	0.1915
Animal 5	0.2242	0.1316	0.1678	0.1497	0.1678	0.1526
Animal 6	0.2014	0.1596	0.1957	0.1444	0.1729	0.1773
Animal 7	0.2145	0.2056	0.1850	0.1779	0.2093	0.1805
Animal 8	0.2046	0.1997	0.1825	0.1662	0.1507	0.1529
Animal 9	0.1979	0.1800	0.1481	0.1677	0.2022	0.1756
Animal 10	0.2152	0.1501	0.1940	0.1334	0.1992	0.1422

	Ovariectomized					
	S-4	S-4	S-4	S-4	S-4	S-4
	0.1 mg/day	0.3 mg/day	0.5 mg/day	0.75 mg/day	1 mg/day	3 mg/day
Animal 1	0.1500	0.1924	0.1747		0.1929	0.2182
Animal 2	0.1602	0.1809	0.1831		0.2160	0.1791
Animal 3	0.1958	0.1660	0.1430	0.1342	0.1743	
Animal 4	0.1900	0.1525	0.1494	0.1529	0.1752	0.1974
Animal 5	0.1544	0.1732	0.1275	0.1848	0.2173	0.1602
Animal 6	0.2041	0.1591	0.1895	0.1747	0.1684	0.1921
Animal 7	0.1943	0.1732	0.1962	0.1700	0.1267	0.1825
Animal 8	0.1775	0.1659	0.1857	0.1985	0.2128	0.1517
Animal 9	0.1957	0.1535	0.1914	0.1978	0.2225	0.2209
Animal 10		0.1581	0.2060	0.1683	0.1831	0.1874

Table B.5: Femoral region 4 BMD as measured by DEXA at day 120.

	Intact		Ovariectomized			
	Vehicle	S-4	Vehicle	DHT	S-4	S-4
	--	1 mg/day	--	1 mg/day	1 mg/day	3 mg/day
Animal 1	0.708	0.736	0.593	0.657	0.832	0.769
Animal 2	0.760	0.798	0.658	0.658	0.728	0.706
Animal 3	0.717	0.724	0.657	0.695	0.744	0.756
Animal 4	0.760	0.715	0.663	0.665	0.749	0.729
Animal 5	0.728	0.763	0.717	0.713	0.704	0.782
Animal 6	0.752	0.756	0.646	0.713	0.794	0.808
Animal 7	0.677	0.795	0.732	0.730	0.701	0.826
Animal 8	0.693	0.757	0.639	0.647	0.702	0.805
Animal 9	0.726	0.752	0.630	0.718	0.715	0.744
Animal 10	0.647		0.643	0.767	0.848	

Table B.6: Cortical thickness of the mid-shaft femur as measured by pQCT at day 120.

	Intact		Ovariectomized			
	Vehicle	S-4	Vehicle	DHT	S-4	S-4
	--	1 mg/day	--	1 mg/day	1 mg/day	3 mg/day
Animal 1	9.850	10.220	8.480	9.52	11.64	12.04
Animal 2	11.150	10.620	8.950	9.53	10.29	9.81
Animal 3	9.740	9.580	9.170	9.60	10.30	10.73
Animal 4	10.800	9.330	9.550	9.15	10.54	10.05
Animal 5	10.620	10.560	9.630	10.06	9.85	10.77
Animal 6	11.510	9.990	8.800	9.61	10.23	11.50
Animal 7	10.080	11.110	10.030	9.93	9.74	12.03
Animal 8	9.890	10.050	8.070	8.95	9.42	11.42
Animal 9	10.210	10.150	8.480	9.96	10.68	10.76
Animal 10	9.290		8.220	10.33	11.61	

Table B.7: Cortical content of the mid-shaft femur as measured by pQCT at day 120.

	Intact		Ovariectomized			
	Vehicle	S-4	Vehicle	DHT	S-4	S-4
	--	1 mg/day	--	1 mg/day	1 mg/day	1 mg/day
Animal 1	11.52	11.65	11.75	12.13	12.09	13.21
Animal 2	12.45	11.51	11.42	12.01	11.81	11.74
Animal 3	11.50	11.45	11.71	11.68	11.74	12.20
Animal 4	11.98	11.18	12.02	11.58	12.00	11.81
Animal 5	12.07	11.87	11.43	11.78	11.80	11.96
Animal 6	12.71	11.41	11.45	11.52	11.34	12.31
Animal 7	12.15	11.94	11.71	11.60	11.78	12.60
Animal 8	11.83	11.33	10.75	11.47	11.45	12.22
Animal 9	11.88	11.63	11.37	11.71	12.44	12.34
Animal 10	11.69		10.92	11.55	11.98	

Table B.8: Periosteal Circumference of the Mid-Shaft Femur as measured by pQCT at day 120.

	Intact		Ovariectomized			
	Vehicle	S-4	Vehicle	DHT	S-4	S-4
	--	1 mg/day	--	1 mg/day	1 mg/day	1 mg/day
Animal 1	1001	1034	848	892	1051	942
Animal 2	986	1075	936	907	961	971
Animal 3	1006	995	904	962	1010	962
Animal 4	1021	977	882	931	962	975
Animal 5	984	1019	995	985	940	989
Animal 6	977	1035	875	984	1064	999
Animal 7	937	1033	991	997	956	1009
Animal 8	961	1044	949	903	968	1011
Animal 9	981	1018	900	985	939	940
Animal 10	921		919	1015	1066	

Table B.9: Total bone mineral density of the mid-shaft femur as measured by pQCT at day 120.

	Intact		Ovariectomized			
	Vehicle	S-4	Vehicle	DHT	S-4	S-4
	--	1 mg/day	--	1 mg/day	1 mg/day	3 mg/day
Animal 1	388.1	397.7	76.2	107.6	156.3	191.6
Animal 2	365.2	498.9	91.9	185.3	124.2	181.0
Animal 3	289.4	405.4	25.0	138.0	108.1	200.3
Animal 4	335.2	455.4	110.7	143.9	113.7	104.9
Animal 5	298.0	450.1	85.4	200.8	74.0	170.4
Animal 6	351.6	433.7	106.4	125.2	114.8	125.3
Animal 7	380.1	440.0	34.8	143.5	117.9	116.1
Animal 8	246.1	528.5	35.6	140.7	84.0	133.1
Animal 9	254.1	398.5	24.5	119.3	130.8	149.7
Animal 10	205.8		0.0	147.5	144.1	

Table B.10: Distal femur trabecular density as measured by pQCT at day 120.

	Intact		Ovariectomized			
	Vehicle	S-4	Vehicle	DHT	S-4	S-4
	--	1 mg/day	--	1 mg/day	1 mg/day	1 mg/day
Animal 1	207.0	222.1	166.4	230.2	262.6	215.1
Animal 2	257.7	251.8	175.4	218.2	209.5	214.2
Animal 3	215.4	234.4	199.4	238.5	239.3	261.7
Animal 4	245.8	211.9	194.3	208.1	236.3	229.5
Animal 5	251.2	263.4	230.5	224.8	243.7	262.4
Animal 6	298.2	215.5	180.6	239.2	242.9	265.8
Animal 7	209.5	257.0	203.0	241.3	212.8	278.5
Animal 8	227.0	231.3	175.1	206.5	221.4	250.8
Animal 9	231.7	238.8	198.4	215.1	234.1	234.4
Animal 10	188.8		186.7	235.0	252.1	

Table B.11: Femur maximum load as measured by three point bending at day 120.

	Intact		Ovariectomized			
	Vehicle	S-4	Vehicle	DHT	S-4	S-4
	--	1 mg/day	--	1 mg/day	1 mg/day	1 mg/day
Animal 1	271.38	367.64	184.31	204.25	171.35	261.96
Animal 2	239.66	267.09	163.28	283.72	280.23	212.24
Animal 3	239.86	165.33	170.90	217.70	191.67	340.01
Animal 4	394.62	273.52	307.17	209.66	311.97	273.55
Animal 5	211.79	348.61	146.66	370.78	226.54	324.51
Animal 6	178.49	280.54	210.85	249.52	272.16	196.18
Animal 7	244.15	255.97	257.42	206.38	87.68	236.03
Animal 8	96.13	252.03	297.54	145.64	110.12	329.58
Animal 9	181.49	284.67	241.98	214.20	165.10	209.59
Animal 10	180.51		189.65	229.81	328.45	

Table B.12: L5 Vertebra biomechanical testing of maximum load at day 120.

Ratio of Dpd/Creatinine (nM/mM)					
	Intact	Ovariectomized			
	Vehicle	Vehicle	DHT	S-4	S-4
	--	--	1 mg/day	1 mg/day	3 mg/day
Animal 1	10.53	37.58	46.37	47.94	33.92
Animal 2	19.62	20.59	30.16	36.34	27.46
Animal 3	7.93	29.35	23.79	38.48	43.31
Animal 4	14.10	32.20	33.25	37.82	45.01
Animal 5	16.04	23.76	30.67	64.11	23.09

Table B.13: Deoxypyridinoline levels as measured by ELISA at day 115.

Osteocalcin (ng/mL)					
	Intact	Ovariectomized			
	Vehicle	Vehicle	DHT	S-4	S-4
	--	--	1 mg/day	1 mg/day	3 mg/day
Animal 1	42.3	46.1	31.6	42.1	41.6
Animal 2	47.1	61.9	29.7	34.2	36.0
Animal 3	32.9	39.2	35.3	44.1	39.8
Animal 4	34.3	50.4	38.4	28.9	41.1
Animal 5	31.1	46.1	37.0	44.5	32.4

Table B.14: Serum osteocalcin levels as measured by ELISA at day 120.

IGF-1 (ng/mL)					
	Intact	Ovariectomized			
	Vehicle	Vehicle	DHT	S-4	S-4
	--	--	1 mg/day	1 mg/day	3 mg/day
Animal 1	563	576	708	695	884
Animal 2	667	264	529	683	780
Animal 3	623	423	456	603	855
Animal 4	614	714	487	706	576
Animal 5	491	673	592	657	805

Table B.15: Serum IGF-1 levels as measured by ELISA at day 120.

APPENDIX C

DATA RELEVANT TO CHAPTER 4

	Intact			Ovariectomized		
	Vehicle	DHT	S-4	Vehicle	DHT	S-4 + Bical
	--	1 mg/day	1 mg/day	--	1 mg/day	0.5 + 1 mg/day
Animal 1	0.2106	0.1994	0.2057	0.1932	0.1891	0.1924
Animal 2	0.2181	0.1973	0.2119	0.1962	0.2008	0.2053
Animal 3	0.2086	0.2188	0.2086	0.2057	0.2053	0.2026
Animal 4	0.2210	0.1898	0.2141	0.2013	0.2035	0.2014
Animal 5	0.2055	0.2134		0.1955	0.1934	0.2067
Animal 6	0.2215	0.2045	0.2074	0.1926		0.1992
Animal 7	0.2274	0.2032	0.2239	0.1953	0.2109	0.2210
Animal 8	0.2020	0.2124	0.2121	0.1976	0.1899	0.2058
Animal 9	0.2064	0.1906	0.2167	0.1987	0.1933	
Animal 10	0.2000	0.2187	0.2248	0.1926	0.2095	0.2043

	Ovariectomized					
	S-4	S-4	S-4	S-4	S-4	S-4
	0.1 mg/day	0.3 mg/day	0.5 mg/day	0.75 mg/day	1 mg/day	3 mg/day
Animal 1	0.1987	0.2150	0.2118	0.2098	0.2219	0.2018
Animal 2	0.2236	0.2012	0.1994	0.1984	0.1987	0.2105
Animal 3	0.1993	0.2064	0.2192	0.2085	0.1981	0.2011
Animal 4	0.2200	0.2129	0.1985	0.2029		0.2020
Animal 5	0.1990	0.2106	0.1938	0.2089	0.2042	0.2113
Animal 6	0.2019	0.2107	0.2064	0.2066	0.1982	0.2100
Animal 7	0.1956	0.2004	0.1966	0.2098	0.2023	0.1999
Animal 8	0.2040	0.2057	0.2139	0.1954	0.1978	0.2038
Animal 9	0.1935	0.2157	0.2157	0.2113	0.2004	0.2099
Animal 10	0.2001	0.2095	0.2015	0.2027	0.2225	0.2083

Table C.1: Whole body BMD as measured by DEXA.

	Intact			Ovariectomized		
	Vehicle	DHT	S-4	Vehicle	DHT	S-4 + Bical
	--	1 mg/day	1 mg/day	--	1 mg/day	0.5 + 1 mg/day
Animal 1	280	314	304	345	343	334
Animal 2	340	350	342	337	366	346
Animal 3	286	389	293	354	393	356
Animal 4	326	331	374	351	351	354
Animal 5	285	348		342	321	303
Animal 6	322	368	296	326		381
Animal 7	304	345	306	347	330	291
Animal 8	341	394	284	293	337	411
Animal 9	310	343	308	315	353	
Animal 10	287	384	298	351	370	345

	Ovariectomized					
	S-4	S-4	S-4	S-4	S-4	S-4
	0.1 mg/day	0.3 mg/day	0.5 mg/day	0.75 mg/day	1 mg/day	3 mg/day
Animal 1	344	394	387	327	395	405
Animal 2	392	350	325	339	386	358
Animal 3	342	297	359	350	350	351
Animal 4	311	352	348	353		395
Animal 5	356	361	319	326	341	350
Animal 6	340	360	359	397	382	367
Animal 7	319	339	364	352	404	386
Animal 8	379	387	387	364	356	391
Animal 9	345	323	384	388	341	398
Animal 10	375	362	360	366	393	411

Table C.2: Body weight as measured by DEXA.

	Intact			Ovariectomized		
	Vehicle	DHT	S-4	Vehicle	DHT	S-4 + Bical
	--	1 mg/day	1 mg/day	--	1 mg/day	0.5 + 1 mg/day
Animal 1	25.8	44.9	30.9	40.3	34.0	34.7
Animal 2	32.4	38.2	21.3	51.1	31.3	39.0
Animal 3	24.5	34.6	30.1	45.0	40.2	36.8
Animal 4	31.1	24.5	25.5	40.0	41.6	31.5
Animal 5	30.4	41.3		36.5	44.6	32.9
Animal 6	28.7	35.2	26.8	43.1		57.5
Animal 7	27.3	38.8	24.6	34.6	35.1	27.0
Animal 8	37.0	42.0	29.5	39.0	29.0	53.7
Animal 9	27.2	35.1	26.8	40.8	36.8	
Animal 10	29.7	39.5	27.0	43.5	35.9	30.7

	Ovariectomized					
	S-4	S-4	S-4	S-4	S-4	S-4
	0.1 mg/day	0.3 mg/day	0.5 mg/day	0.75 mg/day	1 mg/day	3 mg/day
Animal 1	45.8	51.0	37.8	33.8	41.2	48.0
Animal 2	30.2	42.7	29.7	35.7	33.0	30.7
Animal 3	36.4	29.9	29.5	31.6	41.8	39.6
Animal 4	30.0	43.7	38.1	34.1		28.5
Animal 5	35.5	39.0	36.7	32.9	38.5	28.8
Animal 6	40.2	32.8	37.7	38.6	35.5	30.5
Animal 7	35.3	38.6	36.2	27.3	52.1	32.4
Animal 8	55.2	46.6	30.6	37.4	38.8	35.2
Animal 9	36.0	43.1	36.3	35.4	32.9	43.9
Animal 10	26.9	38.7	40.6	34.1	39.2	40.4

Table C.3: Percent fat mass as measured by DEXA.

	Intact			Ovariectomized		
	Vehicle	DHT	S-4	Vehicle	DHT	S-4 + Bical
	--	1 mg/day	1 mg/day	--	1 mg/day	0.5 + 1 mg/day
Animal 1	0.2204	0.1846	0.2216	0.1849	0.2161	0.1838
Animal 2	0.2383	0.2025	0.2200	0.1927	0.2248	0.1633
Animal 3	0.2663	0.2272	0.2058	0.2003	0.2047	0.1869
Animal 4	0.2379	0.1962	0.2381	0.1857	0.2112	0.1926
Animal 5	0.2210	0.2227		0.2041	0.2175	0.2078
Animal 6	0.2618	0.2121	0.2371	0.2049		0.1871
Animal 7	0.2562	0.2125	0.2538	0.2086	0.2355	0.2543
Animal 8	0.1934	0.2016	0.2648	0.2092	0.1940	0.2118
Animal 9	0.2218	0.1844	0.2393	0.1765	0.1866	
Animal 10	0.2191	0.2208	0.2433	0.1559	0.1967	0.1944

	Ovariectomized					
	S-4	S-4	S-4	S-4	S-4	S-4
	0.1 mg/day	0.3 mg/day	0.5 mg/day	0.75 mg/day	1 mg/day	3 mg/day
Animal 1	0.1834	0.2097	0.2150	0.1926	0.1926	0.2304
Animal 2	0.2370	0.2029	0.1792	0.2088	0.1952	0.2130
Animal 3	0.1867	0.2174	0.2271	0.1972	0.1888	0.2271
Animal 4	0.2632	0.1944	0.2009	0.2348	0.1937	0.2349
Animal 5	0.1923	0.2347	0.1613	0.1833		0.2508
Animal 6	0.2099	0.2202	0.1944	0.2161	0.1995	0.2356
Animal 7	0.1861	0.2410	0.1863	0.2047	0.2139	0.2241
Animal 8	0.1901	0.1979	0.2123	0.1734	0.1919	0.2451
Animal 9	0.2002	0.1807	0.2278	0.2077	0.1991	0.2250
Animal 10	0.2130	0.2039	0.2068	0.1923	0.2123	0.2089

Table C.4: L5-L6 BMD as measured by DEXA.

	Intact			Ovariectomized		
	Vehicle	DHT	S-4	Vehicle	DHT	S-4 + Bical
	--	1 mg/day	1 mg/day	--	1 mg/day	0.5 + 1 mg/day
Animal 1	0.1787	0.1739	0.1489	0.1826	0.1755	0.1755
Animal 2	0.1698	0.1885	0.2081	0.1283	0.1854	0.1837
Animal 3	0.2106	0.2309	0.2440	0.1828	0.1299	0.1463
Animal 4	0.2173	0.1764	0.2571	0.1545	0.1609	0.1378
Animal 5	0.2242	0.1623		0.1497	0.1499	0.1679
Animal 6	0.2014	0.2281	0.1491	0.1444		0.1904
Animal 7	0.2145	0.1553	0.1867	0.1779	0.2454	0.2236
Animal 8	0.2046	0.2391	0.2550	0.1662	0.1009	0.1484
Animal 9	0.1979	0.1819	0.1998	0.1677	0.1781	
Animal 10	0.2152	0.1864	0.1288	0.1334	0.1760	0.1509

	Ovariectomized					
	S-4	S-4	S-4	S-4	S-4	S-4
	0.1 mg/day	0.3 mg/day	0.5 mg/day	0.75 mg/day	1 mg/day	3 mg/day
Animal 1	0.1554	0.1502	0.2199	0.2125	0.1692	0.2044
Animal 2	0.2382	0.1697	0.1452	0.2328	0.1966	0.1903
Animal 3	0.1686	0.2148	0.1994	0.1641	0.1873	0.1945
Animal 4	0.2281	0.1848	0.1999	0.1943		0.2060
Animal 5	0.2202	0.2132	0.1521	0.1920	0.1326	0.1914
Animal 6	0.2139	0.1710	0.1544	0.1494	0.2024	0.2143
Animal 7	0.1765	0.1902	0.1821	0.1873	0.1769	0.1469
Animal 8	0.1383	0.1909	0.1774	0.1962	0.1205	0.2331
Animal 9	0.2053	0.1575	0.1591	0.1695	0.1606	0.1554
Animal 10	0.1360	0.1307	0.1925	0.1592	0.1756	0.1970

Table C.5: Femoral region 4 as measured by DEXA.

	Intact	Ovariectomized			
	Vehicle	Vehicle	DHT	S-4	S-4
	--	--	1 mg/day	1 mg/day	3 mg/day
Animal 1	0.708	0.593	0.69	0.652	0.623
Animal 2	0.76	0.658	0.664	0.705	0.634
Animal 3	0.717	0.657	0.713	0.623	0.674
Animal 4	0.76	0.663	0.623	0.677	0.695
Animal 5	0.728	0.717	0.752	0.682	0.684
Animal 6	0.752	0.646	0.635	0.661	0.677
Animal 7	0.677	0.732	0.728	0.643	0.636
Animal 8	0.693	0.639	0.675	0.664	0.722
Animal 9	0.726	0.63	0.832	0.635	0.728
Animal 10	0.647	0.643			0.675

Table C.6: Cortical thickness of the mid-shaft femur as measured by pQCT.

	Intact	Ovariectomized			
	Vehicle	Vehicle	DHT	S-4	S-4
	--	--	1 mg/day	1 mg/day	3 mg/day
Animal 1	9.85	8.48	10.34	9.42	9.01
Animal 2	11.15	8.95	9.64	10.81	9.51
Animal 3	9.74	9.17	10.39	9.33	9.65
Animal 4	10.8	9.55	8.66	9.36	10.49
Animal 5	10.62	9.63	10.64	9.9	10.08
Animal 6	11.51	8.8	9.18	9.42	10.39
Animal 7	10.08	10.03	9.43	9.13	9.65
Animal 8	9.89	8.07	9.53	9.38	10.69
Animal 9	10.21	8.48	11.64	10.07	11.04
Animal 10	9.29	8.22			10.21

Table C.7: Cortical content of the mid-shaft femur as measured by pQCT.

	Intact	Ovariectomized			
	Vehicle	Vehicle	DHT	S-4	S-4
	--	--	1 mg/day	1 mg/day	3 mg/day
Animal 1	388.1	76.2	105.1	99.2	109.7
Animal 2	365.2	91.9	111.5	79.5	109.5
Animal 3	289.4	25.0	123.9	62.7	99.4
Animal 4	335.2	110.7	98.6	60.4	0.0
Animal 5	298.0	85.4	93.2	85.6	0.0
Animal 6	351.6	106.4	110.3	86.3	205.1
Animal 7	380.1	34.8	0.0	101.8	73.0
Animal 8	246.1	35.6	111.1	88.6	95.5
Animal 9	254.1	24.5	118.2	161.6	21.6
Animal 10	205.8	0.0			93.4

Table C.8: Distal femur trabecular density as measured by pQCT.

	Intact		Ovariectomized			
	Vehicle	S-4	Vehicle	DHT	S-4	S-4
	--	1 mg/day	--	1 mg/day	1 mg/day	1 mg/day
Animal 1	207	222	166	206	221	199
Animal 2	258	252	175	217	242	196
Animal 3	215	234	199	213	207	221
Animal 4	246	212	194	244	202	239
Animal 5	251	263	231	187	236	223
Animal 6	298	216	181	245	215	202
Animal 7	210	257	203	185	201	189
Animal 8	227	231	175	215	210	228
Animal 9	232	239	198	216	219	216
Animal 10	189		187			240

Table C.9: Femoral biomechanical testing of maximum load.